# Modulation of VLDL triglyceride metabolism

# Modulation of VLDL triglyceride metabolism

**Proefschrift**

ter verkrijging van
de graad van Doctor aan de Universiteit Leiden,
op gezag van Rector Magnificus prof. mr. P.F. van der Heijden,
volgens besluit van het College voor Promoties
te verdediging op donderdag 16 december 2010
klokke 13.45 uur

door

**Silvia Bijland**

geboren te Zaanstad
in 1980

Promotiecommissie

| | |
|---|---|
| Promotor: | Prof. Dr. Ir. LM Havekes |
| Copromotores: | Dr. Ir. K Willems van Dijk |
| | Dr. PCN Rensen |
| Overige leden: | Prof. Dr. BK Groen (UMCG, Groningen) |
| | Prof. Dr. RR Frants |
| | Prof. Dr. JA Romijn |
| | Dr. HMG Princen (TNO, Leiden) |

The research described in this thesis was financially supported by the Netherlands Organization for Health Care Research Medical Sciences (ZON-MW project nr. 948 000 04) and by grants from the Nutrigenomics Consortium/Top Institute Food and Nutrition (NGC/TIFN) and the Center of Medical Systems Biology (CMSB) established by The Netherlands Genomics Initiative/Netherlands Organization for Scientific Research (NGI/NWO).

Studies presented in this thesis were performed at the department of Human Genetics and the department of Endocrinology, Leiden University Medical Center, Leiden, the Netherlands and at the Gaubius Laboratory, TNO Quality of Life, Leiden, The Netherlands.

Financial support by the Netherlands Heart Foundation for the publication of this thesis is gratefully acknowledged.

Colophon



ISBN: 978949109801 7

Cover design and Illustrations © S. Bijland

Print by F&N Boekservices Eigenbeheer

Financial support for the publication of this thesis was kindly provided by

J.E. Juriaanse Stichting
Novo Nordisk
Servier Nederland Farma B.V.

## Table of contents

# Chapter 1

## General introduction

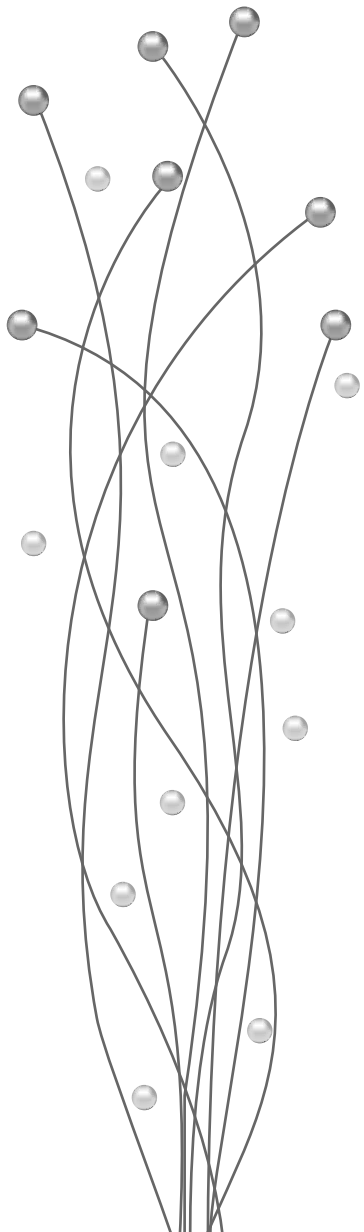

Lipids are essential for life and fulfil multiple functions in energy homeostasis and cellular biology. Two of these lipids are cholesterol, the structural component of cell membranes and steroid hormones, and triglycerides (TG), the main source of energy for both exercise and storage. Excess intake of energy increases the storage of TG and results in overweight and obesity. Since obesity is becoming ever more prevalent in our society due to a sedentary lifestyle combined with a calorie-rich Western diet, it is important to understand pathways involved in the uptake, distribution, oxidation and storage of TG.

In fact, obesity is a global epidemic as stated by the World Health Organization[1] and a major public health concern since excessive overweight is associated with various diseases such as diabetes mellitus type 2 (DM2) and cardiovascular disease (CVD)[2]. The link between TG metabolism, obesity and the development of pathology is subject to intense investigation. TG are composed of a glycerol backbone and three fatty acids (FA). Prior to transmembrane transport, TG are hydrolyzed to FA and after they have been taken up, these FA are re-esterified to TG for storage. Since free FA (FFA) are cytotoxic[3], it is thought that the (mis)handling and distribution of TG derived FA plays a central role in the pathogenesis of overweight related diseases such as DM2 and CVD[4, 5].



**Lipoprotein Metabolism**

The most common lipids in our diet are cholesterol and TG. Since lipids are hydrophobic, they are transported in the circulation in water-soluble spherical particles called lipoproteins. These lipoproteins carry TG and esterified cholesterol (cholesteryl esters, CE) in their core, surrounded by a shell of phospholipids, free cholesterol and proteins termed apolipoproteins (apo's). Based on their composition and origin, lipoproteins can be divided into five major classes e.g. chylomicrons, very low density lipoprotein (VLDL), intermediate density lipoprotein (IDL), low density lipoprotein (LDL) and high density lipoprotein (HDL)[6]. Lipid metabolism can roughly be divided in three major pathways: the exogenous pathway important for transport of dietary lipids, the endogenous pathway important for the transport of lipids during fasting and the reverse cholesterol transport pathway important for the transport of cholesterol from tissues (Fig. 1).

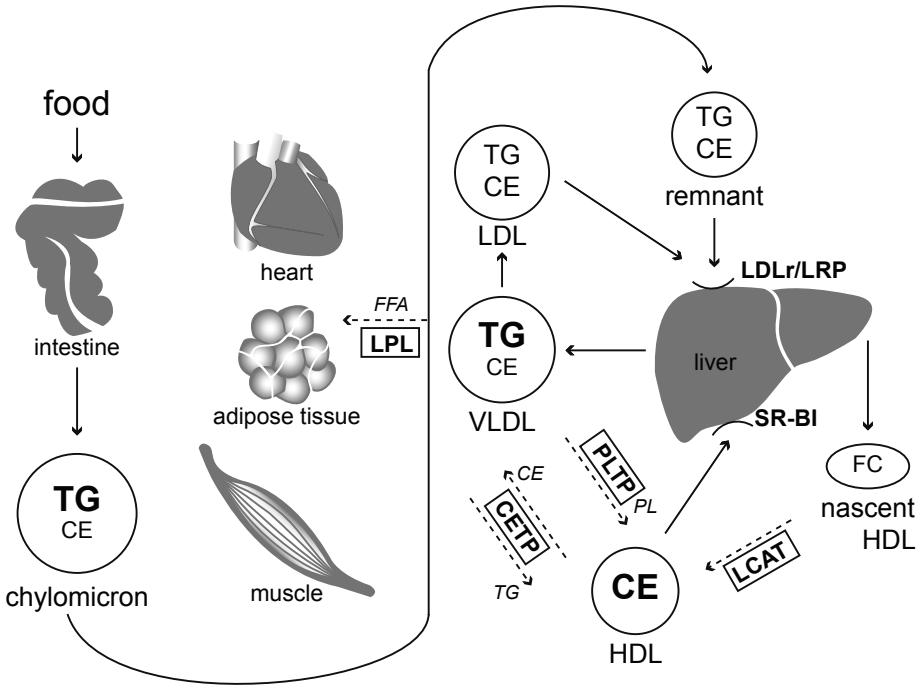


**Figure 1. Schematic overview of lipoprotein metabolism.**
See text for explanation. CE, cholesteryl ester; CETP, cholesteryl ester transfer protein; FC, free cholesterol; FFA, free fatty acids; LCAT, lecithin:cholesterol acyltransferase; LDLr, LDL receptor; LPL, lipoprotein lipase; LRP, LDLr related protein; PL, phospholipid; SR-BI, scavenger receptor BI; TG, triglycerides.

*Exogenous pathway*

In the intestine, dietary lipid is emulsified by the action of bile and TG are hydrolyzed in glycerol and FA by pancreatic lipase[7]. Cholesterol, glycerol and FA are absorbed by the intestinal cells where FA are re-esterified to TG. The TG and cholesterol are packaged in chylomicrons and secreted in the lymph from which they are transported to the blood circulation[8, 9]. Nascent chylomicrons are rich in TG but also contain phospholipids, CE and apolipoproteins apoAI, apoAIV, apoB48 and apoCs[10]. Upon entering the circulation, chylomicrons are processed by lipoprotein lipase (LPL)[8]. LPL hydrolyzes TG, thereby delivering FA to peripheral tissues were it can be used as energy source (heart and skeletal muscle) or can be stored in adipose tissue. The resulting TG depleted remnant chylomicrons are taken up by the liver, mainly via apoE specific recognition sites on the hepatocytes such as the LDL receptor (LDLr) and the LDLr related protein (LRP)[11, 12].

*Endogenous pathway*

Especially in the postprandial state, the liver is the main site of secretion of cholesterol and TG, packaged in VLDL for transport to peripheral tissues. The intracellular formation of VLDL in hepatocytes will be discussed in detail later. After VLDL enters the circulation, the particle is further enriched with apoE and apoCs[10]. Similar to chylomicrons, the TG content of VLDL can be lipolyzed into FA by LPL and used as energy source. VLDL-TG thus predominantly functions as a source of FA under fasting conditions. The processing of VLDL by LPL results in the formation of IDL (or VLDL-remnant) which can be further processed to become cholesterol-rich LDL[10]. The LDLr can bind and internalize both apoE and apoB containing particles[10]. VLDL remnants are predominantly cleared by the liver LDLr via apoE, whereas LDL is depleted from most apolipoproteins except for apoB and is cleared by the liver and peripheral LDLr[10]. High levels of apoB containing lipoproteins (chylomicrons, VLDL, IDL, and LDL) can lead to accumulation of lipids in the vascular wall and the development of atherosclerosis[13, 14].



*Reverse cholesterol transport*

HDL is responsible for the removal of excess cholesterol from peripheral tissues. In the liver and intestine, nascent HDL is formed from apoAI and phospholipids. The biosynthesis of HDL is dependent on the hepatic or intestinal ATP-binding cassette transporter A1 (ABCA1)[15]. In the circulation, HDL is enriched with phospholipids from chylomicrons and VLDL via phospholipid transfer protein (PLTP)[16], and cholesterol from the periphery via ABCA1, ABCGI and probably also scavenger receptor BI (SR-BI)[15, 17]. Cholesterol is subsequently esterified by lecithin:cholesterol acyltransferase (LCAT) into CE that are stored in the core of HDL[17]. The HDL particle expands due to cholesterol accumulation and matures into spherical HDL, which can acquire apolipoproteins including apoAII, apoAIV, apoAV, apoCI, apoCII, apoCIII and apoE[10, 18]. HDL-derived cholesterol can be taken up by the liver via SR-BI[19, 20, 21]. In the liver excess of cholesterol is secreted in the bile thereby maintaining cholesterol homeostasis[22].

The lipids in HDL can be exchanged with other lipoproteins through the interaction with PLTP to exchange phospholipids[16] and cholesteryl ester transfer protein (CETP)[23]. CETP is a glycoprotein that is mainly expressed

by liver, spleen, macrophages and adipose tissue[24]. CETP is predominantly associated with HDL in the circulation and mediates the exchange of CE and TG between apoB containing lipoproteins and HDL[17]. This results in a net flux of TG from (V)LDL to HDL in exchange for CE. The majority of CE from HDL is transferred to apoB containing lipoproteins thereby creating a more atherogenic profile with low levels of HDL-C and high levels of LDL-C. Furthermore, cholesterol transported to LDL by CETP can be taken up by the liver via the LDLr pathway thereby facilitating an alternative route for reverse cholesterol transport mediated by SR-BI.

**VLDL triglyceride and fatty acid metabolism**

*VLDL assembly*

In the liver, TG is secreted in VLDL particles. The assembly of these particles starts in the endoplasmatic reticulum (ER) where newly synthesized apoB is cotranslationally lipidated by microsomal triglyceride transfer protein (MTP)[25, 26]. Each VLDL particle contains one apoB molecule. Since the transcription of apoB is relatively constant, regulation occurs at the posttranscriptional level. Whether apoB is targeted for degradation or lipidated is dependent on the availability of phospholipid and free cholesterol to form the surface monolayer, the availability of neutral lipids (TG and CE) to form the core and the presence of MTP which is necessary for the translocation, folding and lipidation of apoB[27]. When apoB is lipidated and targeted away from proteosomal degradation, a pre-VLDL particle is formed and released in the lumen of the ER where it can either be retained and degraded or further lipidated to form VLDL. This VLDL particle contains only a small amount of TG and is transported to the Golgi complex for secretion. In the Golgi, the VLDL particle can undergo a second step of lipidation in which the particle is loaded with bulk TG after which the mature TG-rich VLDL particle is secreted[25, 27].

The assembly of VLDL is highly dependent on the presence of TG in the hepatocyte. The origin of the FA of these TG is represented in figure 2. Most of the FA used for VLDL-TG secretion originates from the plasma. These FFA are released from the adipose tissue or are spill over from peripheral lipolysis of chylomicron-TG and VLDL-TG and taken up by the liver[28, 29]. Other sources of TG include previously accumulated cytosolic TG stores in the liver, receptor

mediated uptake of TG-rich lipoproteins (TLR), and TG esterification from *de novo* synthesized FA. *De novo* lipogenesis (DNL) in the liver is stimulated in the fed state[28]. FA are depleted from the liver by oxidation of FA (β-oxidation), which lowers the FA available for TG synthesis. A different source for the formation of TG is the phospholipid phosphatidylcholine (PC). Although phospholipids are mainly involved in structuring the VLDL particles, evidence accumulates that phospholipids themselves can also contribute to TG synthesis[30, 31, 32]. However the precise metabolic pathways involved in the conversion of phospholipids to TG are unknown.

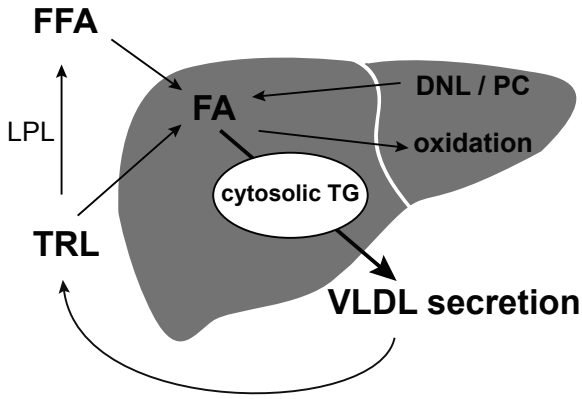




**Figure 2. Schematic overview of sources of fatty acids and TG for VLDL synthesis.**
See text for explanation. DNL, *de novo* lipogenesis; (F)FA, (free) fatty acids; LPL, lipoprotein lipase; PC, phosphatidylcholine; TG, triglycerides; TRL, triglyceride-rich lipoprotein.

*Lipoprotein lipase*

Enzymes responsible for the hydrolysis of TG to FA and glycerol are collectively named lipases[33, 34]. Lipases hydrolyse the ester bonds of mono-, di-, and triglycerides, CE and phospholipids. This family of lipases consists of pancreatic lipase, present in the gut and necessary for the absorption of lipid by the intestine[7], adipose triglyceride lipase (ATGL), hormone sensitive lipase (HSL), endothelial lipase (EL), hepatic lipase (HL) and LPL. LPL is expressed in most tissues, yet most abundantly in tissues that utilize FA for energy or storage (e.g. heart, skeletal muscle and adipose tissue)[33]. To become active, LPL is translocated to the luminal surface of endothelial cells lining the secreting tissues providing a platform for the interaction with TG-rich lipoproteins. This platform consists

of heparin sulfate proteoglycans (HSPGs)[12] and glycosylphosphatidylinositol-anchored high density lipoprotein binding protein 1 (GPIHBP1)[35]. Once TG-rich lipoproteins dock at the platform, LPL mediates the hydrolysis of TG and the released FA are for a large part taken up in the underlying tissue.

The regulation of LPL is tissue-specific and dependent on nutritional status. In the postprandial state, FA are primarily used for storage and therefore LPL activity is high in adipose tissue[36, 37]. During fasting, FA are primarily used as energy substrate and LPL activity is high in muscle[36, 37]. Several factors influence the activity of LPL, some of which are transported by the TG-rich lipoproteins themselves. ApoCII is an essential co-factor for LPL activity[38] and apoAV is a stimulator of LPL mediated lipolysis by guiding the lipoproteins to the lipolysis platform[39, 40]. However, apolipoproteins are also able to inhibit LPL. ApoCIII is a strong LPL inhibitor by affecting both the docking of TG-rich lipoproteins to the lipolytic site as well as directly inhibiting LPL itself[41]. ApoCI is also able to interact with LPL thereby inhibiting its activity[42]. Another group of inhibitors of LPL are the angiopoietin-like protein (Angptl) 3, that suppresses LPL activity and Angptl 4 that inhibits LPL by promoting the conversion of active LPL dimers into inactive LPL monomers[43]. These monomers can be released in the circulation thereby enhancing the binding and/or internalization of lipoproteins[44]. FA derived after lipolysis can be used for β-oxidation or stored in the form of TG by esterification.

*Hormone sensitive lipase*

In the fed state, adipose tissue is the major site of TG storage. There is a continuous cycle of lipolysis and (re-) esterification in the adipose tissue which is mediated by HSL and AGTL, which is termed the futile FA cycle[45, 46]. During intracellular lipolysis, generated glycerol diffuses to the circulation and FA can be released in the circulation or re-esterified to form TG again. The balance between lipolysis and re-esterification therefore determines the plasma levels of FA. During the fed state, the rate of lipolysis by HSL is inhibited by insulin[47] resulting in a net uptake of FA and accumulation of TG in the adipocytes. During fasting, HSL is stimulated by hormones such as glucagon[47] resulting in the release of FA into the circulation. These FA can be oxidized by other tissues, can be taken up by the liver for β-oxidation or can be metabolized into ketone

bodies that can serve as energy source for other tissues. FA from the circulation can also be re-esterified into TG and used as source for VLDL-TG production. This futile cycling of FA between liver and adipose tissue enables the body to adapt rapidly to changes in energy requirement.

*Intracellular FA handling*

FA are an important metabolic substrate but are extremely cytotoxic[3]. Therefore the uptake, transport and storage of FA is intensively regulated and plasma FA levels show relative little variation. After lipolysis, FA are taken up by the underlying tissue by passive diffusion across cell membrane or active transport which is facilitated by FA transporters such as FA translocase CD36[48] and plasma-membrane-associated FA-binding protein (FABPpm)[49]. In the cell, cytosolic FA binding protein (FABPc) and FA transport proteins (FATPs) target the FA to intracellular sites for conversion such as mitochondria for β-oxidation[50]. Diacylglycerol acyltransferases (DGATs) mediate the re-esterification of surplus FA so they can be stored as TG in intracellular lipid droplets. FA also act as important signalling molecules and modulate transcription factors to regulate the expression of genes involved in nutrient sensing and lipid metabolism. This is mediated by G-protein coupled receptors whereby GPR40 and GPR120 are activated by medium and long chain fatty acids[51], and GPR41 and GPR43 are activated by short chain fatty acids[52]. Activation of these FA receptors promotes the secretion of hormones involved in metabolism, such as insulin (GPR40[53], GPR120[54]), leptin (GPR41[55]) and GLP-1 (GPR120[56]), but can also influence our immune response (GPR43[57, 58], GPR120[54]).



**Transcriptional regulation of TG and FA metabolism**

Changes in the expression of genes involved in lipid metabolism are mediated by members of the nuclear receptor superfamily of ligand-dependent transcription factors. These nuclear receptors bind to target genes as heterodimers with retinoid X receptors (RXRs). In the presence of a ligand, these nuclear receptors recruit co-activator complexes resulting in the activation of transcription of the target gene[59]. In the absence of ligand, a co-repressor complex is recruited thereby preventing transcription. Binding of the ligand to the nuclear receptor replaces the co-repressor complex for the co-activator complex thereby

switching from repression to gene activation[59]. A third mechanism through which nuclear receptors act is by transrepression, involving the indirect binding of ligand-bound nuclear receptors to proteins instead of the target gene[59, 60] thereby enabling to control complex gene expression programs. There are several mechanisms through which transrepression can occur including competition and cross-coupling[61]. With competition the activated nuclear receptor competes for the binding of the co-activator complex in situations in which specific co-activators are limited. As a result, less co-activators are available for other transcription factors thereby inhibiting their gene activation. Cross-coupling on the other hand, involves the formation of a complex of the activated nuclear receptor with other activated transcription factors resulting in direct inhibition of each others transcriptional activity.

*PPARs*

Peroxisome proliferators activated receptors (PPARs) play a major role in lipid metabolism. This group of transcription factors consists of three different members that are activated by FA and eicosanoids. PPARα is highly expressed in metabolic active tissue such as liver, heart and muscle[62]. PPARα activation upregulates the expression of genes involved in TG hydrolysis (e.g. apoCIII[63] and LPL[64]) and in FA uptake (e.g. CD36)[65, 66] thereby lowering plasma TG levels. In the liver, PPARα also increases the expression of genes involved in FA import into mitochondria (e.g. CPT1)[67] and β-oxidation (e.g. acyl-CoA synthetase)[62], thereby reducing the intracellular FA concentrations. PPARγ expression is highest in adipose tissue where it affects the expression of genes involved in adipocyte differentiation[68, 69]. Furthermore, PPARγ has a major role in postprandial lipid metabolism. During the postprandial phase, PPARγ expression is highest[70] and upregulates the expression of genes involved in FA uptake and trapping[64, 66], resulting in the storage of lipids in adipocytes[71]. PPARδ is ubiquitously expressed[72] and enhances FA transport and oxidation. This results in depletion of triglyceride stores in tissues such as fat and muscle[73, 74]. Overall, PPARs act as lipid sensors and are able to regulate lipid homeostasis in multiple organs dependent on nutritional and/or energy status.

*SREBP*

Sterol regulatory element binding proteins (SREBPs) are also major regulators of lipid metabolism and are activated when cells become depleted of cholesterol[75]. There are three isoforms, SREBP1a and SREBP1c that share the same gene and SREBP2. SREBP1c is an important downstream target for both the liver X receptor (LXR)[76] and farnesoid X receptor (FXR)[77] and is the major regulator of hepatic FA and TG metabolism[78]. When carbohydrates and saturated FA are abundant, SREBP1c expression is activated and TG storage is increased[78]. While during fasting, SREBP1c is inhibited and FA oxidation is increased[78].

*Xenobiotic receptors*

Activation of the xenobiotic receptors by environmental chemicals and drugs induces the expression of proteins important for the metabolism, deactivation and transport of these chemicals. However, pathways used for xenobiotic metabolism overlap with pathways involved in lipid metabolism. Constitutive androstane receptor (CAR) and pregnane X receptor (PXR) both belong to the nuclear receptor family and decrease the expression of genes involved in β-oxidation[79, 80, 81]. Furthermore, PXR increases the uptake of FA in the liver of mice by increasing the expression of CD36 and increases the hepatic expression of lipogenic genes[82]. Overall activation of xenobiotic receptors can lead to changes in hepatic and plasma lipid profiles[83, 84, 85] and PXR or CAR activating drugs can even lead to lipid accumulation in the liver of patients[86, 87].



*PGC-1*

One of the co-regulators of nuclear receptors involved in the control of energy metabolism is the PPARγ coactivator-1 (PGC-1) family. Several targets of PGC-1 are PPARs[73, 88], PXR[89], CAR[90] and also non-nuclear receptors such as SREBP-1[91] and forkhead box O1 (FOXO1)[92]. In the liver, PGC-1 signalling is increased during fasting and activates gene expression involved in FA oxidation by co-activating PPARα[92, 93]. This increase in FA oxidation is required to produce substrates necessary for the production of glucose and is mediated through PGC-1α and PGC-1β[91, 92, 93]. PGC-1β also activates the expression of genes involved in lipogenesis and VLDL production by co-activating SREBP1c[91].

**The association between lipid and glucose metabolism**

In addition to lipids, carbohydrates are an important source of energy in our diet. Complex carbohydrates such as starch are digested into glucose prior to absorption in the gut. After a meal, blood glucose levels rise, which results in the release of insulin into the circulation by the pancreas. Insulin is a central anabolic hormone that regulates both glucose and lipid metabolism[94]. The main action of insulin is to decrease excessive glucose by stimulating metabolism and storage. The liver is a central player in glucose homeostasis, since it can store glucose in the form of glycogen for later use[95]. However, due to limited glycogen storage insulin promotes *de novo* lipogenesis from excessive glucose to produce FA.

Under fasting conditions, blood glucose levels drop and since the brain is highly dependent on glucose, glucose levels need to be maintained. In response to glucose lowering, insulin is no longer produced by the pancreas to prevent further storage of glucose. In addition, glucose oxidation is lowered and FA oxidation increased in tissue, thereby preventing further usage of glucose. The drop in glucose levels stimulates the production of glucagon by the pancreas. Under the influence of glucagon, glucose can rapidly be mobilized from hepatic glycogen stores (glycogenolysis) and released into the circulation to provide tissues with glucose that can not function without it, such as the brain. When these glycogen stores become depleted, the liver starts producing glucose from substrates such as amino acids and glycerol (gluconeogenesis) to maintain blood glucose levels[96]. During prolonged fasting, glucose is no longer readily available and ketone bodies are used as energy source instead. Ketone bodies are produced in the liver from fatty acids, a process known as ketogenesis, and provide an alternative energy source for tissues, such as the brain, to maintain its function.

**Pathology of lipid and glucose metabolism in the metabolic syndrome**

Since lipid and glucose metabolism are tightly linked, disturbances in one metabolic pathway in general also involves the other. Excessive calorie intake and a diet rich in saturated fat predisposes to obesity and concomitantly dyslipidemia, which is characterized by high levels of TG (hypertriglyceridemia), high levels of small, dense LDL-C and low levels of

HDL-C. This is also known as the metabolic syndrome, which refers to a cluster of correlated disorders including obesity, dyslipidemia, insulin resistance and hypertension[97]. The metabolic syndrome but also all the various components themselves are associated with an increased risk to develop DM2 and CVD[98, 99, 100]. The metabolic syndrome comprises storage of excess TG in non-adipose, resulting in unresponsiveness of this tissue to insulin, also known as insulin resistance[101, 102, 103]. Insulin resistance of the liver results in impaired repression of glucose production in response to insulin, resulting in high blood glucose. To compensate for insulin resistance, the pancreas starts to produce more insulin to maintain normal glucose levels. When the demand on the pancreas to produce insulin exceeds its capacity, the pancreas is damaged, leading to DM2.

A combination of increased storage of TG in the liver and insulin resistance is associated with increased secretion of VLDL-TG[104, 105]. In addition, insulin resistance is also associated with increased lipolysis of TG in adipose tissue by HSL resulting in more FA flux from adipose tissue to the liver, thereby increasing the liver TG stores. The increased production of VLDL-TG by the liver can result in hypertriglyceridemia, thereby providing more apoB lipoprotein acceptors for the transfer of cholesterol by CETP. As a result HDL becomes depleted of cholesterol and LDL-C levels increase[106].



A high level of LDL-C is the major cause of atherosclerosis. Cholesterol rich LDL particles can invade the arterial wall where they are oxidized and cause local damage[13, 14]. Monocytes are attracted to the site of damage and differentiate into macrophages that can incorporate the LDL particles thereby becoming cholesterol rich foam cells[13, 14]. The accumulation of these cholesterol rich foam cells results in the formation of plaques. Rupture of these plaques can lead to an infarct, damaging surrounding tissue[13, 14].

**Models to study lipoprotein metabolism**

Dyslipidemia in humans is a multifactorial disease with both genetic and environmental origins. Due to the complexity of many dyslipidemias, animal models have been developed to investigate specific components of dyslipidemia to gain more insight in the mechanisms involved. Mice are a commonly used model since they are easy to breed, genetically homogeneous and their environment and diet is easily controlled. Moreover, mice can be

genetically manipulated by both changing the expression of endogenous genes and by introducing novel genes. Unfortunately, lipid metabolism in mice is somewhat different compared to humans. Mice are very efficient in clearing apoE-containing lipoproteins from circulation, which results in low levels of apoB containing lipoproteins such as VLDL and LDL. In addition, mice lack the enzyme CETP and have high levels of HDL compared to humans.

Several mouse models have been developed which are more similar to human lipoprotein metabolism such as the LDL receptor-deficient ($LDLr^{-/-}$) and apolipoprotein E-deficient ($ApoE^{-/-}$) (reviewed in[107]). The mouse model used in this thesis to study TG and FA metabolism is the transgenic ApoE*3-Leiden (E3L) mouse. E3L mice carry the human apoCI gene and a variant of the human ApoE*3 gene which causes a genetic form of hyperlipidemia in humans[108, 109]. Expression of these transgenes in E3L mice is associated with decreased LPL activity, a disturbed interaction of lipoproteins with the LDLr and LRP and impaired hepatic clearance of apoE containing lipoproteins. Together this is associated with a more human-like lipoprotein metabolism that is characterized by elevated levels of VLDL and LDL.

On a standard chow diet, E3L mice have moderately increased levels of plasma TG and cholesterol. However, E3L mice are highly responsive to diets rich in fat and cholesterol, resulting in strong increases in plasma TG and cholesterol levels[110]. The E3L mice have been used to study (V)LDL metabolism in response to various hypolipidemic drugs. In contrast to the often used $LDLr^{-/-}$ and $ApoE^{-/-}$ hyperlipidemic mouse models, E3L mice have been shown to respond in a human-like manner to a large number of drugs that modify LDL-C. These drugs include statins[111, 112, 113], fibrates[114, 115] and cholesterol uptake inhibitors[115]. However, mice naturally lack CETP, important for both (V)LDL and HDL cholesterol metabolism. Therefore E3L mice have recently been crossed with mice expressing human CETP under control of its own promoter. The resulting E3L.CETP transgenic mice resemble human lipoprotein metabolism even more closely compared to E3L mice by the redistribution of cholesterol from HDL to (V)LDL[116]. As a result, these E3L.CETP mice respond to both LDL and HDL modifiers[85, 114, 117, 118, 119] and are a valuable model to study the effects of pharmaceuticals on lipoprotein metabolism.

**Outline**

The research in this thesis focuses on the regulation of TG and FA metabolism to get a better understanding of TG and FA metabolism in health and disease. The effect of CETP on TG metabolism is studied by using the E3L mouse model in **Chapter 2**. Previous studies have shown that expression of CETP in E3L mice results in a shift of cholesterol from HDL to apoB containing lipoproteins. Since CETP simultaneously exchanges CE with TG, we set out to evaluate whether the impact of CETP on TG metabolism is similar to the impact of CETP on cholesterol metabolism.

The mechanisms underlying the TG-lowering effect of the PPARα agonist fenofibrate are studied using E3L.CETP mice in **Chapter 3**. This TG-lowering effect of fenofibrate has been attributed to both increased TG clearance and decreased VLDL-TG production. However, since data on the effect of fenofibrate on VLDL production are controversial, we aimed to investigate the mechanism underlying the TG-lowering effect of fenofibrate.

The effects of the antibiotic rifampicine on TG metabolism are discussed in **Chapter 4**. This drug is a potent PXR activator that induces hepatic steatosis in both humans and rodents.



**Chapter 5** describes the effect of perfluoroakyl sulfonates (PFAS) on lipid metabolism. PFAS are very useful for water and oil repellence, but are therefore also extremely resistant to degradation. As a consequence PFAS accumulate in the environment and can be found in the blood of both wildlife as well as humans. PFAS are considered to act as PPARα agonist thereby affecting lipid metabolism. Our aim was to investigate the effects of PFAS on both TG and cholesterol metabolism in E3L.CETP mice.

Hepatic steatosis affects both lipid and glucose metabolism and is associated with insulin resistance. In mice, both prolonged fasting and feeding a high fat diet induces hepatic steatosis, however only after a high fat diet, hepatic steatosis is associated with insulin resistance. **Chapter 6** describes the differences in the hepatic gene expression profile of mice fasted for 16 hours compared to mice fed a high fat diet for 2 weeks.

1

# Chapter 2

## CETP does not affect triglyceride production or clearance in ApoE*3-Leiden mice

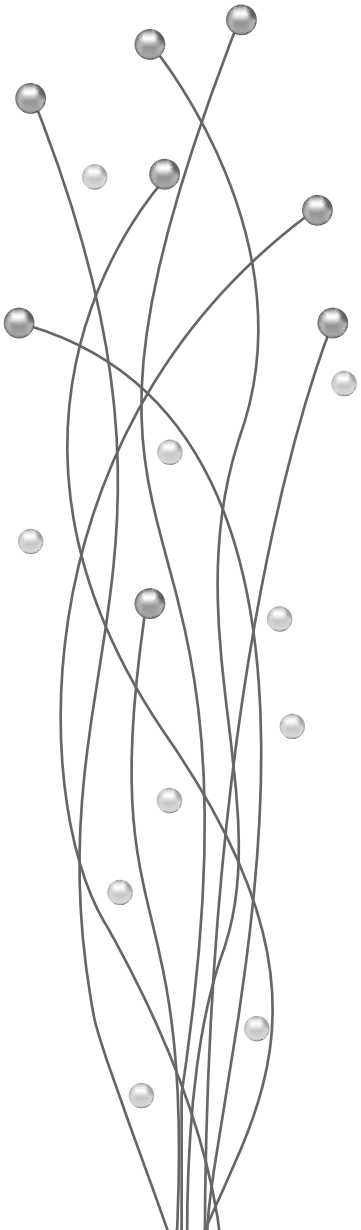

Silvia Bijland
Sjoerd AA van den Berg
Peter J Voshol
Anita M van den Hoek
Hans MG Princen
Louis M Havekes
Patrick CN Rensen
Ko Willems van Dijk

*Journal of Lipid Research 2010*

The cholesteryl ester transfer protein (CETP) facilitates the bidirectional transfer of cholesteryl esters and triglycerides (TG) between HDL and (V)LDL. By shifting cholesterol in plasma from HDL to (V)LDL in exchange for VLDL-TG, CETP aggravates atherosclerosis in hyperlipidemic ApoE*3-Leiden (E3L) mice. The aim of this study was to investigate the role of CETP in TG metabolism and high fat diet-induced obesity by using E3L mice with and without the expression of human CETP gene. On chow, plasma lipid levels were comparable between both male and female E3L and E3L.CETP mice. Further mechanistic studies were performed using male mice. CETP expression increased the level of TG in HDL. CETP did not affect the postprandial plasma TG response, nor the hepatic VLDL-TG and VLDL-apoB production rate. Moreover, CETP did not affect the plasma TG clearance rate or organ-specific TG uptake after infusion of VLDL-like emulsion particles. In line with the absence of an effect of CETP on tissue-specific TG uptake, CETP also did not affect weight gain in response to a high fat diet. In conclusion, the CETP-induced increase of TG in the HDL fraction of E3L mice is not associated with changes in the production of TG or with tissue-specific clearance of TG from the plasma.

**Introduction**

Cardiovascular disease (CVD) is one of the major causes of mortality in the Western world, and dyslipidemia is an important risk factor in the development of CVD. Low levels of HDL-cholesterol (C), high levels of VLDL- and LDL-C and high levels of triglycerides (TG) are independent risk factors for CVD[120, 121]. The ratio of (V)LDL-C to HDL-C is to a great extent affected by the cholesteryl ester transfer protein (CETP).

CETP mediates the bidirectional exchange of cholesteryl esters and TG between HDL and (V)LDL. CETP shifts cholesterol in plasma from HDL to (V)LDL and thereby aggravates atherosclerosis in the E3L mouse model which has a human-like lipoprotein metabolism[116]. The HDL-C-lowering effect of CETP has prompted the development of pharmacological CETP inhibitors, such as torcetrapib, as adjuvant therapy to the widely prescribed LDL-lowering statins. Although the first CETP inhibitor torcetrapib, recently failed[116, 122], at least two novel CETP inhibitors (i.e. JTT-705 and anacetrapib) are currently in different phases of clinical trials[123, 124].

Despite the well described effects of CETP on plasma cholesterol metabolism, the role of CETP in TG metabolism has been studied less well. The torcetrapib and JTT-705 trials showed that inhibition of CETP in humans affects both the cholesterol and TG distribution over lipoproteins[125, 126]. It was also reported that JTT-705 reduces plasma TG in patients with combined hyperlipidemia[127], which may reveal a beneficial effect of CETP inhibition on plasma TG levels. Furthermore, in rabbits, enrichment of HDL with TG by CETP increases the catabolism of HDL by hepatic lipase (HL)[128]. Thus, CETP has the potential to affect TG metabolism, which may have effects on tissue-specific lipid accumulation.

VLDL-derived TG are lipolyzed in peripheral tissues by the enzyme lipoprotein lipase (LPL), whereas HDL-derived TG are presumably lipolyzed by HL and thus shunted to the liver. Therefore, we hypothesized that the CETP mediated net transfer of TG from (V)LDL to HDL modulates the tissue-specific uptake of plasma TG and, as a consequence, affects the development of high fat diet–induced obesity.

## Materials and Methods

*Animals*

Human CETP transgenic mice which express CETP under control of its natural flanking regions (strain 5203)[129] were obtained from Jackson Laboratories (Bar Harbor, MC) and crossbred with E3L mice[108] in our local animal facility to obtain heterozygous E3L.CETP mice[116]. Mice (12-16 weeks old) were housed in a temperature and humidity-controlled environment and were fed a standard chow diet with free access to water. Mice of 12 weeks of age were fed a high fat diet (60 energy% derived from bovine fat; D 12492, Research Diet Services, Wijk bij Duurstede, The Netherlands) for 12 weeks to induce obesity. Body weight was measured during the intervention and the delta was calculated. All animal experiments were approved by the Animal Ethics Committee from the Leiden University Medical Center and The Netherlands Organization for Applied Scientific Research (TNO), Leiden, The Netherlands.



*Plasma parameters*

Plasma was obtained after overnight fasting (unless indicated otherwise) via tail vein bleeding in chilled paraoxon-coated capillary tubes to prevent *ex vivo* lipolysis, and assayed for TG and total cholesterol using commercially available kits 1488872 and 236691 from Roche Molecular Biochemicals (Indianapolis, IN, USA), respectively. Plasma CETP mass was analyzed using the CETP ELISA kit from ALPCO Diagnostics (Salem, NH, USA). FFA were measured using NEFA C kit from Wako Diagnostics (Instruchemie, Delfzijl, the Netherlands). HL activity in plasma was determined by measuring plasma triacylglycerol hydrolase activity as described earlier[130].

*Lipoprotein profiling*

To determine the lipid distribution over plasma lipoproteins, lipoproteins were separated using fast protein liquid chromatography (FPLC). Plasma was pooled per group, and 50 µL of each pool was injected onto a Superose 6 PC 3.2/30 column (Äkta System, Amersham Pharmacia Biotech, Piscataway, NJ, USA) and eluted at a constant flow rate of 50 µL/min in PBS, 1 mM EDTA,

pH 7.4. Fractions of 50 µL were collected and assayed for cholesterol and TG as described above.

*Postprandial response*

Mice were fasted overnight with food withdrawn at 6:00 p.m. the day before the experiment. Mice received an intragastric olive oil load (Carbonell, Cordoba, Spain) of 200 µL. Prior to the bolus and 1, 2, 3, 4, 6 and 10 h after the bolus, blood samples (30 µL) were drawn via tail bleeding for TG determination as described above. The circulating levels were corrected for the levels of TG prior to the bolus and the area under the curve (AUC) was calculated over the period of 0-10 h using GraphPad software.



*Hepatic VLDL-TG and VLDL-apoB production*

Mice were fasted for 4 h with food withdrawn at 5:00 a.m. prior to the start of the experiment. During the experiment, mice were sedated with 6.25 mg/kg acepromazine (Alfasan), 6.25 mg/kg midazolam (Roche), and 0.3125 mg/kg fentanyl (Janssen-Cilag). At t=0 min blood was taken via tail bleeding and mice were i.v. injected with 100 µL PBS containing 100 µCi Trans$^{35}$S label to measure *de novo* total apoB synthesis. After 30 min, the animals received 500 mg of tyloxapol (Triton WR-1339, Sigma-Aldrich) per kg body weight as a 10% (w/w) solution in sterile saline, to prevent systemic lipolysis of newly secreted hepatic VLDL-TG[131]. Additional blood samples were taken at t=15, 30, 60, and 90 min after tyloxapol injection and used for determination of plasma TG concentration. At 120 min, the animals were sacrificed and blood was collected by orbital puncture for isolation of VLDL by density gradient ultracentrifugation. $^{35}$S-labeled total apoB content was measured in the VLDL fraction after precipitation with isopropanol[132, 133, 134].

*In vivo clearance of VLDL-like emulsion particles*

Glycerol tri[$^{3}$H]oleate-labeled VLDL-like emulsion particles (80 nm) were prepared as described by Rensen *et al.*[135]. In short, radiolabeled emulsions were obtained by adding 200 µCi of glycerol tri[$^{3}$H]oleate (triolein, TO) to 100 mg of emulsion lipids before sonication (isotope obtained from GE Healthcare, Little Chalfont, U.K.). Mice were fasted 4 h, sedated as described above and injected

with the radiolabeled emulsion particles (1.0 mg TG in 200 µL PBS) in the tail vein at 9:00 a.m. At indicated time points after injection, blood was taken from the tail vein to determine the serum decay of [$^{3}$H]TO. At 15 min after injection, plasma was collected by orbital puncture and mice were sacrificed by cervical dislocation. Organs were harvested and saponified to determine [$^{3}$H]TO uptake.

*Tissue-specific FFA uptake from plasma TG*

Mice were fasted for 4 h with food withdrawn at 5:00 a.m. prior to the start of the experiment. During the experiment, mice were sedated as described above. At t=0 min blood was taken via tail bleeding and mice received a continuous i.v. infusion of [$^{3}$H]TO-labeled VLDL-like emulsion particles for 2 h (4.4 µCi [$^{3}$H]TO and 1.2 µCi [$^{14}$C]FA)[136]. Blood samples were taken using chilled paraoxon-coated capillaries by tail bleeding at 90 and 120 min of infusion to ensure that steady-state conditions had been reached. Subsequently, mice were sacrificed and organs were quickly harvested and snap-frozen in liquid nitrogen. Analysis and calculations were performed as described[136].



*Statistical analysis*

Differences between groups were determined with the unpaired T-test for normally distributed data (GraphPad Prism 5 software, La Jolla, CA). A P-value of less than 0.05 was considered statistically significant. Data are presented as means ± SEM.

**Results**

*Plasma lipids, lipoprotein profiles and hepatic lipase activity*

To investigate the role of CETP in TG metabolism, male and female E3L and E3L.CETP mice were fasted overnight and plasma lipid levels were determined (Table 1). Expression of CETP had no effect on total plasma lipid levels. Since we did not detect a difference between males and females, we decided to use males only for all subsequent experiments. Plasma lipoprotein profiles were determined on pooled plasma. Expression of CETP resulted in a shift of cholesterol from HDL to VLDL (Fig. 1A), as seen previously[116, 119]. Furthermore,

a small amount of TG was detected in the HDL fraction upon expression of CETP (insert Fig. 1B). HL activity was did not differ between E3L and E3L.CETP mice (3.9 ± 1.5 vs 3.2 ± 1.3 μmol FFA/h/mL, respectively). This indicates that there is exchange of TG from the VLDL to the HDL fraction by CETP, which may be indicative of changes in TG metabolism.



**Table 1.** Plasma parameters after an overnight fast.

| | males | | females | |
|---|---|---|---|---|
| | *E3L* | *E3L.CETP* | *E3L* | *E3L.CETP* |
| triglycerides (mM) | 2.39 ± 0.13 | 2.45 ± 0.26 | 2.59 ± 0.33 | 2.31 ± 0.46 |
| total cholesterol (mM) | 3.26 ± 0.11 | 2.91 ± 0.29 | 3.11 ± 0.23 | 3.09 ± 0.45 |
| free fatty acids (mM) | 1.09 ± 0.06 | 1.18 ± 0.07 | 1.18 ± 0.09 | 1.31 ± 0.10 |
| CETP (μg/mL) | n.d. | 3.78 ± 0.36 | n.d. | 3.51 ± 0.43 |

Plasma was obtained from overnight fasted male and female E3L and E3L.CETP mice on a chow diet (n=12 per group). Plasma triglycerides, total cholesterol, free fatty acids and CETP levels were measured, n.d.; not detected.

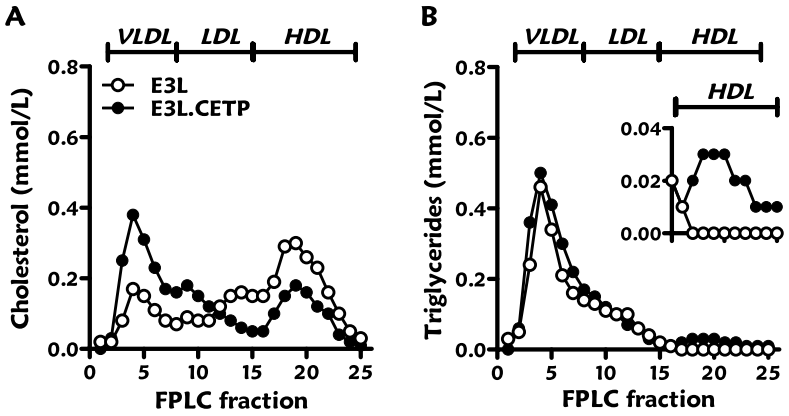


**Figure 1. Plasma lipoprotein profiles.**
12 h fasted mice were bled. Plasma was collected, pooled per group (n=12), and subjected to FPLC to separate lipoproteins Distribution of cholesterol (A) and triglycerides (B) over lipoproteins was determined.

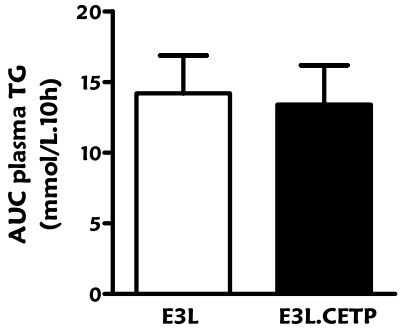


**Figure 2. Postprandial plasma TG response.** Overnight fasted mice received an intragastric olive oil gavage and blood samples were drawn up to 10 h (n=6-9 per group). Plasma TG concentrations were determined and area under the curve ($AUC_{0\text{-}10}$) was calculated.

*Postprandial TG clearance*

To examine whether CETP-mediated transfer of TG from VLDL to HDL influences plasma TG metabolism, we determined postprandial TG response. After an overnight fast, mice received an intragastric gavage of olive oil. Plasma TG concentrations were measured over a 10 h-period and the AUC was calculated. Expression of CETP in E3L mice did not affect the postprandial TG changes in plasma (Fig. 2).



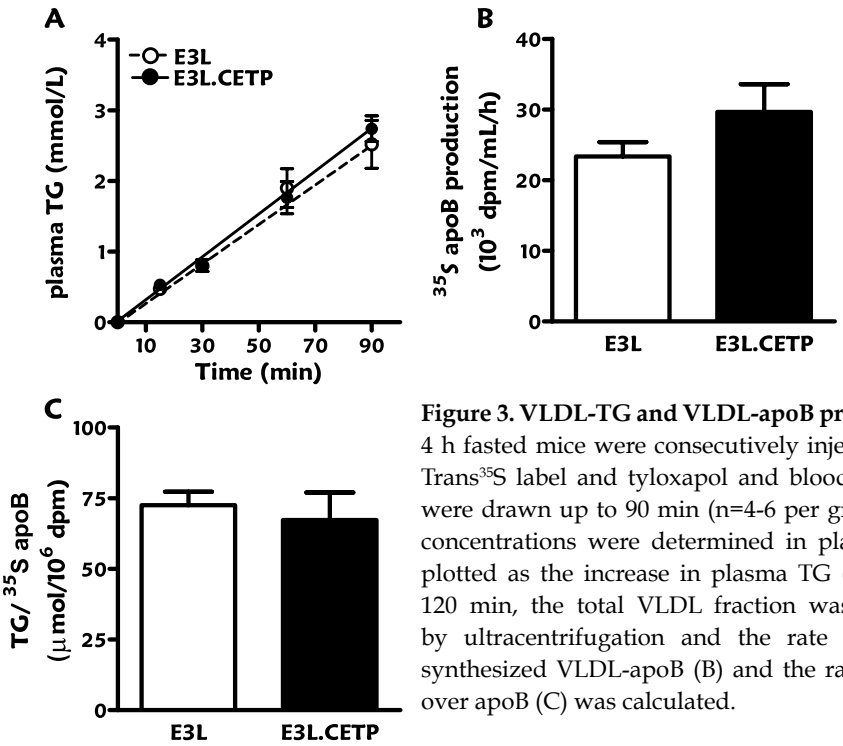


**Figure 3. VLDL-TG and VLDL-apoB production.** 4 h fasted mice were consecutively injected with Trans$^{35}$S label and tyloxapol and blood samples were drawn up to 90 min (n=4-6 per group). TG concentrations were determined in plasma and plotted as the increase in plasma TG (A). After 120 min, the total VLDL fraction was isolated by ultracentrifugation and the rate of newly synthesized VLDL-apoB (B) and the ratio of TG over apoB (C) was calculated.

*VLDL-TG and VLDL-apoB production*

To further examine the effect of CETP on TG metabolism we determined VLDL production. After 4 h of fasting, mice were injected with Trans$^{35}$S and tyloxapol and the accumulation of endogenous VLDL-TG in plasma was measured over time. As is evident from Fig. 3A, the VLDL-TG production rate, as determined from the slope of the curve, was unchanged upon expression of CETP. Furthermore, the rate of VLDL-apoB production (Fig. 3B) as well as the ratio of TG over apoB (Fig. 3C), reflecting the amount of TG per VLDL particle, did not differ between E3L and E3L.CETP mice.

*VLDL-like emulsion-TG clearance*

Clearance of TG from circulation is also a major determinant of TG metabolism and therefore we examined the effect of CETP on TG clearance from VLDL-like emulsions, which have previously been shown to mimic the metabolic behaviour of TG-rich lipoproteins[135, 137]. After 4 h fasting, mice were injected with a bolus of [$^3$H]TO-labeled VLDL-like emulsion particles. The decay of [$^3$H]TO in plasma was not affected by the expression of CETP (Fig. 4). The tissue-specific uptake of [$^3$H]TO was not different between E3L and E3L.CETP mice (data not shown).

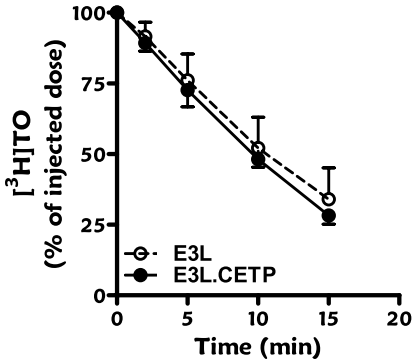


**Figure 4. Plasma TG clearance.**
4 h fasted mice were injected with 1 mg TG as a constituent of VLDL-like [$^3$H]TO-labeled emulsion particles (n=4-8 per group). Blood was collected at the indicated time points and radioactivity was measured in plasma.

To determine the body distribution of TG-derived FA in steady state, [$^3$H]TO-labeled VLDL-like emulsion particles together with albumin-bound [$^{14}$C]FA were continuously infused for 2 h. No difference was observed in the serum half-life of [$^3$H]TO between E3L and E3L.CETP mice (Fig. 5A). Also, the uptake of [$^3$H]TO-derived radioactivity by liver, muscle, white adipose tissue (WAT)

and brown adipose tissue (BAT) was not altered due to the expression of CETP (Fig. 5B). The serum half-life and organ specific uptake of [$^{14}$C]FA were also not changed upon expression of CETP (data not shown).

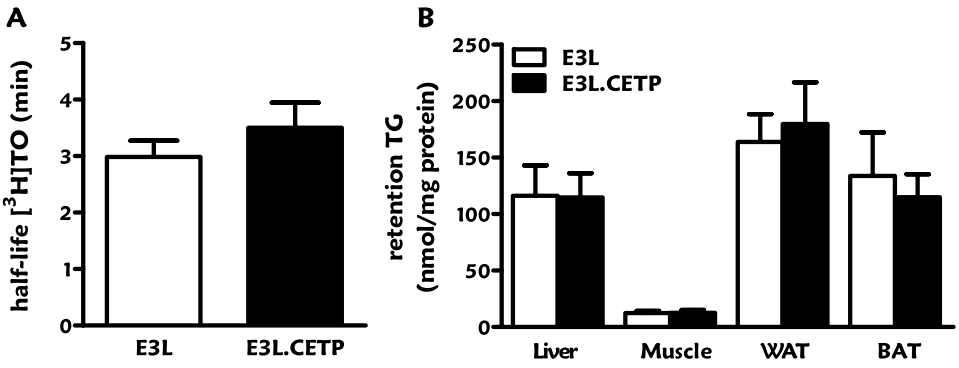


**Figure 5. Plasma derived TG distribution over tissues.**
4 h fasted mice were infused for 2 h with a trace of VLDL-like [$^{3}$H]TO-labeled emulsion particles (n=7 per group). Blood and organs were collected. Radioactivity was measured in plasma lipid fractions after thin layer chromatography and the plasma half-life of [$^{3}$H]TO was calculated (A). The specific [$^{3}$H]TG activity in plasma was calculated based on the TG level, and the uptake of plasma TG by liver, skeletal muscle, white adipose tissue (WAT) and brown adipose tissue (BAT) was calculated (B).



*High fat diet-induced obesity*

We and others have previously shown that modulation of tissue-specific TG-derived FA delivery can have a major impact on the development of high fat diet-induced obesity (reviewed in[138]). To exclude the possibility that CETP expression results in a minor change in tissue-specific TG-derived FA uptake that over a prolonged period would affect the development of obesity, E3L and E3L.CETP mice were fed a high fat diet (60% energy% in the form of fat) for 12 weeks, and body weight was measured over time. The high fat diet did not affect plasma CETP levels in E3L.CETP mice (3.8 ± 0.4 µg/mL on chow and 3.6 ± 0.3 µg/mL on high fat diet). Furthermore the high fat diet resulted in a similar decrease in plasma TG in both E3L and E3L.CETP mice (1.04 ± 0.11 and 0.92 ± 0.14 mmol/L, respectively). CETP did not affect the high fat diet-induced body weight gain at any time point during the 12 weeks (Fig. 6).

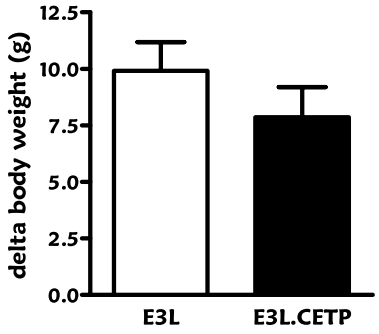


**Figure 6. High fat diet-induced obesity.**
Mice were fed a high fat diet and body weight was measured during the dietary intervention and the increase in bodyweight was calculated (n=12 per group).



**Discussion**

Novel drugs that inhibit CETP activity as therapy to increase HDL-C levels are in various stages of development[123, 124]. The rationale for development of these drugs is based on HDL-lowering effect of CETP due to the redistribution of cholesterol from HDL toward (V)LDL. Since CETP transfers both cholesterol and TG between lipoproteins, we here focused on the effect of CETP on TG metabolism. We studied the effect of CETP expression in E3L mice. The E3L mice display a human-like lipoprotein metabolism, and are an established model for hyperlipidemia and atherosclerosis (as reviewed in[115]). We recently reported the HDL-lowering and pro-atherogenic properties of CETP expression on the E3L background[116]. In this study, after 4 hour fasting, plasma cholesterol were somewhat higher in the E3L.CETP mice. In the current study, we find no changes in plasma total cholesterol and TG after overnight fasting. We do find a small increase in TG in the HDL fraction upon expression of CETP in E3L mice. Despite this relative increase in HDL-TG, CETP did not affect the postprandial TG response, hepatic VLDL-TG production, clearance of TG from VLDL-like emulsion particles and the development of high fat diet-induced obesity. These findings suggest that CETP-mediated transfer of TG from (V)LDL to HDL does not reflect a substantial effect on overall plasma TG metabolism in E3L mice.

There is some controversy on the effects of CETP on TG metabolism in various mouse models. Studies in mice, expressing simian CETP, show that on an atherogenic diet expression of CETP results in increased production

and clearance of TG[139]. Others have demonstrated that mice expressing human CETP when fed a regular chow diet show no alterations in VLDL-TG production[140, 141]. However, Salerno *et al.*[140] showed that CETP-expressing mice have an increased postprandial TG response and decreased clearance of TG from the circulation. This was attributed to a decrease in LPL activity and LPL gene transcription. We did not find changes in the postprandial TG response or in the clearance of TG from the circulation in E3L.CETP mice versus E3L mice. We also did not find an effect of CETP in E3L mice on high fat diet-induced obesity. Since modification of tissue-specific FA delivery can significantly affect high-fat diet-induced obesity, this further confirms the absence of even a subtle effect of CETP on tissue-specific TG-derived FA uptake. It seems likely that the explanation for the discrepancy of our data with those of Salerno *et al.*[140] is associated with the more human-like lipoprotein metabolism on the E3L background as indicated by presence of a substantial amount of apoB-containing lipoproteins.

Enrichment of HDL with TG has a major impact on HDL metabolism. In humans, it has been demonstrated that cholesterol and apoAI within TG-rich HDL are cleared more rapidly as compared to those within TG-poor HDL[142]. Similar observations have been made in various animal models[128, 143, 144]. Thus, CETP-mediated TG enrichment of HDL has measurable effects on the kinetics of HDL-C and HDL-apoAI. Although these changes in HDL kinetics have the potential to have a substantial effect on TG metabolism, our results implicate that the CETP-mediated TG transfer does not alter the kinetics of TG clearance from the circulation.



This may be explained by the apparently small contribution of HDL-TG to the overall flux of TG. Especially in the postprandial state, the amount of TG in chylomicrons exceeds the amount of TG in HDL by far, even when CETP activity is high. Alternatively, HDL-TG may be readily lipolyzed by HL and the fate of the resulting FA may not be quantitatively different from FA derived from VLDL-TG. During lipolysis of VLDL-TG by LPL, a significant fraction of FA leaks to the circulation and is subsequently cleared by the liver[136]. Since it has been postulated that HDL-TG-derived FA are also cleared by the liver[128], the fate of a substantial fraction of VLDL-TG derived FA and HDL-TG derived FA will thus be indistinguishable.

In conclusion, we show that expression of CETP does not affect overall TG metabolism and high fat diet-induced obesity in E3L mice. This implicates that, at least under relatively normolipidemic conditions, pharmacological CETP inhibition is unlikely to disturb TG metabolism.



**Acknowledgements**

This work was supported by grants from the Nutrigenomics Consortium/ Top Institute Food and Nutrition (NGC/TIFN) and the Center of Medical Systems Biology (CMSB) established by The Netherlands Genomics Initiative/ Netherlands Organization for Scientific Research (NGI/NWO) and by the Netherlands Organization for Health Care Research Medical Sciences (ZON-MW project nr. 948 000 04). The authors are grateful to M.C. Maas and A.P. Tholens for excellent technical assistance.

# Chapter 3

## Fenofibrate increases VLDL-triglyceride production despite reducing plasma triglyceride levels in ApoE*3-Leiden.CETP mice

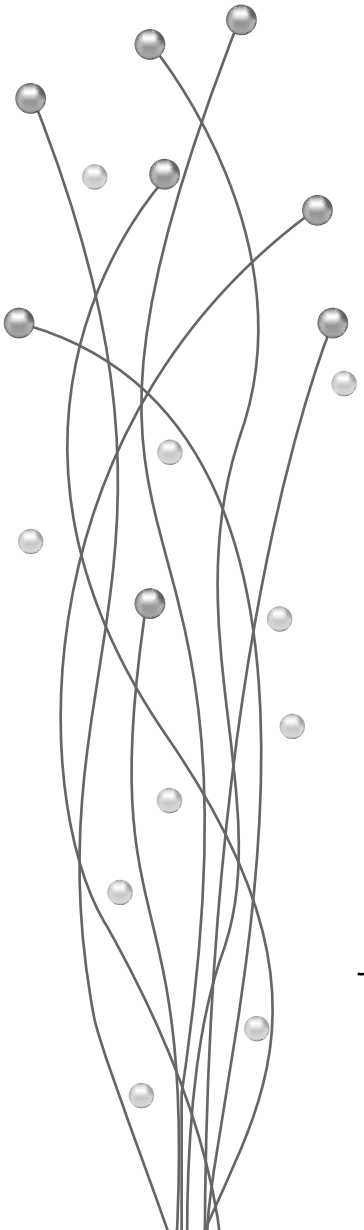

Silvia Bijland
Elsbet J Pieterman
Annemarie CE Maas
José WA van der Hoorn
Marjan J van Erk
Jan B van Klinken
Louis M Havekes
Ko Willems van Dijk
Hans MG Princen
Patrick CN Rensen

*Journal of Biological Chemistry 2010*

The PPARα activator fenofibrate efficiently decreases plasma triglycerides (TG), which is generally attributed to enhanced VLDL-TG clearance and decreased VLDL-TG production. However, since data on the effect of fenofibrate on VLDL production are controversial, we aimed to investigate in (more) detail the mechanism underlying the TG-lowering effect by studying VLDL-TG production and clearance using ApoE*3-Leiden.CETP mice, a unique mouse model for human-like lipoprotein metabolism. Male mice were fed a Western-type diet for 4 weeks, followed by the same diet without or with fenofibrate (30 mg/kg bodyweight/day) for 4 weeks. Fenofibrate strongly lowered plasma cholesterol (-38%; $P<0.001$) and TG (-60%; $P<0.001$) caused by reduction of VLDL. Fenofibrate markedly accelerated VLDL-TG clearance, as judged from a reduced plasma half-life of intravenously injected glycerol tri[$^3$H]oleate-labeled VLDL-like emulsion particles (-68%; $P<0.01$). This was associated with an increased post-heparin LPL activity (+110%; $P<0.0001$) and an increased uptake of VLDL-derived fatty acids by skeletal muscle, white adipose tissue and liver. Concomitantly, fenofibrate markedly increased the VLDL-TG production rate (+73%; $P<0.0001$) but not the VLDL-apoB production rate. Kinetic studies using [$^3$H]palmitic acid showed that fenofibrate increased VLDL-TG production by equally increasing incorporation of re-esterified plasma FA and liver TG into VLDL, which was supported by hepatic gene expression profiling data. We conclude that fenofibrate decreases plasma TG by enhancing LPL-mediated VLDL-TG clearance, which results in a compensatory increase in VLDL-TG production by the liver.

## Introduction

The lipid-lowering agent fenofibrate reduces plasma triglyceride (TG) levels and increases HDL-cholesterol (HDL-C) levels, which generates a less atherogenic lipid phenotype[120, 121]. Fenofibrate acts through activation of peroxisome proliferator-activated receptor alpha (PPARα) thereby altering the expression of genes involved in lipid metabolism[145, 146, 147]. Several mechanisms of action have been proposed through which fenofibrate lowers TG levels, including increased VLDL-TG clearance and decreased hepatic TG production[147].

VLDL-TG clearance is governed by lipoprotein lipase (LPL), of which the expression is potently induced by PPARα[64]. In addition, it has been shown that PPARα agonists down-regulate the expression of the LPL inhibitor apoCIII, and up-regulate the expression of the LPL activator apoAV[63]. Altogether this results in an increase in LPL-mediated lipolysis and clearance of VLDL. Indeed, two human studies show that fenofibrate increases the fractional catabolic rate (FCR) of VLDL-apoB in patients with hypertriglyceridemia without or with type 2 diabetes[148, 149], which is associated with increased LPL activity[148].

Hepatic VLDL production is dependent on the availability of fatty acids (FA) which is determined by *de novo* FA synthesis, FA/TG uptake from the circulation and β-oxidation of FA in the liver. PPARα has been shown to influence VLDL production in mice. PPARα deficiency in mice increased hepatic VLDL-TG production[150, 151], and the selective PPARα agonist Wy14643 lowered VLDL-TG production, at least in severely hypertriglyceridemic Angptl4 transgenic mice[152]. Limited data exist on the specific effect of fenofibrate on hepatic VLDL production. Although in vitro experiments using cultured hepatocytes show that fenofibrate, among other fibrates, decreases the production of both VLDL-TG and apoB[153, 154], in patients with the metabolic syndrome, fenofibrate treatment had no effect on the VLDL-apoB production rate[149].

Our aim was to investigate in detail the mechanism underlying the VLDL-TG lowering effect of fenofibrate *in vivo*. We used ApoE*3-Leiden. CETP (E3L.CETP) mice[108, 116] that express human CETP under control of its natural flanking regions[129]. These mice have an attenuated clearance of apoB-containing lipoproteins and, therefore, show a human-like lipoprotein profile on a cholesterol-rich Western-type diet[114, 116]. Our data show that treatment of

E3L.CETP mice on a Western-type diet with fenofibrate decreases plasma VLDL-TG as explained by increased VLDL-TG clearance resulting from enhanced LPL activity, but increases VLDL-TG production by increasing lipidation of apoB with TG that is equally derived from esterification of plasma FA and hepatic stores.

**Materials and Methods**

*Animals*

Hemizygous human CETP transgenic mice, expressing a human CETP minigene under the control of its natural flanking regions[129] were purchased from the Jackson Laboratory (Bar Harbor, ME) and crossbred with hemizygous E3L mice[108] at our Institutional Animal Facility to obtain E3L.CETP mice[116]. In this study, male E3L.CETP and wild-type mice (both C57Bl/6 background) were used, housed under standard conditions in conventional cages with free access to food and water. At the age of 12 weeks, mice were fed a semi-synthetic cholesterol-rich diet, containing 0.25% (w/w) cholesterol, 1% (w/w) corn oil and 14% (w/w) bovine fat (Western-type diet) (Hope Farms, Woerden, The Netherlands) for four weeks. Upon randomization according to plasma total cholesterol (TC) and triglyceride (TG) levels, mice received Western-type diet without or with 30 mg/kg bodyweight/day (0.03%, w/w) fenofibrate (Sigma, St. Louis, MO, USA). This dose is relevant to the human situation, as it corresponds with 210 mg fenofibrate per day for a 70 kg-person taking into account a 10-fold higher (drug) metabolism in mice. Experiments were performed after 4 h of fasting at 12:00 pm with food withdrawn at 8:00 am. The institutional Ethical Committee on Animal Care and Experimentation has approved all experiments.



*Plasma parameters*

Plasma was obtained via tail vein bleeding as described[130] and assayed for TC and TG, using the commercially available enzymatic kits 236691 and 11488872 (Roche Molecular Biochemicals, Indianapolis, IN, USA), respectively. The distribution of lipids over plasma lipoproteins was determined using fast protein liquid chromatography (FPLC). Plasma was pooled per group, and 50

µL of each pool was injected onto a Superose 6 PC 3.2/30 column (Äkta System, Amersham Pharmacia Biotech, Piscataway, NJ, USA) and eluted at a constant flow rate of 50 µL/min in PBS, 1 mM EDTA, pH 7.4. Fractions of 50 µL were collected and assayed for TC and TG as described above. HDL was isolated after precipitation of apoB-containing lipoproteins from 20 µL EDTA plasma by adding 10 µL heparin (LEO Pharma, The Netherlands; 500 U/mL) and 10 µL 0.2 M $MnCl_2$. The mixtures were incubated for 20 min at room temperature and centrifuged for 15 min at 13,000 rpm at 4°C. HDL-C was measured in the supernatant using enzymatic kit 236691 (Roche Molecular Biochemicals, Indianapolis, IN, USA).



*In vivo clearance of VLDL-like emulsion particles*

Glycerol tri[$^3$H]oleate (triolein, TO)- and [1α,2α(n)-$^{14}$C]cholesteryl oleate (CO)-double labeled VLDL-like emulsion particles (80 nm) were prepared as described by Rensen *et al*.[135]. In short, radiolabeled emulsions were obtained by adding 100 µCi of [$^3$H]TO and 10 µCi of [$^{14}$C]CO to 100 mg of emulsion lipids before sonication (isotopes obtained from GE Healthcare, Little Chalfont, U.K.). Mice were fasted for 4 h, sedated with 6.25 mg/kg acepromazine (Alfasan), 6.25 mg/kg midazolam (Roche), and 0.3125 mg/kg fentanyl (Janssen-Cilag) and injected with the radiolabeled emulsion particles (1.0 mg TG in 200 µL PBS) via the tail vein. At indicated time points after injection, blood was taken from the tail vein to determine the serum decay of [$^3$H]TO and [$^{14}$C]CO. At 30 min after injection, plasma was collected by orbital puncture and mice were sacrificed by cervical dislocation. Organs were harvested and saponified to determine [$^3$H]TO and [$^{14}$C]CO uptake.

*Hepatic lipase and lipoprotein lipase assay*

To liberate LPL from endothelium, 4 h fasted mice were injected intra-peritoneally with heparin (0.5 U/g bodyweight; Leo Pharmaceutical Products BV., Weesp, The Netherlands) and blood was collected after 20 min. Total hepatic lipase (HL) and LPL activity was analyzed as modified from Zechner[155]. In short, 10 µL of post-heparin plasma was incubated with 0.2 mL of TG substrate mixture containing triolein (4.6 mg/mL) and [3H]TO (2.5 µCi/mL) 130 for 30 min at 37°C in the presence or absence of 1 M NaCl, which completely inhibits

LPL activity, to estimate both the HL and LPL activity. The LPL activity was calculated as the fraction of total triacylglycerol hydrolase activity that was inhibited by the presence of 1 M NaCl and is expressed as the amount of free FA released per hour per mL of plasma.

*Hepatic VLDL-TG and VLDL-apoB production*

Mice were fasted for 4 h prior to the start of the experiment. During the experiment, mice were sedated as described above. At t=0 min blood was taken via tail bleeding and mice were i.v. injected with 100 µL PBS containing 100 µCi Trans$^{35}$S label to measure *de novo* total apoB synthesis. After 30 min, the animals received 500 mg of tyloxapol (Triton WR-1339, Sigma-Aldrich) per kg body weight as a 10% (w/w) solution in sterile saline, to prevent systemic lipolysis of newly secreted hepatic VLDL-TG[131]. Additional blood samples were taken at t=15, 30, 60, and 90 min after tyloxapol injection and used for determination of plasma TG concentration. At 120 min, the animals were sacrificed and blood was collected by orbital puncture for isolation of VLDL by density gradient ultracentrifugation. $^{35}$S-apoB was measured in the VLDL fraction after apoB-specific precipitation with isopropanol[134, 133, 132].



*Hepatic lipid analysis*

Livers were isolated and partly homogenized (30 sec at 5,000 rpm) in saline (approx. 10% wet w/v) using a mini-bead beater (Biospec Products, Inc., Bartlesville, OK, USA). Lipids were extracted as described[156] and separated by high performance thin layer chromatography (HPTLC). Lipid spots were stained with color reagent (5 g $MnCl_2.4H_2O$, 32 mL 95-97% $H_2SO_4$ added to 960 mL of $CH_3OH$:$H_2O$ 1:1 v/v) and quantified using TINA® version 2.09 software (Raytest, Straubenhardt, Germany).

*Hepatic gene expression analysis*

Total RNA was extracted from individual livers using RNA-Bee (Bio-Connect, Huissen, The Netherlands) and glass beads according to the manufacturer's instructions. The RNA was further purified using the nucleospin RNA II kit (Machery-Nagel, Düren, Germany) according to the manufacturer's instructions. The integrity of each RNA sample obtained was examined by

Agilent Lab-on-a-chip technology using a RNA 6000 Nano LabChip kit and a Bioanalyzer 2100 (Agilent Technologies, Amstelveen, The Netherlands). The Affymetrix 3′ IVT-Express labeling Kit (#901229) and the protocols optimized by Affymetrix were used to synthesize Biotin-labeled cRNA (from 100 ng of total RNA) for microarray hybridization. For the hybridization 15 µg cRNA was used for further fragmentation and finally 10 µg for the hybridizations. The quality of intermediate products (that is, biotin-labeled cRNA and fragmented cRNA) was again checked.

Microarray analysis was carried out using an Affymetrix technology platform and Affymetrix GeneChip® mouse genome 430 2.0 arrays. Briefly, fragmented cRNA was mixed with spiked controls and hybridized with murine GeneChip® 430 2.0 arrays. The hybridization, probe array washing and staining, and washing procedures were executed as described in the Affymetrix protocols, and probe arrays were scanned with a Hewlett-Packard Gene Array Scanner (ServiceXS, Leiden, The Netherlands). Quality control of microarray data was performed using BioConductor packages (including simpleaffy and affyplm), through the NuGO pipeline that is available as a Genepattern procedure on http://nbx2.nugo.org[157]. All samples passed the QC. Raw signal intensities (from CEL-files) were normalized using the GCRMA algorithm (gc-rma slow). For annotation of probes and summarization of signals from probes representing one gene the custom MNBI CDF-file was used (based on EntrezGene, version 11.0.2) (http://brainarray.mbni.med.umich.edu/Brainarray/Database/CustomCDF/cdfreadme.htm). This resulted in expression values for 16331 genes, represented by unique Entrez gene identifiers. Genes were filtered for expression above 5 in 3 or more samples, resulting in a set of 11587 genes that was used for further analysis. Gene expression data were log-transformed (base 2).

Statistical analysis on resulting data was performed using the moderated t-test (Limma: http://bioinf.wehi.edu.au/limma/) with correction for multiple testing[158]. Cut-off for statistically significant changes was set at corrected P-value (q-value) <0.05. In addition, T-profiler analysis[159] was performed using expression values corrected for mean expression in the control group. This analysis resulted in scores (t-scores) and significance values for functional gene sets and biological processes (based on gene ontology annotation). Gene sets

and biological processes with significant scores (>4 or <-4) in 5 or 6 animals per group were selected. A hierarchical clustering of these pathways and biological processes and their scores in all samples was generated in GenePattern (Broad Institute, MIT, USA)[160].

*Analysis of pathways contributing to hepatic VLDL-TG secretion*

Mice were fasted for 2 h with food withdrawn at 8:00 a.m. prior to the start of the experiment. During the experiment, mice were sedated as described above. At t=-2 h mice received a continuous i.v. infusion of $^{3}$H-labeled FA ([9,10(n)-$^{3}$H] palmitic acid in sterile saline with 2% BSA) at a rate of 100 µL/h (1.6 µCi/h). Blood samples were taken at t=-30 and 0 min, and the mice received 500 mg of tyloxapol (Triton WR-1339, Sigma-Aldrich) per kg body weight as a 10% (w/w) solution in sterile saline. Additional blood samples were taken at t=15, 30, 60, and 90 min after tyloxapol injection. All blood samples were taken using chilled paraoxon-coated capillaries.

Plasma TG and FA were determined as described above. The amount of $^{3}$H-activity in the FA and TG fraction of all plasma samples was determined after lipid extraction from plasma according to Bligh and Dyer[156]. The lipid fraction was dried under nitrogen, dissolved into chloroform/methanol (5:1 [vol/vol]) and subjected to thin layer chromatography (TLC) on silica gel plates by using hexane/diethylether/acetic acid (83:16:1, vol/vol/vol) as resolving solution. Triolein and palmitic acid were used as internal standards. Plasma samples obtained at t=-30 and 0 min were used to ensure steady state was reached for the specific activity (SA) of both [$^{3}$H]FA as well as [$^{3}$H]TG prior to the tyloxapol injection.

The production rate of [$^{3}$H]TG and TG was calculated from the slope of the curve from t=0 to t=90 min and expressed as dpm/min and nmol/min, respectively. As the production rate of [$^{3}$H]TG represents the rate of FA produced as TG, the production rate of FA within TG was calculated by multiplying the TG production rate by 3. This production rate represents the total rate of FA incorporation into VLDL-TG. The specific activity (SA) of the VLDL precursor pool (pTG) is given by the ratio of [$^{3}$H]TG production and TG production (Equation 1; production rate is indicated with an accent ‘). The relative contribution of plasma FA to the VLDL-TG precursor pool can

be estimated by dividing the SA of the pTG pool by the average SA of plasma FFA (Equation 2; average was taken over the time interval t=-30 to +60 min). Equation 2 gives the ratio of the rate of incorporation of FA in VLDL-TG, that is directly derived from plasma ($V_1$), and the total rate of FA incorporation into VLDL-TG ($V_1+V_2$; see also Fig. 6C); the contribution of liver TG to VLDL-TG is represented by $V_2$. By Equation 1 and 2 and the definition $(TG)' = V_1+V_2$, we obtain an expression for $V_1$ (Equation 3).

Equation 1: SA pTG = ([$^3$H]TG)′ / (TG)′ [dpm/μmol TG]

Equation 2: Contribution of plasma FA to VLDL-TG production
= (SA pTG / SA-$FA_{t-30-+60}$)*100 (%)

Equation 3: $V_1$ = ([$^3$H]TG)′ / SA-$FA_{t-30-+60}$ [nmol/min]



*Statistical analysis*

All data are presented as means ± SEM unless indicated otherwise. Data were analyzed using the unpaired Student's t test. P-values less than 0.05 were considered statistically significant.

**Results**

*Fenofibrate decreases VLDL and increases HDL in E3L.CETP mice*

To confirm that fenofibrate decreases VLDL-TG in E3L.CETP mice, mice were fed a cholesterol-rich Western-type diet for 4 weeks (t0). Mice were randomized, and fed the same diet without (time-matched control group) or with fenofibrate (30 mg/kg bodyweight/day) for another 4 weeks (t4). At both t0 and t4, plasma was assayed for lipids (Fig. 1). As compared to the time-matched control group, fenofibrate decreased plasma cholesterol (-38%; 5.0±0.2 versus 8.0±0.7 mmol/L; P<0.001) (Fig. 1A). Lipoprotein profiling showed that this was the net effect of a large reduction of VLDL-C (~85%) and an increase in HDL-C (~55%) (Fig. 1B). The increase in HDL-C was confirmed by directly measuring HDL-C in plasma after precipitation of apoB-containing lipoproteins (+52%; 2.1±0.1 versus 1.4±0.1 mmol/L; P<0.001) (Fig. 1C).

The decrease in VLDL-C was accompanied by a large reduction in plasma TG (-60%; 0.7±0.2 versus 1.9±0.2; P<0.001) (Fig. 1D), which was specific for VLDL (not shown).

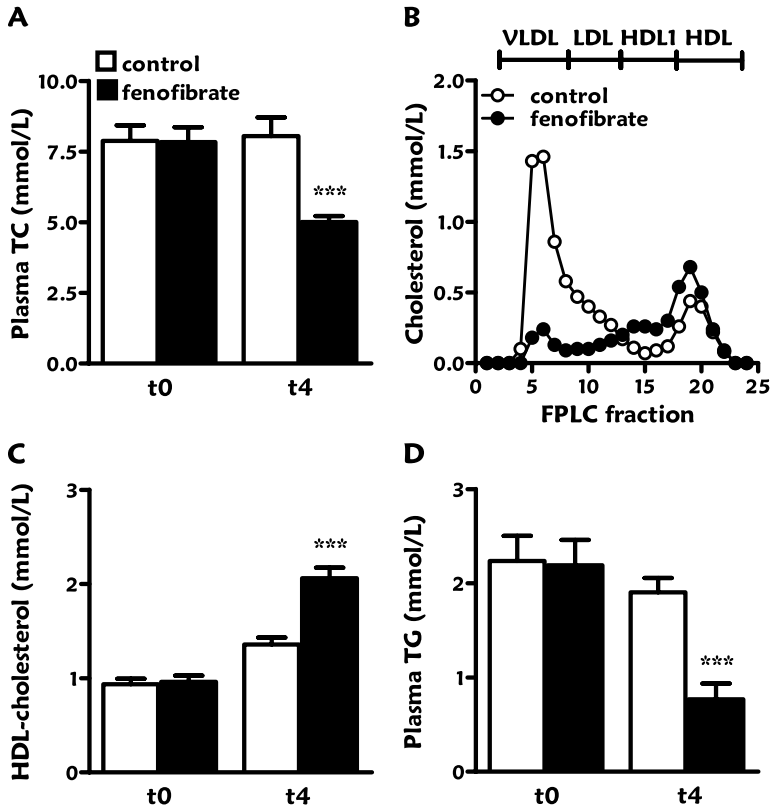


**Figure 1. Fenofibrate decreases VLDL-TG and VLDL-cholesterol in E3L.CETP mice.** Mice received a Western-type diet without and with fenofibrate (0.03% w/w). At baseline (t0) and after 4 weeks of intervention (t4), 4 h-fasted blood was taken and plasma was assayed for total cholesterol (A). After 4 weeks of intervention cholesterol distribution over lipoproteins was determined (B). At t0 and t4, HDL-cholesterol (C) and TG (D) were also assayed. Data are means ± SEM (n=8). ***P<0.001.



*Fenofibrate increases VLDL-TG clearance by enhancing VLDL-TG hydrolysis and hepatic uptake of VLDL remnants*

Plasma VLDL-TG levels are determined by the balance between VLDL-TG production and VLDL-TG clearance. To evaluate whether an increased VLDL-TG clearance may contribute to the fenofibrate-mediated reduction in VLDL-TG levels, control and fenofibrate-treated E3L.CETP mice were injected with

[$^{3}$H]TO- and [$^{14}$C]CO-labeled VLDL-like emulsion particles and the plasma clearance was determined (Fig. 2). Fenofibrate reduced the plasma half-life of [$^{3}$H]TO as compared to time-matched control mice by -68% (t1/2 = 6.8±0.9 min versus 21.0±6.3 min; P<0.005) (Fig. 2A) as reflected by an increase in uptake of [$^{3}$H]TO-derived activity by liver, skeletal muscle and white adipose tissue (Fig. 2B). Likewise, fenofibrate reduced the plasma half-life of [$^{14}$C]CO by -80% (t1/2 = 11.0±1.7 min versus 56.6±11.7 min; P<0.005) (Fig 2C), as mainly reflected by an increased uptake of [$^{14}$C]CO by the liver (Fig. 2D).



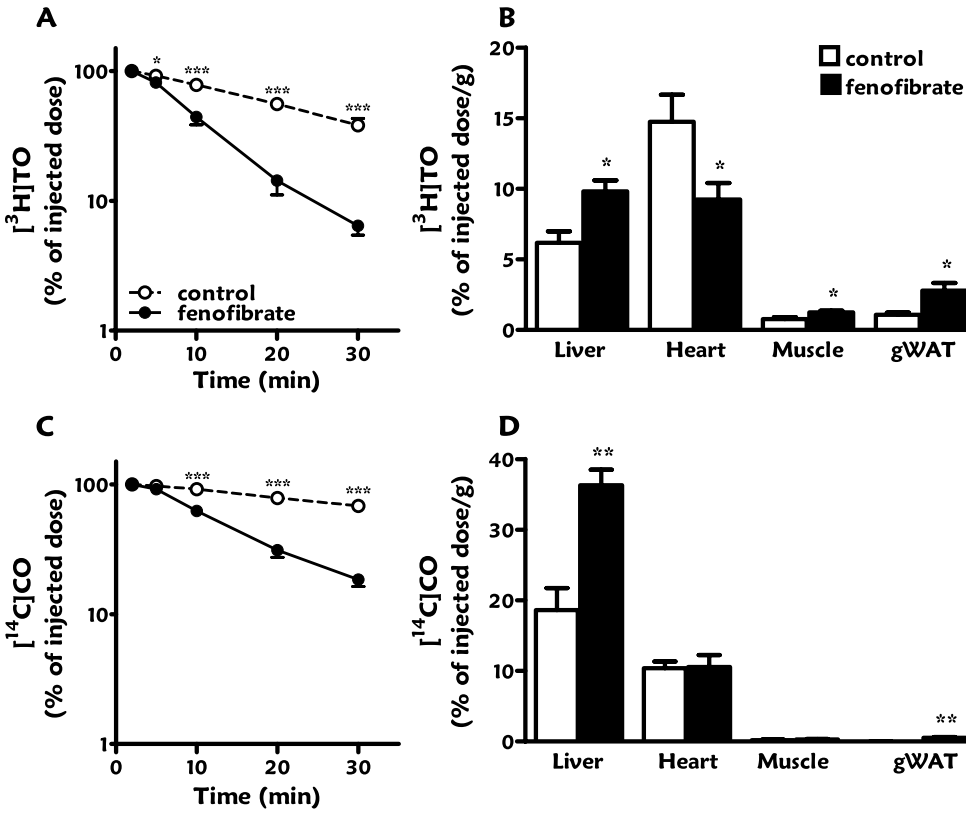


**Figure 2. Fenofibrate increases the clearance of VLDL-like emulsion particles in E3L.CETP mice.**

Mice received a Western-type diet without or with fenofibrate (0.03% w/w). After 4 h fasting, mice were injected with [$^{3}$H]TO and [$^{14}$C]CO-labeled VLDL-like emulsion particles (1 mg TG) and plasma samples were taken at indicated time points to determine the plasma clearance of [$^{3}$H]TO (A) and [$^{14}$C]CO (C). At 30 min after injection, the uptake of $^{3}$H-activity (B) and $^{14}$C-activity (D) was determined in liver, heart, skeletal muscle and gonadal white adipose tissue (gWAT). Data are means ± SEM (n=5). *P<0.05; **P<0.01; ***P<0.001.

To determine whether the accelerated clearance of VLDL-like emulsion particles was due to an increase in the lipolytic activity of plasma, HL and LPL activity was determined in plasma after heparin injection (Fig. 3). Fenofibrate increased postheparin plasma HL activity by +67% (12.3±1.4 versus 7.4±0.9 μmol FFA/h/mL; P<0.0001) as well as postheparin plasma LPL activity by +110% (25.1±3.1 versus 12.0±2.5 μmol FFA/h/mL; P<0.0001).

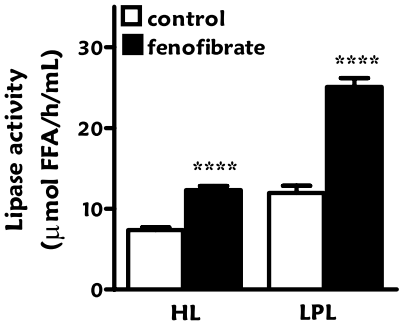


**Figure 3. Fenofibrate increases hepatic lipase and lipoprotein lipase activity in postheparin plasma of E3L.CETP mice.**
Mice received a Western-type diet without or with fenofibrate (0.03% w/w). After 4 h fasting, heparin was injected and postheparin plasma was collected. Plasma was incubated with a [$^{3}$H] TO-containing substrate mixture in the absence or presence of 1 M NaCl, to estimate both the HL and LPL activity. Data are means ± SEM (n=8). ****P<0.0001



*Fenofibrate increases VLDL-TG production but not VLDL-apoB production*

To determine the effect of fenofibrate on VLDL-TG production by the liver, control and fenofibrate-treated E3L.CETP mice were injected with Trans$^{35}$S and tyloxapol and VLDL production was determined (Fig. 4). Surprisingly, fenofibrate caused an increase in the accumulation of plasma TG (Fig. 4A). The VLDL-TG production rate, as determined from the slope of the curve, was increased by +73% (11.8±0.6 versus 6.8±0.5 μmol TG/h; P<0.0001) (Fig. 4B). The rate of VLDL-apoB production was not altered (Fig. 4C), indicating that fenofibrate increases the lipidation of VLDL particles in the liver rather than the number of VLDL particles secreted from the liver. Fenofibrate thus increased the amount of TG per mg of VLDL protein by +58% (48.3±4.0 versus 30.9±2.7 μmol/mg; P<0.01) (Fig. 4D).

To exclude the possibility that the paradoxical increase VLDL-TG production was specific for E3L.CETP mice, we also determined the effect of fenofibrate on VLDL production in wild-type mice (Fig. 5). Like in E3L.CETP mice, fenofibrate increased the VLDL-TG production rate (10.0±0.3 versus 7.3±0.3 μmol TG/h; P<0.0001) (Fig. 5A, B). Furthermore, fenofibrate slightly

decreased the VLDL-apoB production rate (32.2±1.7 versus 37.3±1.6; P<0.05) (Fig. 5C) and increased the amount of TG per mg of VLDL protein (28.4±0.7 versus 25.4±0.8 μmol/mg; P<0.05) (Fig. 5D).



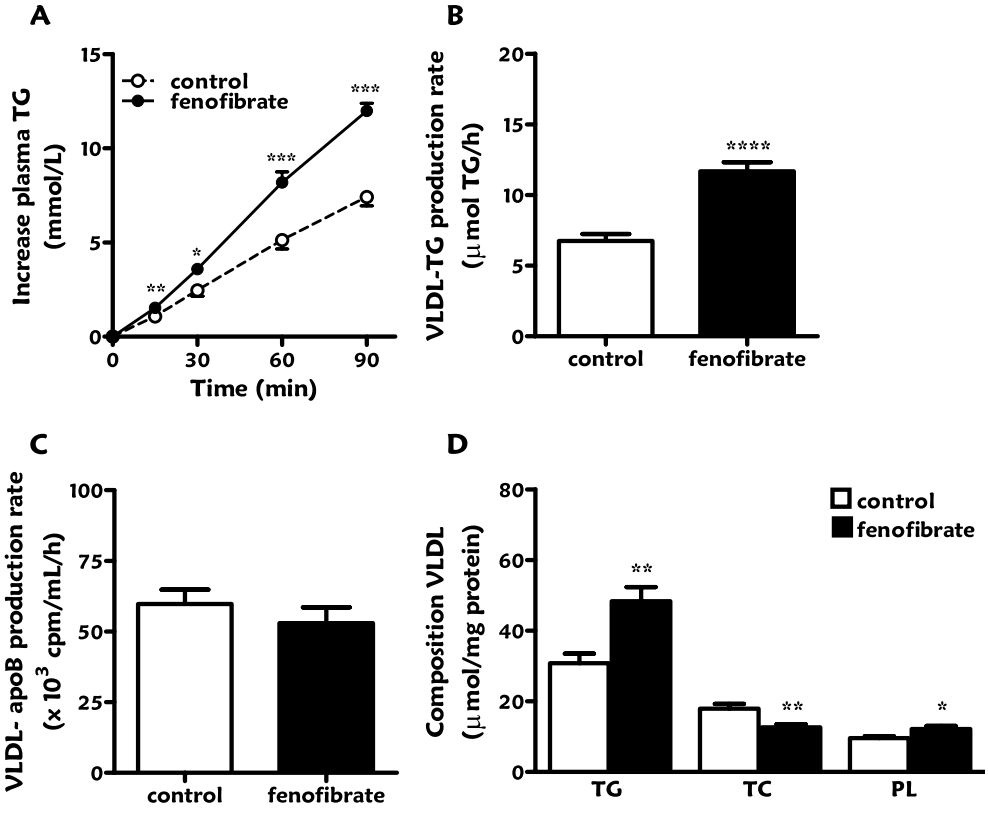


**Figure 4. Fenofibrate increases hepatic VLDL-TG production in E3L.CETP mice.**
Mice received a Western-type diet without or with fenofibrate (0.03% w/w). After 4 h fasting, mice were consecutively injected with Trans$^{35}$S label (t=-30 min) and tyloxapol (t=0 min) and blood samples were drawn up to 90 min after tyloxapol injection. Plasma TG concentrations were determined and plotted as the increase in plasma TG as compared to baseline (A). The rate of TG production was calculated from the slopes of the curves from the individual mice (B). After 120 min, the total VLDL fraction was isolated by ultracentrifugation and the rate of newly synthesized VLDL-$^{35}$S-apoB (C) as well as the amount of triglycerides (TG), total cholesterol (TC) and phospholipids (PL) per mg VLDL protein (D) was measured. Data are means ± SEM (n=9). *P<0.05; **P<0.01; ***P<0.001; ****P<0.0001

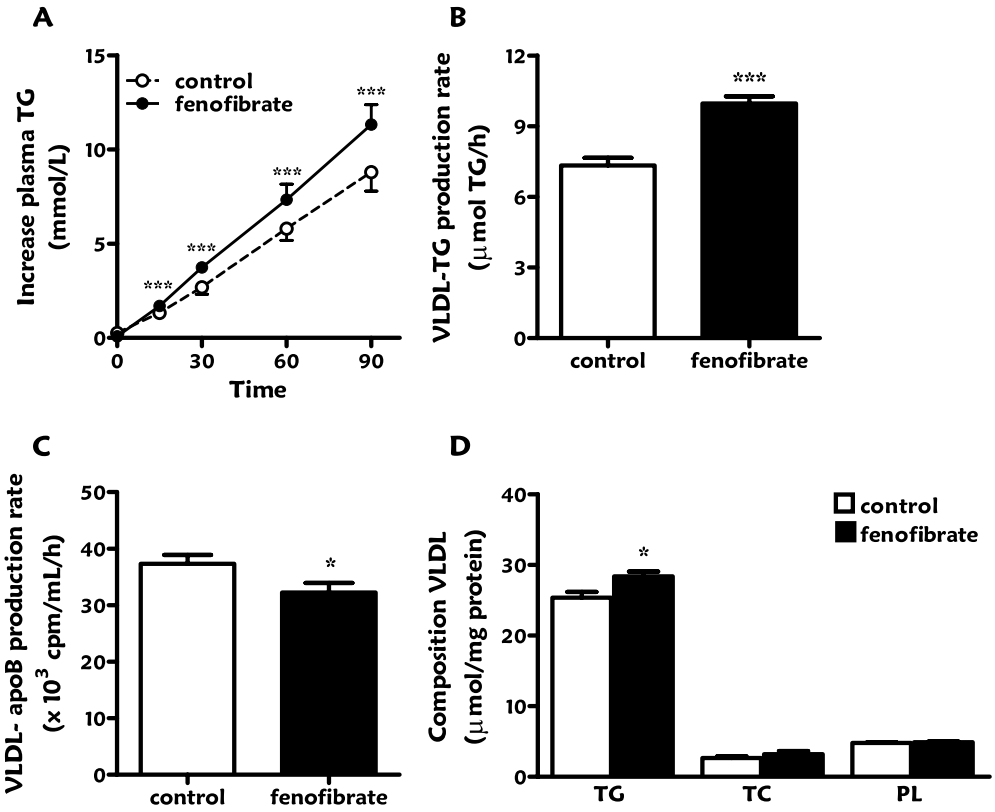




**Figure 5. Fenofibrate increases hepatic VLDL-TG production in wild-type mice.** Mice received a Western-type diet without or with fenofibrate (0.03% w/w). After 4 h fasting, mice were consecutively injected with Trans$^{35}$S label and tyloxapol and blood samples were drawn up to 90 min after tyloxapol injection. Plasma TG concentrations were determined and plotted as the increase in plasma TG (A). The rate of TG production was calculated from the slopes of the curves from the individual mice (B). After 120 min, the total VLDL fraction was isolated by ultracentrifugation and the rate of newly synthesized VLDL-apoB (C) as well as the amount of triglycerides (TG), total cholesterol (TC) and phospholipids (PL) per mg protein (D) was measured. Data are means ± SD (n=8-10). *P<0.05; ***P<0.001.

*Fenofibrate decreases hepatic lipid content*

Since an increase in VLDL production may result from an increased hepatic TG content[161, 27], we determined the effect of fenofibrate on hepatic lipid levels (Fig. 6). However, fenofibrate in fact tended to reduce the hepatic TG content by -20% (59.9±6.5 versus 74.5±7.2 mg/mg protein; P=0.162) (Fig. 6A). In addition, fenofibrate decreased the hepatic free cholesterol content by -19%

(11.7±0.3 versus 14.3±0.6 mg/mg protein; P<0.01) (Fig. 6B) as well as the hepatic cholesteryl ester content by -51% (11.9±0.6 versus 24.6±1.4; P<0.0001) (Fig. 6C).

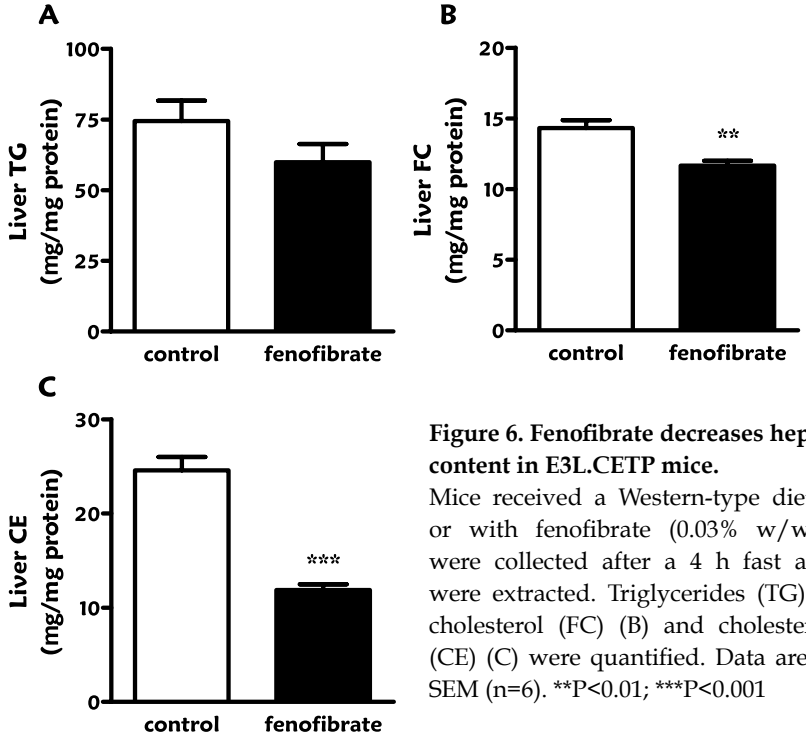


**Figure 6. Fenofibrate decreases hepatic lipid content in E3L.CETP mice.**
Mice received a Western-type diet without or with fenofibrate (0.03% w/w). Livers were collected after a 4 h fast and lipids were extracted. Triglycerides (TG) (A), free cholesterol (FC) (B) and cholesteryl esters (CE) (C) were quantified. Data are means ± SEM (n=6). **P<0.01; ***P<0.001

*Fenofibrate increases expression of hepatic genes involved in FA uptake and transport*
To further investigate the mechanism(s) by which fenofibrate affects VLDL-TG metabolism, we determined the hepatic expression profile of 16331 well characterized mouse genes. As compared to the control group, fenofibrate resulted in 2924 differentially expressed genes. Pathway analysis, based on gene ontology annotation, revealed that fenofibrate up-regulated gene sets related to PPAR activation and lipid/energy metabolism and down-regulated gene sets related to inflammation (Supplemental Fig. 1).

A selection of genes involved in VLDL metabolism is depicted in Table 1. As expected, fenofibrate upregulated genes involved in FA oxidation including *Cpt1a*, *Cpt1b, Acox1, Acaa1a, Acaa1b* and *Acaa2*. In line with our observation that fenofibrate increases VLDL-TG clearance and LPL activity in postheparin plasma, fenofibrate largely upregulated *Lpl* and slightly decreased *Apoc3*.

Fenofibrate did not largely affect FA/TG synthesis genes, apart from increasing Dgat1. Rather, fenofibrate upregulated genes involved in FA uptake (*Cd36, Ldlr*), FA transport (*Slc27a1, Slc27a2, Slc27a4* and *Slc27a5*), FA binding (*Fabp1, Fabp2, Fabp4* and *Fabp7*), FA activation (*Acsl1, Acsl3, Acsl4* and *Acsl5*) and VLDL assembly (*Mttp*). Taken together, these data suggest that fenofibrate increases hepatic VLDL-TG secretion through increased hepatic uptake, intracellular trafficking and secretion of excess FA derived from extrahepatic LPL-derived lipolysis, rather than by increased *de novo* FA synthesis.

**Table 1.** Effect of fenofibrate on hepatic expression of genes involved in VLDL metabolism

| Protein | Gene | Fold change (vs control) | Corrected P-value |
|---|---|---|---|
| **FA oxidation** | | | |
| CPT1a | *Cpt1a* | **+1.28** | **0.010** |
| CPT1b | *Cpt1b* | **+6.08** | **<0.001** |
| ACO | *Acox1* | **+1.51** | **<0.001** |
| Thiolase | *Acaa1a* | **+1.89** | **<0.001** |
| Thiolase | *Acaa1b* | **+1.29** | **<0.001** |
| Thiolase | *Acaa2* | **+1.21** | **<0.001** |
| **Lipolysis** | | | |
| LPL | *Lpl* | **+4.63** | **<0.001** |
| ApoCI | *Apoc1* | -1.03 | 0.235 |
| ApoCII | *Apoc2* | -1.04 | 0.402 |
| ApoCIII | *Apoc3* | **-1.08** | **0.014** |
| ApoAV | *Apoa5* | -1.15 | 0.065 |
| GPIHBP1 | *Gpihbp1* | 1.08 | 0.344 |
| **FA/TG synthesis** | | | |
| SREBP1a/c | *Srebf1* | -1.11 | 0.350 |
| FAS | *Fasn* | +1.90 | 0.068 |
| DGAT1 | *Dgat1* | **+1.48** | **0.002** |
| DGAT2 | *Dgat2* | **-1.17** | **0.046** |
| SCD1 | *Scd1* | +1.24 | 0.207 |
| SCD2 | *Scd2* | +1.09 | 0.247 |

| Protein | Gene | Fold change (vs control) | Corrected P-value |
|---|---|---|---|
| **FA uptake and transport** | | | |
| FATPa1 | *Slc27a1* | **+4.59** | **<0.001** |
| FATPa2 | *Slc27a2* | **+1.15** | **0.001** |
| FATPa4 | *Slc27a4* | **+3.30** | **<0.001** |
| FATPa5 | *Slc27a5* | -1.07 | 0.181 |
| CD36 | *Cd36* | **+3.42** | **<0.001** |
| LDLR | *Ldlr* | **+1.52** | **0.016** |
| PCSK9 | *Pcsk9* | +1.64 | 0.110 |
| **FA binding and activation** | | | |
| FABP1 | *Fabp1* | **+1.10** | **0.012** |
| FABP2 | *Fabp2* | **+1.36** | **0.006** |
| FABP4 | *Fabp4* | **+2.19** | **<0.001** |
| FABP6 | *Fabp6* | +1.05 | 0.412 |
| FABP7 | *Fabp7* | **-3.48** | **<0.001** |
| ACSL1 | *Acsl1* | **+2.15** | **<0.001** |
| ACSL3 | *Acsl3* | **+3.07** | **<0.001** |
| ACSL4 | *Acsl4* | **+1.58** | **<0.001** |
| ACSL5 | *Acsl5* | **+1.49** | **0.001** |
| **VLDL assembly** | | | |
| ApoB | *Apob* | -1.02 | 0.374 |
| ApoBEC | *Apobec1* | 1.00 | 0.515 |
| MTP | *Mttp* | **+1.42** | **<0.001** |

Mice received a Western-type diet without or with fenofibrate (0.03% w/w). Livers were collected after a 4 h fast, total RNA was extracted, and gene expression analysis was performed using Affymetrix GeneChip mouse genome 430 2.0 arrays. Data are expressed as mean fold change as compared to the control group (n=6 per group). Values in bold are considered significant (corrected P-value or q-value <0.05).

*Fenofibrate increases VLDL-TG production by equally increasing incorporation of re-esterified plasma FA and liver-derived TG into VLDL*

We next investigated whether the increase in VLDL-TG production is solely the result of an increased flux of plasma FA towards the liver, and subsequent incorporation into nascent VLDL after re-esterification into TG. Hereto, we continuously infused [$^3$H]palmitic acid while measuring the linear accumulation of VLDL-derived TG and [$^3$H]TG in plasma after injection of tyloxapol (Fig. 7).

Fenofibrate not only increased the production rate of both VLDL-TG (+31%; P<0.05) (Fig. 7A), which is consistent with Fig 4A, but also increased the production rate of VLDL-[$^3$H]TG (+63%; P<0.05) (Fig. 7B). Fig. 7C schematically represents the model used to determine the contribution of plasma FA ($V_1$) as compared to contribution of liver TG ($V_2$) to the VLDL-TG production ($V_1$ + $V_2$). Calculating the ratio of $V_1$ over $V_1$+$V_2$ shows that the estimated contribution of re-esterification of plasma FA to the total VLDL production was

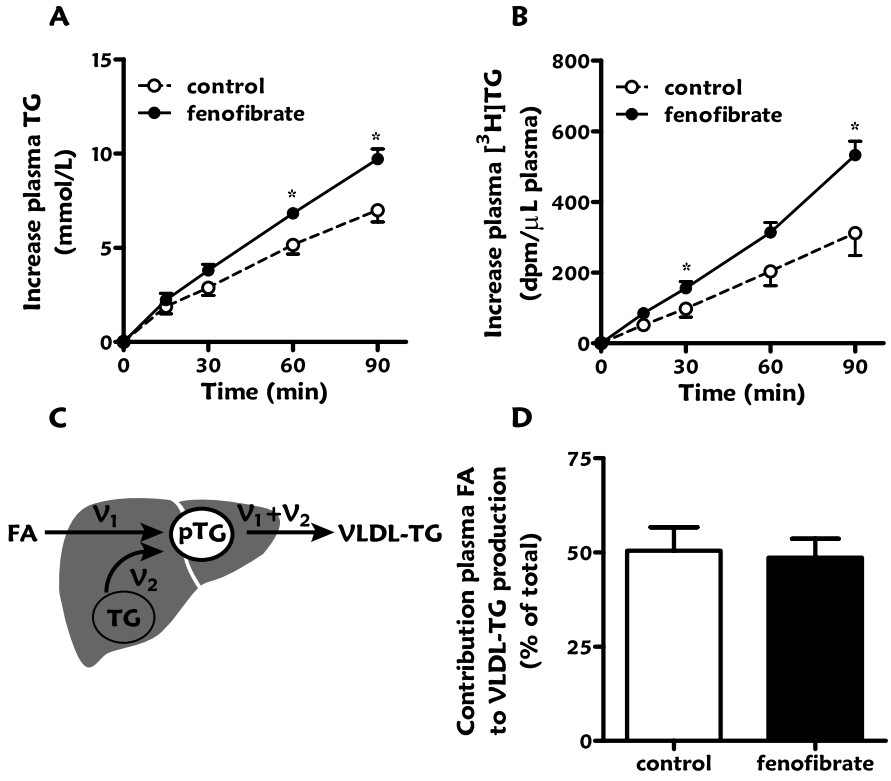




**Figure 6. Fenofibrate equally increases the incorporation of both plasma FA and liver TG in VLDL-TG in E3L.CETP mice.**

Mice received a Western-type diet without or with fenofibrate (0.03% w/w). Mice were continuously infused with [$^3$H]palmitic acid after 2 h of fasting, and received tyloxapol after 4 h of fasting, and the increase in plasma TG (A) and [$^3$H]TG (B) was subsequently measured. According to the equations as schematically represented (C), the relative contribution of re-esterified plasma FA to VLDL-TG production was calculated (D). Data are means ± SEM (n=5). *P<0.05. V1, incorporation rate of plasma FA in VLDL-TG; V2, incorporation rate of liver TG in VLDL-TG; pTG, VLDL precursor pool.

equal for both control and fenofibrate treated mice (46±15% vs 49±11%; n.s.) (Fig. 7D). These data imply that fenofibrate increases VLDL-TG production by equally increasing incorporation of re-esterified plasma FA and liver-derived TG. Indeed, fenofibrate increased VLDL-TG production by an increased incorporation of plasma FA (+38%) as well as liver TG (+25%).

**Discussion**

We investigated the mechanisms underlying the effect of fenofibrate on VLDL metabolism. Our data show that fenofibrate decreases plasma TG levels in E3L.CETP mice, which is solely explained by an increased LPL-mediated TG clearance from plasma. Despite the generally accepted dogma that fenofibrate reduces VLDL-TG production thereby contributing to the plasma TG-lowering effect, fenofibrate in fact increases VLDL-TG production as caused in part by an increased flux of FA to the liver.



In this study, we have used E3L.CETP mice to study the effect of fenofibrate on VLDL metabolism, at a dose relevant to clinical practice in humans. We have previously observed that these mice show a human-like response to drug interventions aimed at reducing plasma levels of apoB-containing lipoproteins, including atorvastatin[118], niacin[117] and fenofibrate[114]. In the present study, we confirmed that fenofibrate effectively reduces plasma TG levels (-60%) and cholesterol levels (-38%), which was the combined result of a decrease in VLDL-C (~85%) and an increase in HDL-C (~55%). Recently, we have shown that the HDL-raising effect of fenofibrate is explained by a reduction in hepatic cholesterol levels, which decreases hepatic CETP expression and consequently reduces plasma CETP levels[114], an effect that has also been observed in humans[162].

Since plasma VLDL-TG levels are determined by the balance between VLDL-TG production and VLDL-TG clearance, we evaluated the individual contribution of both pathways to the TG-lowering effect of fenofibrate. We observed that the TG-lowering effect of fenofibrate can be fully explained by an accelerated TG clearance from plasma. Fenofibrate appeared to increase the total triacylglycerol hydrolase capacity of plasma, as evidenced by increased HL activity (+67%) and LPL activity (+110%) in post-heparin plasma, which is

likely due to increased whole-body expression of the lipase genes as reflected by a large 4.6-fold increase in hepatic Lpl mRNA. It is likely that fenofibrate further increases TG clearance by indirectly enhancing LPL activity via reduced hepatic mRNA expression of the main LPL inhibitor apoCIII. These changes are consistent with previous observations on the effects of fibrates on LPL[64] and apoCIII[63] in rodents. Likewise, fibrates have been shown to increase LPL activity[148, 163] and decrease apoCIII synthesis[63, 149, 164] in humans.

In contrast to the generally accepted view that a reduction of the VLDL-TG production contributes to the TG-lowering effect of fenofibrate, we now clearly demonstrate that fenofibrate in fact increases the VLDL-TG production in E3L.CETP mice. To exclude that this effect would be genotype-specific, we confirmed that fenofibrate increases VLDL-TG production in wild-type mice. In both mouse types, fenofibrate did not increase the VLDL-apoB production rate, implying that fenofibrate increases the lipidation of VLDL particles rather than affecting the VLDL particle production rate.

It is tempting to speculate about the mechanism(s) underlying the increasing effect of fenofibrate on VLDL-TG production. VLDL-TG production is determined by the balance between hepatic FA β-oxidation, FA/TG entry into the liver, hepatic FA/TG synthesis and hepatic TG stores. Fenofibrate increased hepatic genes involved in FA β-oxidation, which was expected from its PPARα agonistic activity[165, 166, 167]. Affymetrix analysis indicated that hepatic genes involved in FA/TG synthesis were generally not affected. However, many genes involved in FA uptake and transport (*Slc27a, Cd36, Ldlr*), FA binding and activation (*Fabp, Acsl*) and FA esterification (*Dgat1*) were upregulated, in addition to *Mttp* that is crucial for VLDL assembly. In general, these data are in line with previous reports that PPARα induces genes involved in TG synthesis and apoB lipidation[168, 169]. Collectively, these data suggest that fenofibrate may increase the uptake of FA by the liver, followed by the intrahepatic binding, activation, esterification, and ultimately secretion of FA as VLDL-TG. Indeed, by performing kinetic analyses using intravenously injected $^{3}$H-FA, we demonstrated that fenofibrate increased the incorporation rate of plasma FA into nascent VLDL-TG. At the same time, fenofibrate also increased the incorporation rate of a hepatic pool of FA/TG into nascent VLDL-TG. The observed tendency towards a reduction in liver TG content can

thus be explained by a combination of an increased FA β-oxidation as well as an increased secretion of hepatic TG stores incorporated in VLDL.

Taken together, the effect of fenofibrate with respect to reduction of plasma TG levels is primarily caused by an enhanced TG hydrolysis in the capillary bed of LPL-expressing tissues such as skeletal muscle and white adipose tissue. Liberated FA are not only taken up by these tissues, but also redirected towards the liver as bound to albumin[136]. An increased FA flux towards the liver may then drive increased lipidation of nascent VLDL particles without influencing the VLDL particle production rate as judged from an unaltered VLDL-apoB production rate. Although the effect of fenofibrate on the VLDL-TG production rate has not been studied in humans, fenofibrate has been shown to reduce VLDL-apoB levels without affecting the VLDL-apoB production rate[170, 149], which is agreement with our data.



So, how can we reconcile our data with the accepted dogma that fenofibrate would decrease VLDL-TG production? First, it has been generally assumed that, via increased FA β-oxidation, fenofibrate reduces the amount of FA available for VLDL-TG output[147]. However, we previously showed that specific inhibition of FA β-oxidation using methyl palmoxirate does not affect VLDL-TG production despite increasing hepatic TG content[171]. Moreover, this simplified assumption does not take into account that fenofibrate in fact increases the liver-directed flux of FA/TG. Second, a few models have suggested that fenofibrate reduces VLDL-TG production[150, 151, 172, 173]. For example, mice deficient for PPARα have increased VLDL-TG production[150, 151]. However, this could easily be caused by compensatory changes resulting from complete deficiency of PPARα. It would thus be more relevant to study PPARα activation instead of complete PPARα deficiency. Activation of PPARα has been shown to inhibit VLDL-TG secretion by primary rat hepatocytes in vitro[172]. This can indeed be explained by an increase in FA β-oxidation, but it should be realized that such a study set-up obviously does not take into account an increased FA flux from peripheral tissues towards hepatocytes. A single *in vivo* study in mice, which were deficient for the LDL receptor (LDLr) and fed a high fat diet, showed that fenofibrate reduced VLDL-TG production[173]. It is likely that the absence of the LDLr may have prevented the efficient hepatic uptake of VLDL remnants in that study. We observed that fenofibrate increased both the plasma clearance

and liver uptake of VLDL core remnants. Furthermore, fenofibrate decreased the hepatic cholesterol content (which was also observed in the LDLr-deficient mice[173] and resulted in an expected increase in hepatic LDLr expression in our study. It is thus conceivable that the LDLr plays an important role in the influx of remnant-TG upon treatment with fenofibrate. In addition, an alternative uptake route of VLDL remnants, in case of LDLr-deficiency, may result in a different intracellular distribution of remnant-derived TG that is a less accessible source for VLDL-TG production.

In conclusion, our data demonstrate that fenofibrate decreases plasma TG by enhancing LPL-mediated VLDL-TG clearance. As a consequence, fenofibrate increases VLDL-TG production by the liver as caused by 1) enhanced hepatic FA/TG uptake resulting from strongly accelerated peripheral LPL-mediated VLDL-TG hydrolysis, and 2) increased incorporation of TG from a separate pool in the liver resulting from *de novo* FA/TG synthesis and/or lipoprotein uptake. Since the primary mechanism of action underlying the lipid-lowering effect of fibrates (i.e. increased LPL-mediated VLDL-TG clearance) is different as compared to that of statins (i.e. decreased hepatic VLDL-TG and VLDL-C output), future studies addressing the combined action of these two drug classes on lipid metabolism and their combined effect on atherosclerosis development are thus warranted.



**Acknowledgements**

This work was performed within the framework of the Leiden Center for Cardiovascular Research LUMC-TNO and supported by grants from the Nutrigenomics Consortium/Top Institute Food and Nutrition (TiFN), the Center for Medical Systems Biology (CMSB) and the Netherlands Consortium for Systems Biology (NCSB), within the framework of the Netherlands Genomics Initiative (NGI/NWO), the Netherlands Organization for Health Care Research Medical Sciences (ZON-MW project nr. 948 000 04), the Netherlands Organization for Scientific Research (NWO VIDI grant 917.36.351 to PCN Rensen). PCN Rensen is an Established Investigator of the Netherlands Heart Foundation (2009T038). We thank Marian Bekkers, Simone van der Drift-Droog and Karin Toet for excellent technical assistance.

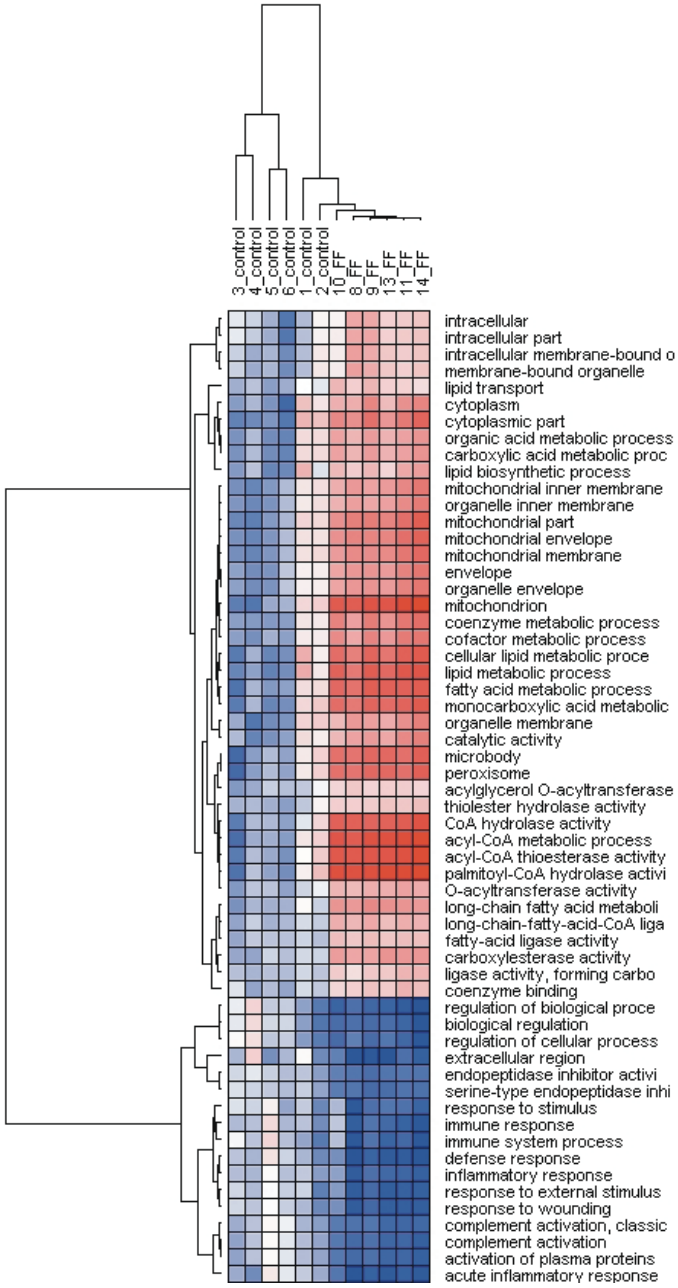


**Supplemental Figure 1. Hierarchical clustering of scores for biological processes.**
T-profiler analysis was performed using expression values corrected for mean expression in the control group. Pathways and biological processes with significant scores (>4 or <-4) in 5 or 6 animals of the fenofibrate group were selected. A hierarchical clustering of these pathways and biological processes and their scores in all samples was generated in GenePattern (Broad Institute, MIT, USA). Red indicates positive score (majority of genes in set are up-regulated), blue indicate negative score (majority of genes in set are down-regulated).

# CHAPTER 4

## Rifampicin decreases plasma cholesterol by impairing HDL and VLDL patricle production in ApoE*3-Leiden.CETP mice

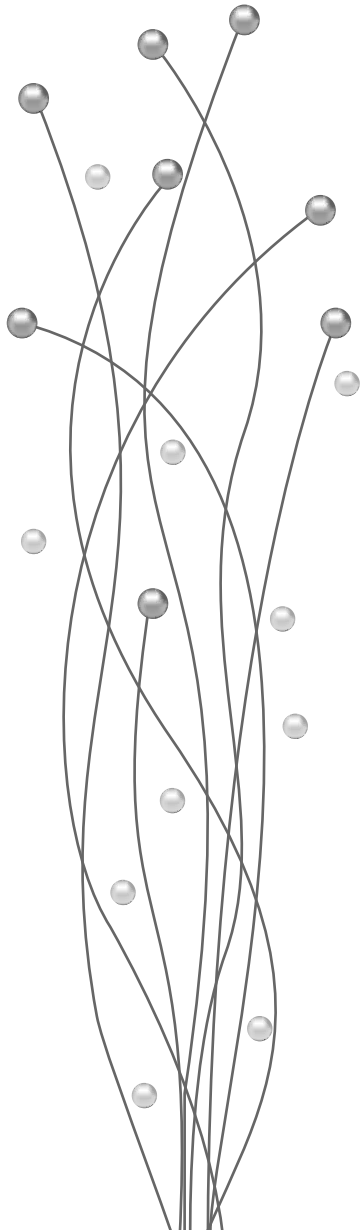

Silvia Bijland*
Willeke de Haan*
Johannes WA Smit
Louis M Havekes
Hans MG Princen
Ko Willems van Dijk
Patrick CN Rensen

* both authors contributed equally

*Manuscript in preparation*

Rifampicin, an antibiotic used for the treatment of tuberculosis, is associated with disturbances in hepatic and plasma lipid metabolism. The aim of this study was to evaluate the effect of rifampicin on lipoprotein metabolism in ApoE*3-Leiden.CETP mice, a well-established model for human-like lipoprotein metabolism, and to investigate the underlying mechanisms. Female mice were fed a diet with increasing amounts of rifampicin (up to 0.10% w/w). Rifampicin dose-dependently decreased plasma cholesterol, explained by a reduction in both HDL-C and VLDL-C. The reduction in HDL-C was caused by a reduction in hepatic HDL particle synthesis (reduction in apoAI) and HDL maturation (reduction in LCAT, HL and PLTP), most likely caused by rifampicin-mediated PXR activation. The reduction in VLDL-C was caused by a reduction in hepatic VLDL particle synthesis, despite clear induction of hepatic steatosis. We conclude that rifampicin dose-dependently reduces plasma HDL-C by inhibiting HDL particle synthesis and maturation and reduces plasma VLDL-C by inhibiting VLDL particle synthesis.

## Introduction

Rifampicin (RIF) is an antibiotic used for the treatment of tuberculosis[174]. Treatment with RIF has been associated with hepatic lipid accumulation in some clinical cases[175, 176, 177]. In addition, RIF has been reported to cause hyperlipidemia in humans[178]. RIF is an agonist of the pregnane X receptor (PXR)[179], which is a xenochemical sensing nuclear receptor that regulates the expression of genes involved in drug and xenobiotic metabolism. PXR activation in rodents induces hepatic steatosis[82, 180, 181] associated with increased expression of the fatty acid transporter CD36 and lipogenic genes including stearoyl CoA desaturase-1 (SCD1)[82]. In addition PXR activation has been shown to reduce hepatic b-oxidation and ketogenesis, which can further contribute to the increase in hepatic lipid content[81]. Taken together, PXR activation most likely explains the hepatic steatosis associated with RIF treatment.

Recently, we[85] and others[182] have shown that the specific PXR agonist 5-pregnen-3β-ol-20-one-16α-carbonitrile (PCN), reduces plasma HDL levels by inhibiting HDL synthesis and/or maturation, and increases plasma VLDL levels[182]. Since RIF also activates PXR, RIF can be expected to have similar effects on plasma lipoprotein metabolism. However, the effects of RIF on lipoprotein metabolism have been poorly investigated, especially in absence of tuberculosis, a Gram-negative bacterial infection that may also affect lipoprotein metabolism[183].

The aim of the present study was to evaluate the effect of RIF on plasma lipoprotein metabolism and to investigate the underlying mechanisms. We used ApoE*3-Leiden.CETP (E3L.CETP) mice[108, 116] that express human CETP under control of its natural flanking regions[129]. These mice have an attenuated clearance of apoB-containing lipoproteins and, therefore, show a human-like lipoprotein profile on a cholesterol-rich Western-type diet as characterized by increased plasma levels of cholesterol (C) and TG[114, 116]. Our results show that RIF decreased plasma HDL-C and, in contrast to PCN, decreased VLDL-C, due to decreased HDL and VLDL particle production.

## Materials and Methods

*Animals*

Female ApoE*3-Leiden.CETP (E3L.CETP) transgenic mice that express human CETP under control of its natural flanking regions were housed under standard conditions with access to water and food ad libitum. Mice were fed a diet enriched with 15% cacao butter (Diet T; AB Diet Services, Woerden, The Netherlands) for 3 weeks to increase plasma cholesterol levels from 2 mM to ~6 mM. Blood was collected after a 4 h fast from the tail vein into EDTA-containing cups, and mice were randomized into 3 groups according to their plasma total cholesterol, TG and HDL-C. Subsequently, mice were fed control diet (diet T) or the same diet with rifampicin (RIF; Sigma) at increasing doses of 0.01%, 0.03% and 0.10% (corresponding with ~11, 33 and 110 mg/kg/day) for three weeks each. In a separate experiment, mice were fed diet T without or with 0.1% RIF after randomization. Experiments were performed after 4 h of fasting with food withdrawn at 8:00 am. All experiments were approved by the institutional committee on animal care and experimentation.



*Hepatic mRNA expression*

Total mRNA extraction from liver tissue samples was performed using TRIzol (Invitrogen, Carlsbad, CA, USA) according to manufacturer's instructions. mRNA quality was confirmed with lab-on-a-chip (Bio-Rad Laboratories, Hercules, CA, USA), and mRNA was converted to single-stranded cDNA using the RevertAid First Strand cDNA Synthesis Kit (Fermentas, Ontario, Canada). RT-PCR was performed using the IQ5 multicolor real-time PCR detection system using the SYBR Green RT-PCR mix (Bio-Rad Laboratories, Hercules, CA, USA). mRNA levels were normalized to mRNA levels of hypoxanthine-guanine phosphoribosyl transferase (HPRT), cyclophilin and glyceraldehyde-3-phosphate dehydrogenase (GAPDH). Primers are listed in Table I.

*Hepatic lipid analysis*

Liver samples (~50 mg) were homogenized (20 sec at 4,800 rpm) in ice-cold methanol (10 µL/mg tissue) using a Mini Bead Beater (BioSpec Products, Bartlesville, USA). Tissue homogenates (45 µL ~ 4.5 mg tissue) were diluted

with ice-cold methanol (450 µL) and ice-cold chloroform (1350 µL), and further shaken (20 sec at 4800 rpm) to extract lipids from the tissue samples. Mixtures were centrifuged (15 min at 14,000 rpm; 4°C) and supernatant was transferred into a new tube, dried under nitrogen gas. Lipids were dissolved in 100 µL 2% Triton-X100. Total cholesterol, TG and phospholipid levels were assayed as described above.

**Table 1.** List of primers

| Gene | Forward primer | Reverse primer |
|---|---|---|
| *Abca1* | CCCAGAGCAAAAAGCGACTC | GGTCATCATCACTTTGGTCCTTG |
| *Apoa1* | GGAGCTGCAAGGGAGACTGT | TGCGCAGAGAGTCTACGTGTGT |
| *Apob* | GCCCATTGTGGACAAGTTGAT C | CCAGGACTTGGAGGTCTTGGA |
| *Cd36* | GCAAAGAACAGCAGCAAAATC | CAGTGAAGGCTCAAAGATGG |
| *CETP* | CAGATCAGCCACTTGTCCAT | CAGCTGTGTGTTGATCTGGA |
| *Cyclo* | CAAATGCTGGACCAAACACAA | GCCATCCAGCCATTCAGTCT |
| *Cyp3A11* | CTTTCCTTCACCCTGCATTCC | CTCATCCTGCAGTTTTTTCTGGAT |
| *Cyp7a1* | CAGGGAGATGCTCTGTGTTCA | AGGCATACATCCCTTCCGTGA |
| *Fas* | ATTGCATCAAGCAAGTGCAG | GAGCCGTCAAACAGGAAGAG |
| *Gapdh* | TGCACCACCAACTGCTTAGC | GGCATGGACTGTGGTCATGAG |
| *Hl* | CAGCCTGGGAGCGCAC | CAATCTTGTTCTTCCCGTCCA |
| *HMGCoA* | CCGGCAACAACAAGATCTGTG | ATGTACAGGATGGCGATGCA |
| *Hprt* | TTGCTCGAGATGTCATGAAGGA | AGCAGGTCAGCAAAGAACTTATAG |
| *Lcat* | GGCAAGACCGAATCTGTTGAG | ACCAGATTCTGCACCAGTGTGT |
| *Ldlr* | GCA TCA GCT TGG ACA AGG TGT | GGG AAC AGC CAC CAT TGT TG |
| *Lxra* | CTGCACGCCTACGTCTCCAT | AAGTACGGAGGCTCACCAGCT |
| *Pltp* | TCAGTCTGCGCTGGAGTCTCT | AAGGCATCACTCCGATTTGC |
| *Scd1* | GCGATACACTCTGGTGCTCA | CCCAGGGAAACCAGGATATT |
| *Sr-b1* | GTTGGTCACCATGGGCCA | CGTAGCCCCACAGGATCTCA |
| *Srebp1c* | GGAGCCATGGATTGCACATT | GGCCCGGGAAGTCACTGT |

*Plasma lipid and lipoprotein analysis*

Plasma total cholesterol and triglycerides (TG) were measured using commercially available enzymatic kits (236691 and 1488872, respectively, Roche Molecular Biochemicals, Indianapolis IN, USA) according to the manufacturer's instructions. Phospholipids were determined using an enzymatic Phospholipids kit (Spinreact,

Sant Esteve de Bas, Spain). Plasma HDL-C was measured after precipitation of the apoB-containing lipoproteins from 20 µL EDTA plasma by adding 10 µL heparin (LEO Pharma, The Netherlands; 500 U/mL) and 10 µL 0.2 M $MnCl_2$. Mixtures were incubated during 20 min at room temperature and centrifuged for 15 min at 13,000 rpm at 4°C. In the supernatant HDL-C was measured. To determine the lipid distribution over plasma lipoproteins, lipoproteins were separated using FPLC. Plasma was pooled per group, and 50 µL of each pool was injected onto a Superose 6 HR 10/30 column (Äkta System, Amersham Pharmacia Biotech, Piscataway, NJ, USA) and eluted at a constant flow rate of 50 µL/min in PBS, 1 mM EDTA, pH 7.4. Fractions of 50 µL were collected and assayed for TG and cholesterol as described above.

*Plasma CETP activity*

Total (lipoprotein-independent) CETP activity was measured as the transfer of [$^3$H] cholesteryl oleate (CO) from LDL to HDL[184], exactly as described[185]. Endogenous (lipoprotein-dependent) CETP activity was determined by a fluorescent method using liposomes enriched with nitrobenzoxadiazole-labeled cholesteryl esters (RB-CETP, Roar Biomedical, New York)[185, 186].



*Plasma apoAI protein*

Plasma was pooled per group and lipoproteins were separated using FPLC. Each fraction (7.5 µL) was run on a 4-20% SDS-PAGE gel (Bio-Rad Laboratories, Hercules CA, USA). Gels were stained with Coomassie brilliant blue, and apoAI within the main HDL fraction (fraction 18) was quantified by densitometry using the Quantity One (Bio-Rad Laboratories, Hercules CA, USA).

*Hepatic ABCA1 and SR-BI protein*

Immunoblot analysis of hepatic ABCA1 and SR-BI was performed as described[187]. In short, liver samples were lysed, cell debris was removed, and protein concentration was determined. Equal amounts of protein (20 µg) were separated on 7.5% SDS-PAGE gels and transferred to nitrocellulose membrane. Immunolabeling was performed using murine monoclonal αABCA1 (AC-10) or rabbit polyclonal αSRBI (anti-BI[495]) as primary antibody and goat-anti-mouse IgG and goat-anti-rabbit IgG, respectively, as secondary antibodies. Immunolabeling was detected by enhanced chemiluminescence.

*Hepatic VLDL-TG and VLDL-apoB production*

Mice were fasted for 4 h prior to the start of the experiment. During the experiment, mice were sedated by i.p. injection of 6.25 mg/kg acepromazine (Alfasan), 6.25 mg/kg midazolam (Roche) and 0.3125 mg/kg fentanyl (Janssen-Cilag). At t=0 min blood was taken via tail bleeding and mice were i.v. injected with 100 µL PBS containing 100 µCi Trans$^{35}$S-label (MP Biomedicals, Irvine, USA) to measure *de novo* total apoB synthesis. After 30 min, the animals received 500 mg of tyloxapol (Triton WR-1339, Sigma-Aldrich) per kg body weight as a 10% (w/w) solution in sterile saline, to prevent systemic lipolysis of newly secreted hepatic VLDL-TG [131]. Additional blood samples were taken at t=15, 30, 60, and 90 min after tyloxapol injection and used for determination of plasma TG concentration. After 90 min, the animals were sacrificed and blood was collected by orbital bleeding for isolation of VLDL by density gradient ultracentrifugation to measure $^{35}$S-apoB in the VLDL fraction[132, 133].

*In vivo clearance of VLDL-like emulsion particles*

Glycerol tri[$^{3}$H]oleate (triolein, TO)- and [1α,2α(n)-$^{14}$C]cholesteryl oleate (CO)-double labeled VLDL-like emulsion particles (80 nm) were prepared as described by Rensen *et al*.[135]. Mice were fasted 4 h and sedated as described above and a large bolus of VLDL-like emulsion particles (1.0 mg TG in 200 µL PBS) containing 100 µCi [$^{3}$H]TO and 10 µCi [$^{14}$C]CO was injected into the tail. At 2, 5, 10, 20 and 30 min blood samples (50 µL) were taken from the tail vein. $^{3}$H and $^{14}$C activities were counted in 10 µL serum and corrected for total serum volume. At the end of the experiment, organs (i.e. liver, heart, perigonadal fat, spleen and skeletal femoralis muscle) were collected, saponified by overnight incubation at 60°C in 500 µL Solvable (Perkin-Elmer, Wellesley, USA), and radioactivity was measured. The half-life of VLDL-[$^{3}$H]TO and [$^{14}$C]CO were calculated from the slope after linear fitting of semi-logarithmic decay curves.

*Statistical analysis*

Data are presented as means ± SEM. Statistical differences were assessed using the Student T Test unless stated otherwise. GraphPad (Prism 5 software, La Jolla, CA) was used for statistical analysis. A P-value of less than 0.05 was considered statistically significant.

## Results

*Rifampicin is an activator of PXR in mice*

E3L.CETP mice were fed a control diet or a diet with increasing doses of RIF (0, 0.01, 0.03 and 0.10%). To verify that RIF activates PXR in these mice, we determined the effect of RIF on hepatic gene expression of the well-established PXR target genes *Cyp3a11* and *Cyp7a11* (Table 2). Indeed, RIF strongly upregulated *Cyp3a11* (9-fold) and down-regulated *Cyp7a1* (-60%), indicating that RIF is indeed a potent PXR agonist in E3L.CETP mice. Since it is known that PXR activation causes hepatic steatosis, the effect of RIF treatment on the liver lipid content was evaluated (Fig. 1). RIF increased the liver weight (+74%; P<0.001) (Fig. 1A), which was accompanied by increased hepatic levels of TG (+242%; P<0.001), TC (+229%; P<0.01), and phospholipids (+52%; P<0.05) (Fig. 1B), fully consistent with PXR agonism[85].

**Table 2.** Rifampicin affects hepatic gene expression



| | control | RIF |
|---|---|---|
| PXR targets | | |
| *Cyp3a11* | 1.00 ± 0.38 | 8.83 ± 2.56*** |
| *Cyp7a1* | 1.00 ± 0.41 | 0.44 ± 0.22** |
| HDL metabolism | | |
| *Abca1* | 1.00 ± 0.16 | 0.81 ± 0.21 |
| *Apoa1* | 1.00 ± 0.38 | 0.42 ± 0.09** |
| *CETP* | 1.00 ± 0.53 | 0.53 ± 0.19 |
| *Hl* | 1.00 ± 0.28 | 0.64 ± 0.14* |
| *Lcat* | 1.00 ± 0.23 | 0.72 ± 0.16* |
| *Pltp* | 1.00 ± 0.29 | 0.50 ± 0.15** |
| *Sr-b1* | 1.00 ± 0.28 | 0.64 ± 0.19* |

| | control | RIF |
|---|---|---|
| VLDL metabolism | | |
| *ApoB* | 1.00 ± 0.25 | 0.68 ± 0.16* |
| *Cd36* | 1.00 ± 0.26 | 0.91 ± 0.59 |
| *Fas* | 1.00 ± 0.38 | 0.34 ± 0.13** |
| *HMGcoA* | 1.00 ± 0.37 | 0.36 ± 0.11** |
| *LDLr* | 1.00 ± 0.25 | 0.47 ± 0.33** |
| *Lxr* | 1.00 ± 0.18 | 0.93 ± 0.26 |
| *Scd1* | 1.00 ± 0.27 | 0.49 ± 0.18** |
| *Srebp1c* | 1.00 ± 0.38 | 0.61 ± 0.25* |

E3L.CETP mice were fed a control diet or a diet with increasing doses of RIF (0, 0.01, 0.03, and 0.10%) for three weeks each. After the last treatment period, liver gene expression was quantified by RT-PCR. Data are calculated as fold difference as compared to the control group. Values are means ± SD (n= 6-7 per group); * P<0.05, ** P<0.01 versus control group.

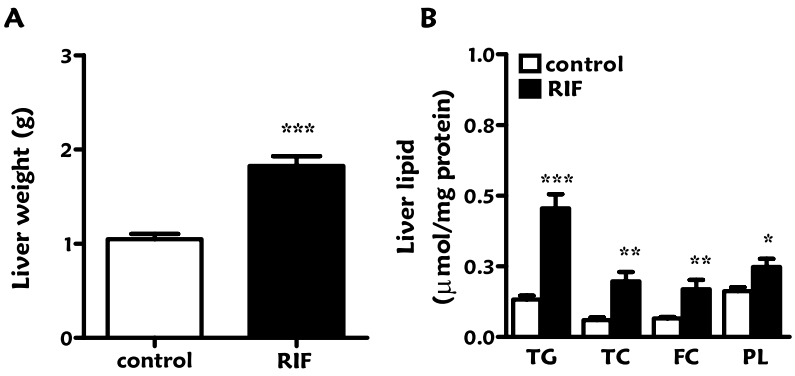


**Figure 1. Rifampicin increases liver lipids.**
E3L.CETP mice were fed a control diet (time-matched control group) or a diet with increasing doses of RIF (0, 0.01, 0.03 and 0.10%) for three weeks each. After the last treatment period (0.10% RIF), mice were sacrificed and livers were isolated and weighed (A). Livers were homogenized, lipids were extracted, and triglycerides (TG), total cholesterol (TC), and phospholipids (PL) were determined per mg cell protein (B). Values are means ± SEM (n= 6-7 per group). *P<0.05; **P<0.01, ***P<0.001 versus control group.



*Rifampicin decreases plasma VLDL-C and HDL-C levels*

Next, we investigated the dose-dependent effect of RIF (0, 0.01, 0.03 and 0.10%) on plasma lipids (Fig. 2). Whereas RIF did not affect plasma TG levels (Fig. 2A), RIF dose-dependently decreased plasma cholesterol levels up to -60% (P<0.001) (Fig. 2B). Lipoprotein profiling showed that the highest dose of RIF (0.10%) did not affect the distribution of TG over lipoproteins (Fig. 2C), and that the reduction in total cholesterol by RIF was caused by a combined reduction in HDL-C and VLDL-C (Fig. 2D). Quantitative analysis showed that RIF (0.10%) caused a reduction in both non HDL-C (-59%; P<0.01) (Fig. 2E) and HDL-C (-71%; P<0.001) (Fig. 2F). However, the absolute reduction in plasma TC, induced by RIF (-4.9 mM), was mainly explained by a reduction in non HDL-C (-4.2 mM).

*Rifampicin decreases HDL production and maturation*

We have previously observed that a decrease in the hepatic cholesterol content of E3L.CETP mice e.g. by treatment with fenofibrate[114], atorvastatin[118] and niacin[117] decreased both the hepatic expression of CETP and the activity of CETP in plasma. Since RIF strongly increased the hepatic cholesterol content, we questioned whether the reduction in plasma HDL may be related to

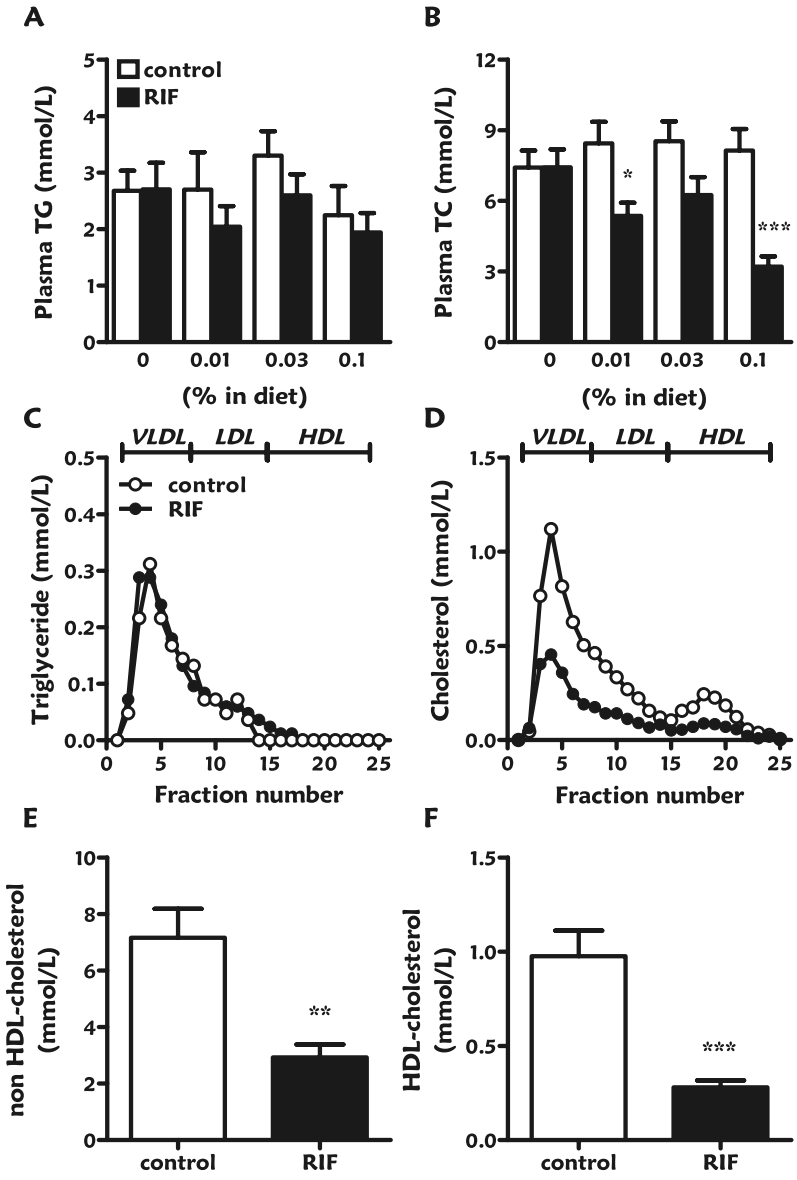


**Figure 2. Rifampicin dose-dependently reduces plasma cholesterol.**
APOE*3-Leiden.CETP (E3L.CETP) mice were fed a control diet (time-matched control group) or a diet with increasing doses of rifampicin (RIF) (0, 0.01, 0.03 and 0.10%) for three weeks each. Before treatment and at the end of the 3-week periods, blood was drawn and plasma was assayed for triglycerides (TG; A), total cholesterol (TC; B). After 3 weeks of intervention with 0.10% RIF, the distribution of TG (C) and TC (D) over lipoproteins was determined in pooled plasma. Total plasma was assayed for HDL-C (F) and non-HDL cholesterol was calculated (E). Values are means ± SEM (n= 7 per group); * P<0.05, ** P<0.01, ***P<0.001 versus control group.

increased plasma CETP activity. Therefore, the effect of RIF on CETP activity was determined in plasma (Fig. 3). It appeared that 0.10% RIF decreased the total exogenous plasma activity of CETP (-45%; P<0.001) (Fig. 3A) without affecting the endogenous CETP activity (Fig. 3B), which can thus not explain the reduction in HDL-C.

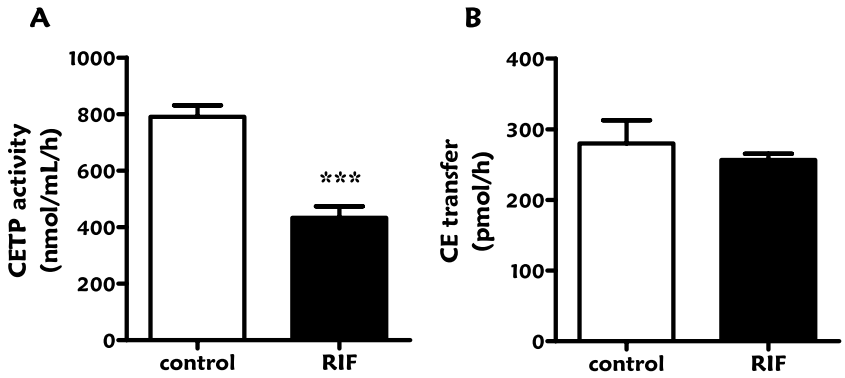


**Figure 3. Rifampicin decreases plasma CETP activity.**
E3L.CETP mice were fed a control diet (time-matched control group) or a diet with increasing doses of RIF (0, 0.01, 0.03 and 0.10%) for three weeks each. After the last treatment period (0.10% RIF), blood was drawn and plasma was assayed for total CETP activity (A) and endogenous CETP activity (B). Values are means ± SEM (n= 7 per group); *** P<0.001 versus control group.

To gain further insight into the mechanism(s) underlying the HDL-decreasing effect of RIF, we performed hepatic gene expression analysis (Table I). With respect to HDL metabolism, RIF decreased mRNA of proteins involved in HDL assembly including *Abca1* (-20%, which did not reach significance) and *Apoa1* (-50%). In addition, RIF decreased the expression of genes involved in HDL maturation such as *Lcat* (-30%), *Hl* (-30%) and *Pltp* (-50%), as well as the gene involved in hepatic clearance of HDL-C, *Sr-b1* (-40%). We next evaluated whether the relatively large effects of RIF on the hepatic expression of *Apoa1* and *Sr-b1* were indeed reflected by lower protein levels (Fig. 4). RIF decreased HDL-apoAI in pooled plasma by -37% (Fig. 4A). Western blot analysis of hepatic homogenates indicated that RIF did not substantially reduce hepatic ABCA1 protein (-14%), but markedly reduced SR-BI protein (-57%, P<0.05) (Fig. 4B). Collectively, these data imply that RIF reduces HDL mainly via inhibiting hepatic HDL particle synthesis (i.e. reduction in apoAI) and HDL maturation (i.e. reduction in LCAT, HL and PLTP), similar to the rodent specific PXR agonist PCN[85].

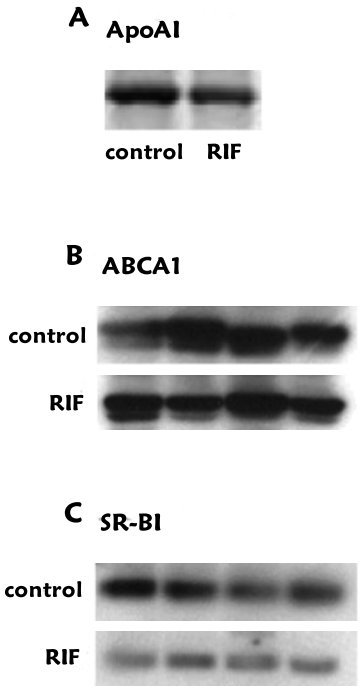


**Figure 4. Rifampicin reduces plasma apoAI and hepatic SR-BI protein.**
E3L.CETP mice were fed a control diet or a diet with increasing doses of RIF (0, 0.01, 0.03, and 0.10%) for three weeks each. After the last treatment period (0.10% RIF), pooled plasma was assayed for apoAI (A). Mice were sacrificed and livers were isolated. Livers were homogenized and equal amounts of hepatic proteins were separated by SDS-PAGE and transferred to nitrocellulose membrane. ABCA1 (B) and SR-BI (C) were visualized by immunolabeling. Results of 4 individual mice per group are shown.



*Rifampicin decreases VLDL production without largely affecting VLDL clearance*

To elucidate the mechanism underlying the VLDL-C-decreasing effect of RIF, we first investigated the hepatic expression of genes involved in VLDL metabolism (Table I). RIF decreased mRNA of *apoB* (-20%), required for VLDL production. RIF did not affect expression of *Cd36*, involved in fatty acid uptake. Although RIF did not affect the expression of *Lxr*, RIF decreased the expression of the LXR target genes *Srebp1c* (-40%), *Fas* (-65%) and *Scd1* (-50%), involved in fatty acid synthesis. Expression of the *Ldlr*, involved in the uptake of VLDL remnants and LDL, was also decreased (-50%). Since these data suggest that RIF may decrease the hepatic assembly of VLDL, we evaluated the effect of RIF on VLDL production (Fig. 5). RIF reduced VLDL-TG production to some extent (-20%; $P=0.084$) (Fig. 6 A, B) and markedly reduced the VLDL-apoB production rate (-50%; $P<0.001$) (Fig. 6C). As a consequence, RIF thus selectively increased the ratio of TG over apoB (+64%; $P<0.01$) without affecting the relative TC and PL content (Fig. 6D). Since each VLDL particle contains a single molecule of apoB, these data show that RIF reduces the production of VLDL particles that are nevertheless rich in TG.

To determine whether increased VLDL-TG clearance also contributes to the effect of RIF on VLDL levels, mice were injected with [$^{3}$H]TO [$^{14}$C]CO-labeled VLDL-like emulsion particles and the plasma clearance was determined (Fig. 6). As compared to control mice, RIF had no significant effect on the clearance rate of [$^{3}$H]TO ($t_{½}$ = 5.4 ± 0.6 vs 7.5 ± 1.4 min; Fig. 6A) or [$^{14}$C]CO ($t_{½}$ = 23.2 ± 5.6 vs 23.9 ± 4.2 min; Fig. 6B). However, RIF reduced the uptake of [$^{14}$C]CO by the liver (21.1 ± 4.1% versus 10.5 ± 2.7%; P<0.01) (Fig. 6C).

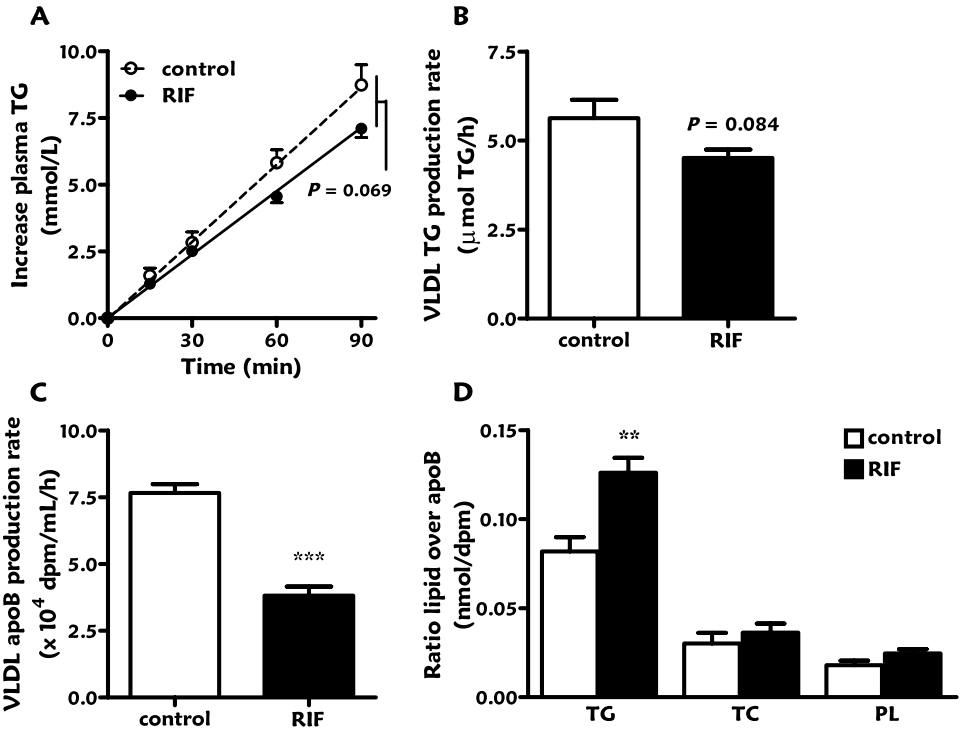


**Figure 5. Rifampicin decreases hepatic VLDL particle production.**
E3L.CETP mice were fed a control diet (time-matched control group) or a diet with 0.10% RIF for 3 weeks. Mice were consecutively injected with Trans$^{35}$S label and tyloxapol and blood samples were drawn up to 90 min after tyloxapol injection. Plasma TG concentrations were determined and plotted as the increase in plasma TG relative to t=0 (A). The TG production rate was calculated from the slopes of the curves from the individual mice (B). After 120 min, the total VLDL fraction was isolated by ultracentrifugation and the rate of newly synthesized VLDL-apoB was determined (C). The ratio of TG over apoB production was calculated (D). Values are means ± SEM (n= 5 per group). ***P<0.001 versus control group.

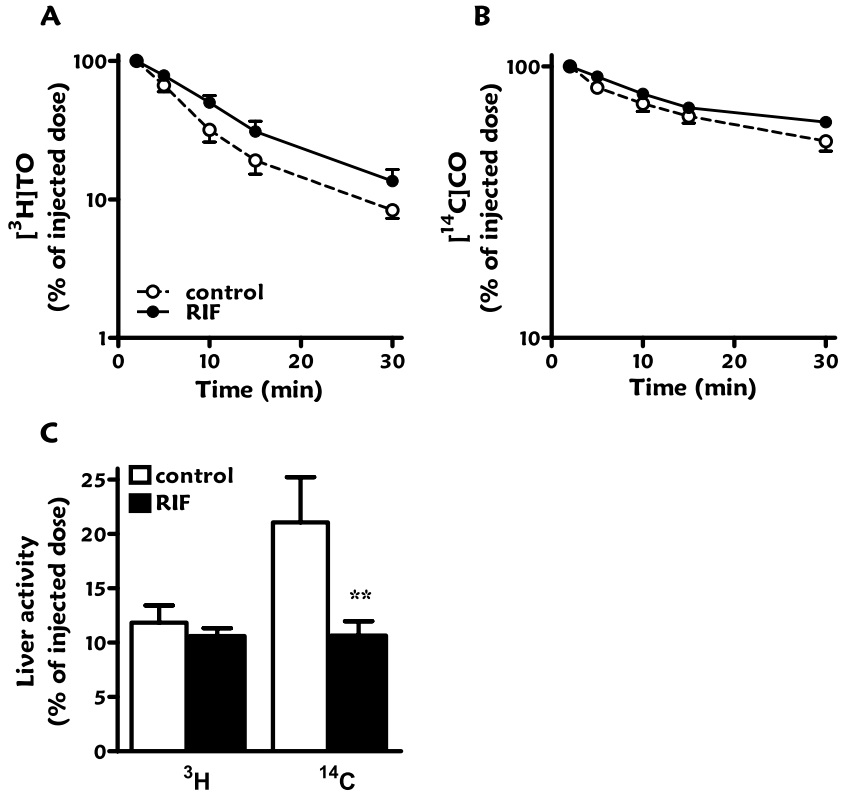




**Figure 6. Rifampicin does not affect the clearance of VLDL-like emulsion particles.** E3L.CETP mice were fed a control diet (time-matched control group) or a diet with 0.10% RIF for 3 weeks. Mice were injected with VLDL-like glycerol tri[$^{3}$H]oleate [$^{14}$C]cholesteryl oleate double labeled VLDL-like emulsion particles (1 mg TG) and plasma samples were taken at indicated time points to determine the plasma clearance of [$^{3}$H]TO (A) and [$^{14}$C]CO (B). At 30 min after injection, liver was harvested to determine the uptake of $^{3}$H and $^{14}$C (C) activity. Values are means ± SEM (n= 5-6 per group). *P<0.05; **P<0.01 versus control group.

## Discussion

Rifampicin (RIF) is an antibiotic used for the treatment of tuberculosis and has been reported to cause hepatic lipid accumulation[175, 176, 177] and hyperlipidemia in humans[178]. Here, we have evaluated the effect of RIF on lipoprotein metabolism in E3L.CETP mice, which is a well-established model for human-like lipoprotein metabolism[114, 116]. We show that RIF dose-dependently decreased both VLDL-C and HDL-C without affecting TG levels. Mechanistic studies showed that the decrease in HDL-C was likely caused by impaired HDL production, and inhibited HDL maturation, and that the decrease in

VLDL-C was caused by impaired production of VLDL particles that were nevertheless rich in TG.

We have previously reported the response of E3L.CETP mice to the PXR agonist 5-pregnen-3β-ol-20-one-16α-carbonitrile (PCN)[85]. PCN considerably increased hepatic Cyp3a11 expression and reduced Cyp7a1 expression, which is in accordance with its PXR agonistic activity. Here, we report that RIF has a similar effect on these P450 enzymes. In addition, both RIF and PCN increased liver weight and increased levels of hepatic TG, total cholesterol and phospholipid resulting in a fatty liver[85]. PXR agonism is associated with hepatic steatosis[82 81] and our gene expression data suggest that RIF increases hepatic lipid content via PXR. Therefore, we can conclude that RIF is indeed a potent PXR agonist in mice.

Similar to PCN[85], RIF dose-dependently decreased HDL-C levels. HDL synthesis, maturation and clearance all determine plasma HDL-C levels. The reduction in HDL-C can be explained by reduced hepatic expression of apoAI, important for the generation of discoidal HDL precursors[188]. In fact, this is similar to the effect of PCN on the expression of genes involved in HDL formation[85]. Both RIF and PCN[85] markedly reduced hepatic *Apoa1* mRNA (~50-60%) as reflected by decreased plasma apoAI protein (~40%). In addition, they tended to reduce hepatic *Abca1* mRNA (~20%) and protein (~15-20%), which is in line with effects of RIF in HepG2 cells and PCN in primary rat hepatocytes[189]. In addition, RIF decreased the expression of genes involved in HDL maturation such as *Hl* (~40%), *Lcat* (~30%) and *Pltp* (~50%). A reduction in both LCAT[190] and PLTP[191] might contribute to the reduction in plasma HDL levels. Since these data are similar to the effect of PCN on HDL metabolism[85], RIF activates PXR and reduces HDL cholesterol by reducing HDL assembly and maturation in E3L.CETP mice. Another important protein in HDL maturation is CETP, involved in the transfer of cholesterol from HDL to VLDL. Previous studies with fenofibrate[114], atorvastatin[118] and niacin[117] showed that HDL-C levels increased in response to a decrease in CETP expression in E3L.CETP mice. This decrease in CETP expression was associated with lower hepatic lipid levels. Since RIF increased hepatic lipid levels, an increase in CETP expression might be causing the reduction of HDL-C. However, RIF did not significantly affect hepatic CETP expression (not shown) and reduced rather

than increased CETP activity[192]. Finally, similar to PCN, RIF significantly reduced hepatic SR-BI mRNA and protein levels in E3L.CETP mice. In mice, SR-BI appears solely responsible for the selective clearance of cholesteryl esters from HDL[19]. Decreased SR-BI expression would thus cause the accumulation of enlarged HDL[193]. However, since endogenous CETP activity is unchanged and enlarged HDL is a preferred substrate of CETP, this likely explains the normal HDL particle size observed after treatment with RIF. Altogether, these data show that RIF lowers HDL-C by decreasing HDL synthesis, maturation and clearance. Since these effects on HDL metabolism are similar to those seen with the PXR activator PCN[85], we conclude that the reduction in HDL-C by RIF is mediated by activation of PXR.

Despite similarities in the effects of RIF and PCN on HDL metabolism, RIF differentially affected plasma TG and VLDL-C as compared to PCN[85]. RIF did not affect plasma TG levels and reduced VLDL-C levels causing a decrease in total cholesterol whereas PCN increased plasma TG together with a small increase in plasma cholesterol, as reflected by increased VLDL levels[85]. Plasma VLDL levels are determined by the rates of VLDL production and VLDL clearance. Upon RIF treatment, hepatic VLDL particle production was reduced, explaining the reduction in VLDL-C. The reduced VLDL particle production was associated with reduced hepatic apoB expression. However, since total TG levels were unaffected, the produced VLDL particles were enriched with TG. PXR-mediated TG enrichment of VLDL has been shown before in LDLr knockout mice treated with PCN[182]. VLDL-TG production is determined by hepatic FA uptake and *de novo* lipogenesis. We did not detect changes in the expression of CD36, important for the uptake of plasma derived FA. However the expression of genes involved in *de novo* lipogenesis including SREBP1c, FAS and SCD1 was reduced. Changes in the expression of these genes were not detected in the LDLr knockout mice treated with PCN[182], however similar changes were seen in E3L.CETP mice treated with PCN (personal communication W. de Haan).VLDL-TG clearance was not affected upon treatment with RIF.

In conclusion we show that RIF treatment in E3L.CETP mice lowers HDL-C by reducing HDL synthesis and maturation, which can be attributed to PXR activation. The impairment of VLDL particle production by RIF cannot be

explained by activation of PXR and may be caused by PXR-selective or non-PXR mediated mechanisms.

**Acknowledgements**

This work was performed in the framework of the Leiden Center for Cardiovascular Research LUMC-TNO, and supported by grants from the Nutrigenomics Consortium/Top Institute Food and Nutrition (TIFN) and the Center for Medical Systems Biology (CMSB), within the framework of the Netherlands Genomics Initiative (NGI/NWO), the Netherlands Organization for Health Care Research Medical Sciences (ZON-MW project nr. 948 000 04), the Netherlands Heart Foundation (NHS grant 2003B136 to PCNR) and the Netherlands Organization for Scientific Research (NWO VIDI grant 917.36.351 to PCNR). PCNR is an Established Investigator of the Netherlands Heart Foundation (grant 2009T038).

# CHAPTER 5

## Perfluoroalkyl sulfonates cause alkyl chain length-dependent hepatic steatosis and hypolipidemia mainly by impairing lipoprotein production in ApoE*3-Leiden.CETP mice

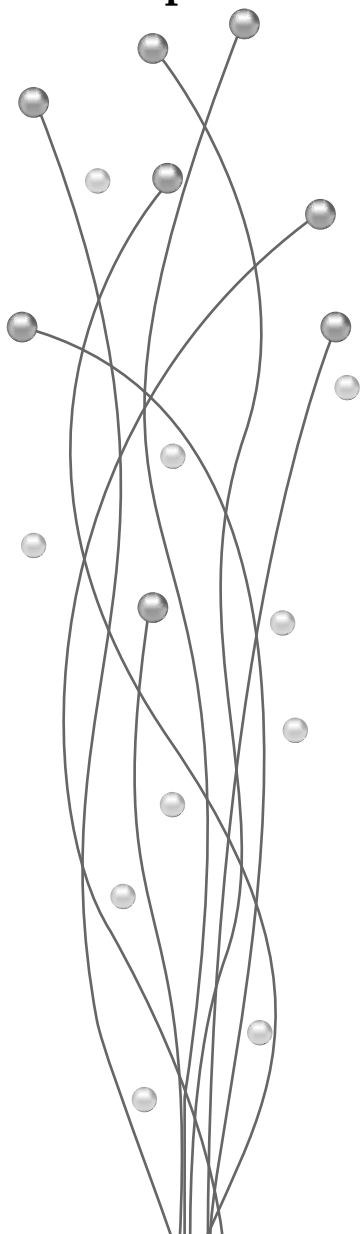

Silvia Bijland*
Patrick CN Rensen*
Elsbet J Pieterman
Annemarie CE Maas
José W van der Hoorn
Marjan J van Erk
Louis M Havekes
Ko Willems van Dijk
Shu-Ching Chang
David J. Ehresman
John L. Butenhoff
Hans M.G. Princen

* both authors contributed equally

*Submitted*

Perfluorobutane sulfonate (PFBS), perfluorohexane sulfonate (PFHxS), and perfluorooctane sulfonate (PFOS) are stable perfluoroalkyl sulfonate (PFAS) surfactants, and PFHxS and PFOS are frequently detected in human biomonitoring studies. Some epidemiological studies have shown modest positive correlations of serum PFOS with nonHDL-C. This study investigated the mechanism underlying the effect of PFAS surfactants on lipoprotein metabolism. ApoE*3-Leiden.CETP mice were fed a Western-type diet with PFBS, PFHxS or PFOS (30, 6 and 3 mg/kg/day, respectively) for 4-6 weeks. While PFBS modestly reduced only plasma TG, PFHxS and PFOS markedly reduced TG, nonHDL-C and HDL-C. The decrease in VLDL was caused by enhanced LPL-mediated VLDL-TG clearance, and by decreased production of VLDL-TG and VLDL-apoB. Reduced HDL production related to decreased apoAI synthesis resulted in decreased HDL. PFHxS and PFOS increased liver weight and hepatic TG content. Hepatic gene expression profiling data indicated that these effects were the combined result of PPARα and PXR activation. In conclusion, the potency of PFAS to affect lipoprotein metabolism increased with increasing alkyl chain length. PFHxS and PFOS reduce plasma TG and TC mainly by impairing lipoprotein production, implying that the reported positive correlations of serum PFOS and nonHDL-C are associative rather than causal.

**Introduction**

Perfluoroalkyl sulfonates (PFAS) including perfluorobutane sulfonate (PFBS), perfluorohexane sulfonate (PFHxS), and perfluorooctane sulfonate (PFOS) are exceptionally stable surfactant molecules that are representative members of the perfluoroalkyl sulfonate (PFAS) class of perfluoroalkyls. Due to their unique physical and chemical properties PFAS have been used, either directly or by use of N-alkyl functionalized perfluoroalkyl sulfonamides, in industrial and consumer products with applications requiring stability toward corrosion and heat, strong surface-tension reduction, and resistance to water and oil. Applications have included paper and textile coatings, food packaging, surfactants, repellents and fire-retardant foams[194, 195]. Although used directly as surfactants or ion-pairing agents, these molecules can also result from metabolic[196, 197] or environmental[198] degradation of N-substituted perfluoroalkyl sulfonamides.

In 2001, the widespread distribution of PFOS and PFHxS in humans and PFOS in wildlife was reported[199, 200]. Since that time, due to their structural stability, widespread dissemination in the environment, and poor elimination in most species, particularly humans[201], PFHxS and PFOS have been detected frequently in biological and environmental matrices[202]. These findings led the major United States manufacturer, 3M Company, to discontinue manufacture of PFOS, PFHxS, and materials that could generate these compounds via degradation by the end of 2002. International regulatory action has been taken to further restrict the use of PFOS and materials that may generate PFOS[202]. PFBS has a more favorable toxicological and environmental profile than either PFHxS or PFOS. In fact, the geometric mean serum elimination half-lives of PFOS and PFHxS determined for 26 retired production workers were, in years, 4.8 (95% CI 4.0-5.8) and 7.3 (95% CI 5.8-9.2), respectively[201]. In contrast, PFBS had a serum elimination half-life of 25.8 days (95% CI 16.6-40.2) among six production workers removed from exposure[203]. Several epidemiological studies have shown modest positive correlations of serum lipids with serum PFOS in non-occupationally-exposed populations[204, 205] as well as some occupationally-exposed populations[206], while no correlations of serum PFOS

with HDL-C have been noted[206, 204]. However, it is still unclear whether these correlations are causal or associative.

In toxicological studies using cynomolgus monkeys[207], rats[208, 209, 210] and pregnant mice[211], PFOS was shown to reduce serum total cholesterol and otherwise induce changes in plasma lipid metabolism, and to increase liver TG. PFHxS was also shown to reduce serum total cholesterol in rat[212], and PFBS was not[213]. However, the mechanism(s) underlying the effects of PFBS, PFHxS and PFOS on lipoprotein metabolism, as well as the importance of the alkyl chain length to these effects, have not been addressed thoroughly. Thus, the objective of this study was to investigate the mechanism(s) underlying the effects of PFHxS and PFOS on lipoprotein metabolism, and to assess the importance of the alkyl chain length by comparing the effects between PFBS and PFHxS and PFOS. ApoE*3-Leiden.CETP (E3L.CETP) mice[116] were used, which have attenuated clearance of apoB-containing lipoproteins and exhibit a human-like lipoprotein metabolism on a Western-type diet.



## Materials and Methods

*Animals*

In this study, male E3L.CETP mice on a C57Bl/6 background[116] were used, housed under standard conditions in conventional macrolon cages (2-4 mice/cage, wood dust bedding) with free access to food and water. At the age of 8-10 weeks, mice were fed a semi-synthetic Western-type diet, containing 0.25% (w/w) cholesterol, 1% (w/w) corn oil and 14% (w/w) bovine fat (Hope Farms, Woerden, The Netherlands) for 4 weeks in three independent experiments. Upon randomization according to body weight, total plasma cholesterol (TC) and TG levels, mice received the Western-type diet without or with PFBS (0.03% ~30 mg/kg/day), PFHxS (0.006% ~6 mg/kg/day) or PFOS (0.003% ~3 mg/kg/day) for 4-6 weeks. Test materials were provided by 3M Company, St. Paul, MN, USA, and included potassium PFOS (FC-95, Lot 217, 87.6% purity), potassium PFHxS (L-9051, 99.9% purity), and potassium PFBS (L-7038, 98.2% pure). Experiments were performed after 4 h of fasting with food withdrawn at 8:00 am. The institutional Ethical Committee on Animal Care and Experimentation approved all experiments.

*Determination of serum concentrations of PFBS, PFHxS, and PFOS*
Serum concentrations of PFBS, PFHxS, and PFOS were determined using an LC-MS/MS method as described[214].

*Plasma lipid and lipoprotein analysis*
Plasma was obtained via tail vein bleeding and assayed for TC and TG, using the commercially available enzymatic kits 236691 and 11488872 (Roche Molecular Biochemicals, Indianapolis, IN, USA), respectively. Free fatty acids (FA) were measured using NEFA-C kit from Wako Diagnostics (Instruchemie, Delfzijl, the Netherlands) and glycerol was measured using the free glycerol determination kit (Sigma, St. Louis, USA). The distribution of lipids over plasma lipoproteins was determined using fast protein liquid chromatography (FPLC). Plasma was pooled per group, and 50 µL of each pool was injected onto a Superose 6 PC 3.2/30 column (Äkta System, Amersham Pharmacia Biotech, Piscataway, NJ, USA) and eluted at a constant flow rate of 50 µL/min in PBS, 1 mM EDTA, pH 7.4. Fractions of 50 µL were collected and assayed for TC as described above. HDL was isolated by precipitation of apoB-containing lipoproteins from 20 µL EDTA plasma by adding 10 µL heparin (LEO Pharma, The Netherlands; 500 U/mL) and 10 µL 0.2 M $MnCl_2$. The mixtures were incubated for 20 min at room temperature and centrifuged for 15 min at 13,000 rpm at 4°C. HDL-C was measured in the supernatant using enzymatic kit 236691 (Roche Molecular Biochemicals, Indianapolis, IN, USA). Plasma CETP mass was analyzed using the CETP ELISA kit from ALPCO Diagnostics (Salem, NH, USA). Plasma apoAI concentrations were determined using a sandwich ELISA [117], with diluted mouse plasma (dilution 1:400,000). Purified mouse apoAI from Biodesign International (Saco, USA) was used as a standard.

*In vivo clearance of VLDL-like emulsion particles*
Glycerol tri[$^3$H]oleate (triolein, TO)-labeled VLDL-like emulsion particles (80 nm) were prepared as described by Rensen *et al*[135]. In short, radiolabeled emulsions were obtained by adding 100 µCi of [$^3$H]TO to 100 mg of emulsion lipids before sonication (isotopes obtained from GE Healthcare, Little Chalfont, UK). Mice were fasted for 4 h, sedated with 6.25 mg/kg acepromazine (Alfasan), 6.25 mg/kg midazolam (Roche), and 0.3125 mg/kg fentanyl (Janssen-Cilag)

and injected with a large bolus of radiolabeled emulsion particles (1.0 mg TG in 200 µL PBS) via the tail vein. At indicated time points after injection, blood was taken from the tail vein to determine the serum decay of [$^{3}$H]TO. At 30 min after injection, plasma was collected by orbital puncture and mice were sacrificed by cervical dislocation. Organs (i.e. liver, heart, perigonadal fat, spleen and skeletal femoralis muscle) were harvested and saponified in 500 µL Solvable (Perkin-Elmer, Wellesley, USA) to determine [$^{3}$H]TO uptake. The half-life of VLDL-[$^{3}$H]TO was calculated from the slope after linear fitting of semi-logarithmic decay curves.

*Hepatic lipase and lipoprotein lipase assay*

Lipolytic activity of both lipoprotein lipase (LPL) and hepatic lipase (HL) was determined as described previously[215]. To liberate LPL from endothelium, 4 h fasted mice were injected intraperitoneally with heparin (0.5 U/g bodyweight; Leo Pharmaceutical Products BV., Weesp, The Netherlands) and blood was collected after 20 min. 10 µL of post-heparin plasma was incubated with 0.2 mL of TG substrate mixture containing triolein (4.6 mg/mL) and [$^{3}$H]TO (2.5 µCi/mL) for 30 min at 37°C in the presence or absence of 1 M NaCl, which completely inhibits LPL activity, to estimate both the HL and LPL activity. The LPL activity was calculated as the fraction of total triacylglycerol hydrolase activity that was inhibited by the presence of 1 M NaCl and is expressed as the amount of free FA released per hour per mL of plasma.



*Hepatic VLDL-TG and VLDL-apoB production*

Mice were fasted for 4 h prior to the start of the experiment. During the experiment, mice were sedated as described above. At t=0 min blood was taken via tail bleeding and mice were i.v. injected with 100 µL PBS containing 100 µCi Trans$^{35}$S-label (ICM Biomedicals, Irvine, USA) to measure *de novo* total apoB synthesis. After 30 min, the animals received 500 mg of tyloxapol (Triton WR-1339, Sigma-Aldrich) per kg body weight as a 10% (w/w) solution in sterile saline, to prevent systemic lipolysis of newly secreted hepatic VLDL-TG[131]. Additional blood samples were taken at t=15, 30, 60, and 90 min after tyloxapol injection and used for determination of plasma TG concentration. After 90 min, the animals were sacrificed and blood was collected by orbital

puncture for isolation of VLDL by density gradient ultracentrifugation. $^{35}$S-apoB was measured in the VLDL fraction after apoB-specific precipitation with isopropanol[132, 133, 134].

*Hepatic lipid analysis*

Livers were isolated and partly homogenized (30 sec at 5,000 rpm) in saline (approx. 10% wet w/v) using a mini-bead beater (Biospec Products, Inc., Bartlesville, OK, USA). Lipids were extracted as described[216] and separated by high performance thin layer chromatography (HPTLC). Lipid spots were stained with color reagent (5 g $MnCl_2.4H_2O$, 32 mL 95-97% $H_2SO_4$ added to 960 mL of $CH_3OH$:$H_2O$ 1:1 v/v) and quantified using TINA® version 2.09 software (Raytest, Straubenhardt, Germany).

*Fecal excretion of bile acids and neutral sterols*

Fecal secretion of neutral sterols and bile acids was determined in feces, collected during a 48-72 h time period at 2 consecutive time points, by gas chromatographic (GS) analysis as described previously[217].

*In vivo clearance of autologous HDL*

One mouse of each experimental group was used to obtain autologous HDL that was radiolabeled with [$^3$H]CO as described[114]. Mice were injected via the tail vein with a trace of autologous radiolabeled HDL (0.1 µCi in 200 µL PBS). At the indicated time points after injection, blood was collected to determine the plasma decay of [$^3$H]CO. The fractional catabolic rate was calculated after curve fitting. Taking into account that plasma levels of HDL-C were changed upon treatment, the FCR was also calculated from these data as mM HDL-C cleared per hour, based on the actual level of HDL-C in the various groups.

*Hepatic gene expression analysis*

Total RNA was extracted from individual livers using RNA-Bee (Bio-Connect, Huissen, The Netherlands) and glass beads according to the manufacturer's instructions. The RNA was further purified using the nucleospin RNA II kit (Machery-Nagel, Düren, Germany) according to the manufacturer's instructions. The integrity of each RNA sample obtained was examined by

Agilent Lab-on-a-chip technology using a RNA 6000 Nano LabChip kit and a Bioanalyzer 2100 (Agilent Technologies, Amstelveen, The Netherlands). The Affymetrix 3' IVT-Express labeling Kit (#901229) and the protocols optimized by Affymetrix were used to synthesize Biotin-labeled cRNA (from 100 ng of total RNA) for microarray hybridization. For the hybridization 15 µg cRNA was used for further fragmentation and finally 10 µg for the hybridizations. The quality of intermediate products (that is, biotin-labeled cRNA and fragmented cRNA) was again checked.

Microarray analysis was carried out using an Affymetrix technology platform and Affymetrix GeneChip® mouse genome 430 2.0 arrays. Briefly, fragmented cRNA was mixed with spiked controls and hybridized with murine GeneChip® 430 2.0 arrays. The hybridization, probe array washing and staining, and washing procedures were executed as described in the Affymetrix protocols, and probe arrays were scanned with a Hewlett-Packard Gene Array Scanner (ServiceXS, Leiden, The Netherlands). Quality control of microarray data was performed using BioConductor packages (including simpleaffy and affyplm), through the NuGO pipeline that is available as a Genepattern procedure on http://nbx2.nugo.org[157]. All samples passed the QC. Raw signal intensities (from CEL-files) were normalized using the GCRMA algorithm (gc-rma slow). For annotation of probes and summarization of signals from probes representing one gene the custom MNBI CDF-file was used (based on EntrezGene, version 11.0.2) (http://brainarray.mbni.med.umich.edu/Brainarray/Database/CustomCDF/cdfreadme.htm). This resulted in expression values for 16331 genes, represented by unique Entrez gene identifiers. Genes were filtered for expression above 5 in 3 or more samples, resulting in a set of 11587 genes that was used for further analysis. Gene expression data were log-transformed (base 2).



Statistical analysis on resulting data was performed using the moderated t-test (Limma: http://bioinf.wehi.edu.au/limma/) with correction for multiple testing[158]. Cut-off for statistically significant changes was set at corrected P-value (q-value) <0.05. In addition, T-profiler analysis[159] was performed using expression values corrected for mean expression in the control group. This analysis resulted in scores (t-scores) and significance values for functional gene sets and biological processes (based on gene ontology annotation). Gene sets

and biological processes with significant scores (>4 or <-4) in 5 or 6 animals per group were selected. A hierarchical clustering of these pathways and biological processes and their scores in all samples was generated in GenePattern (Broad Institute, MIT, USA)[160]. The data discussed in this publication have been deposited in NCBI's Gene Expression Omnibus and are accessible through GEO Series accession number GSE22940 (accession for reviewers available).

*Statistical analysis*

All data are presented as means ± SEM unless indicated otherwise. Most data were analyzed using SPSS. A Kruskall-Wallis test for several independent samples was used, followed by a Mann-Whitney test for independent samples. P-values less than 0.05 were considered statistically significant. Serum PFBS, PFHxS, and PFOS data were analyzed using the Tukey-Kramer HSD test for multiple comparisons of means in JMP™ 5.1 (Cary, NC, USA).

**Results**

*Serum concentrations of PFBS, PFHxS, and PFOS*

Serum concentrations of PFAS for the various experiments performed to measure all biochemical and physiological parameters are presented in Table I. Mean serum concentrations after 4-6 weeks of feeding were 33-38 μg/mL (PFBS), 188-218 μg/mL (PFHxS) and 86-125 μg/mL (PFOS). Serum concentrations of PFBS measured in the three experiments were not different from each other. Even with much higher daily intakes of PFBS than either PFHxS or PFOS, the mean PFBS concentrations, on a molar basis, were approximately 25% those of PFHxS and 50-75% those of PFOS and. Serum PFHxS concentrations were approximately 2-3 times those of PFOS, corresponding to the difference in daily intakes of PFHxS as compared to PFOS.

*PFBS, PFHxS and PFOS decrease plasma triglyceride levels*

To investigate the effect of PFAS on lipoprotein metabolism in E3L.CETP mice, mice were fed a Western-type diet for 4 weeks. Mice were randomized (t0), and fed the same diet without or with different PFAS (0.03% PFBS, 0.006% PFHxS or 0.003% PFOS) for another 4 weeks (t4). Body weight and food intake

did not differ between groups throughout the intervention period (data not shown). At both t0 and t4, plasma was assayed for lipids (Fig. 1). As compared to the control group, plasma TG levels were decreased by both PFBS (-37%; P<0.01), PFHxS (-59%; P<0.0001) and PFOS (-50%; P<0.001) (Fig. 1A).

**Table 1.** Mean serum concentrations of perfluoroalkyl sulfonates.

| | | Serum concentration (mean ± SD); µg/mL (µM)[b] | | |
|---|---|---|---|---|
| **Compound (µmoles/kg)[a]** | **% in diet** | **Experiment 1 (6 weeks, n=8)** | **Experiment 2 (4 weeks, n=6)** | **Experiment 3 (4 weeks, n=6)** |
| PFBS | 0.03 (1003)[a] | 36.7 ± 7.4$^{A,*}$ (123 ± 25)[b] | 37.8 ± 6.6$^{A}$ (126 ± 22) | 32.7 ± 10.2$^{A}$ (109 ± 34) |
| PFHxS | 0.006 (150) | 217.6 ± 13.3$^{A}$ (545 ± 33) | 197.3 ± 10.4$^{A,B}$ (494 ± 26) | 188.3 ± 31.5$^{B}$ (472 ± 72) |
| PFOS | 0.003 (60) | 124.7 ± 8.1$^{A}$ (250 ± 16) | 85.6 ± 9.5$^{B}$ (172 ± 19) | 95.3 ± 4.2$^{B}$ (191 ± 9) |

Mice received a Western-type diet without or with 0.03% PFBS, 0.006% PFHxS or 0.003% PFOS during the indicated time periods, and plasma concentrations of PFBS, PFHxS, and PFOS were measured.



* Values that share the same capital letter designation within a row of data are not statistically significantly different (P<0.05) by the Tukey-Kramer HSD test.

[a] Dietary concentrations in parentheses are in units of µmoles/kg of diet.

[b] Fluorochemical serum concentrations in parentheses are in µM.

*PFHxS and PFOS decrease plasma VLDL- and HDL-cholesterol levels*

Besides TG metabolism, PFAS also affected cholesterol metabolism. Plasma TC levels tended to be decreased by PFBS (-16%: n.s.) and were significantly decreased by PFHxS (-67%: P<0.0001) and PFOS (-60%: P<0.0001) (Fig. 1B). The tendency towards reduction of total cholesterol by PFBS was caused by a selective reduction in VLDL-cholesterol, whereas PFHxS and PFOS reduced both VLDL-cholesterol and HDL-cholesterol (Fig. 1C). Quantitative analysis showed that nonHDL-cholesterol was decreased by PFBS (-28% P=0.065), PFHxS (-68% P<0.0001) and PFOS (-60% P<0.0001) (Fig. 1D). In addition, HDL-cholesterol was only decreased by PFHxS (-62%; P<0.001) and PFOS (-74% P<0.0001) (Fig. 1E), which was accompanied by even larger reductions in plasma apoAI induced by PFHxS (-76%; P<0.0001) and PFOS (-81%; P<0.0001) (Fig. 1F).

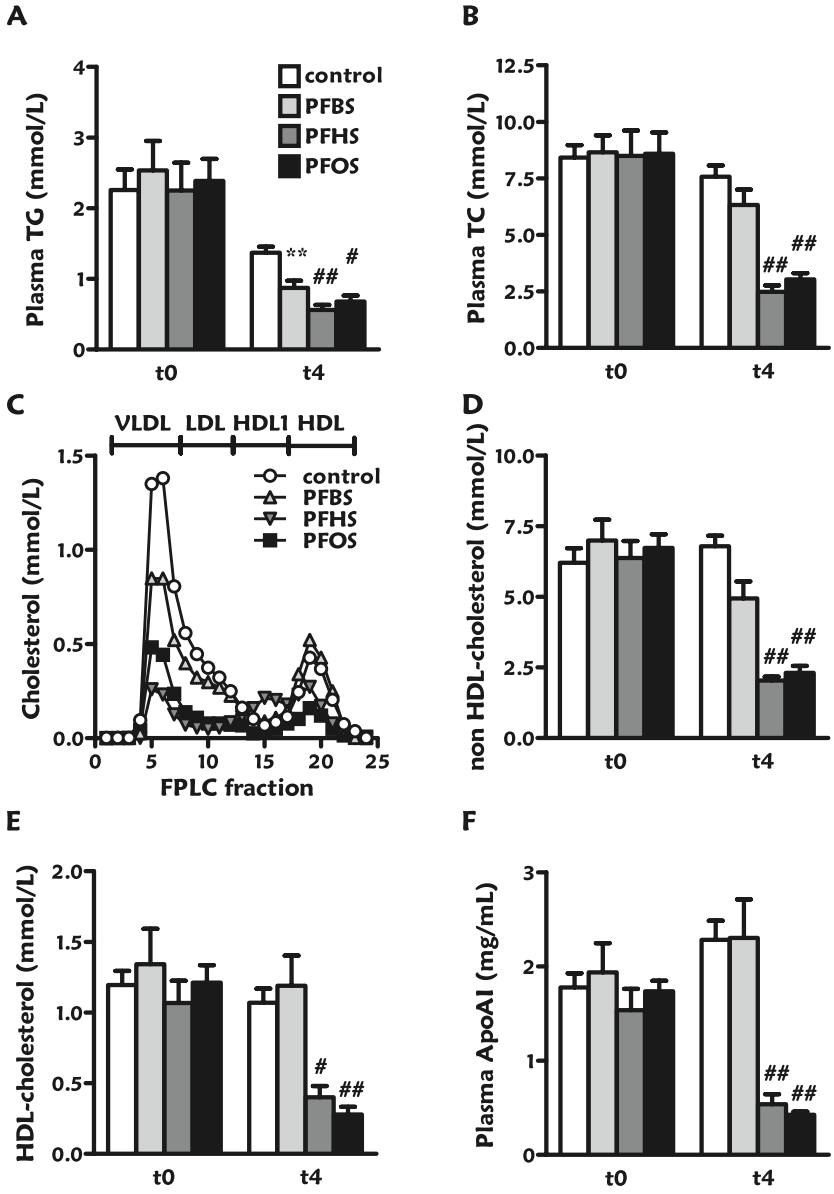


**Figure 1. Effect of perfluoroalkyl sulfonates on plasma triglycerides, total cholesterol and HDL-cholesterol.**

Mice received a Western-type diet without and with 0.03% PFBS, 0.006% PFHxS or 0.003% PFOS for 4 weeks. At baseline (t0) and after 4 weeks of intervention (t4), 4 h-fasted blood was taken and plasma was assayed for triglycerides (A) and total cholesterol (B). After 4 weeks of intervention, cholesterol distribution over lipoproteins was determined (C). Plasma at t0 and t4 were also assayed for nonHDL-cholesterol (D), HDL-cholesterol (E) and apoAI (F). Data are means ± SEM (n = 6). **P<0.01; #P<0.001; ##P<0.0001 as compared to the control group.

*PFBS, PFHxS and PFOS increase VLDL-triglyceride clearance*

Plasma VLDL-TG levels are determined by the balance between VLDL-TG production and VLDL-TG clearance. To evaluate whether an increased VLDL-TG clearance may have attributed to the reduction in VLDL-TG levels caused by all PFAS, the plasma clearance of [$^3$H]TO-labeled VLDL-like emulsion particles was determined (Fig. 2). As compared to control mice, the plasma half-life of [$^3$H]TO was reduced by PFBS (-51%, P<0.05), PFHxS (-61%, P<0.001) and PFOS (-52%, P<0.01) (Fig. 2A,B), reflected by a significant increase in the uptake of [$^3$H]TO-derived activity by the liver and trends towards an increased uptake by skeletal muscle and white adipose tissue (Fig. 2C).



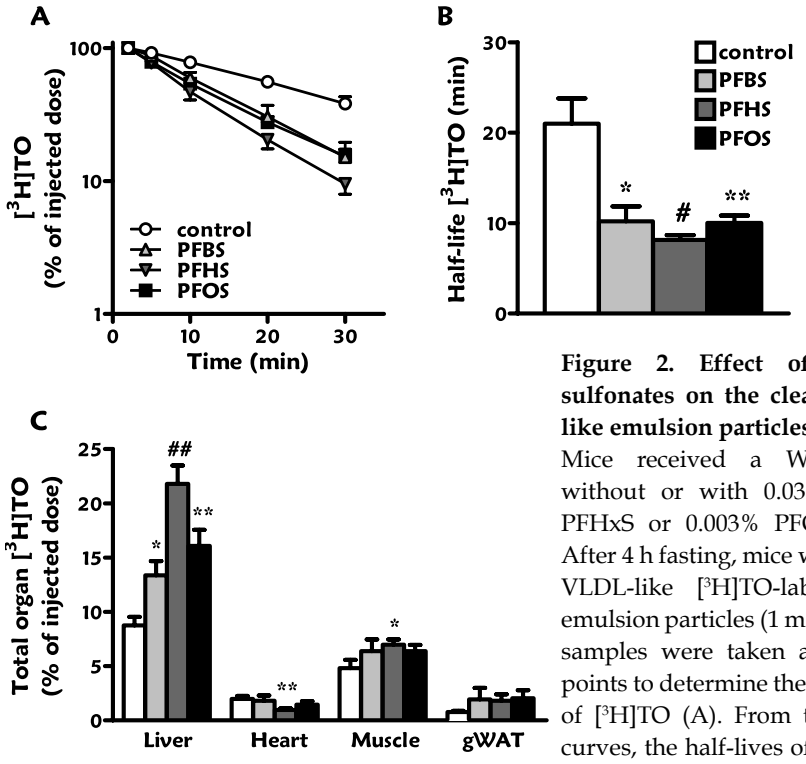


**Figure 2. Effect of perfluoroalkyl sulfonates on the clearance of VLDL-like emulsion particles.**

Mice received a Western-type diet without or with 0.03% PFBS, 0.006% PFHxS or 0.003% PFOS for 4 weeks. After 4 h fasting, mice were injected with VLDL-like [$^3$H]TO-labeled VLDL-like emulsion particles (1 mg TG) and plasma samples were taken at indicated time points to determine the plasma clearance of [$^3$H]TO (A). From the slopes of the curves, the half-lives of $^3$H-activity were calculated (B). At 30 min after injection, various organs [liver, heart, skeletal muscle and gonadal white adipose tissue (gWAT)] were harvested to determine the uptake of $^3$H-activity (C). Data are means ± SEM (n = 4-6). *P<0.05; **P<0.01; $^{\#}$P<0.001; $^{\#\#}$P<0.0001 as compared to the control group.

Since these data are consistent with an increased lipolytic processing, HL and LPL activity were determined in post-heparin plasma (Fig. 3). HL activity was decreased to some extent by PFBS (-28%; P<0.05) and increased by PFHxS (+15%; n.s.) and PFOS (+22%; P<0.05). LPL activity tended to be increased by PFBS (+20%; n.s.) and was significantly and markedly increased by PFHxS (+74%; P<0.001) and PFOS (+54%; P<0.001).

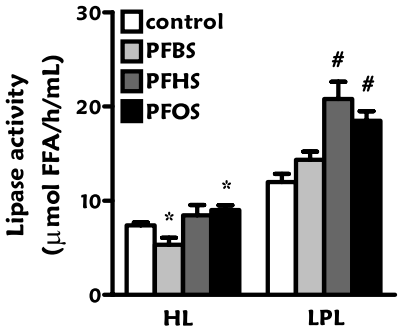


**Figure 3. Effect of perfluoroalkyl sulfonates on plasma hepatic lipase and lipoprotein lipase activity.**
Mice received a Western-type diet without or with 0.03% PFBS, 0.006% PFHxS or 0.003% PFOS for 4 weeks. After 4 h fasting, heparin was injected and postheparin plasma was collected. Plasma was incubated with a [$^3$H]TO-containing substrate mixture in the absence or presence of 1 M NaCl, to estimate both the HL and LPL activity. Data are means ± SEM (n = 8). *P<0.05; #P<0.001 as compared to the control group.

*PFHxS and PFOS decrease VLDL production*

We next determined whether a reduction in VLDL-TG production may also have contributed to the TG-lowering effect of PFAS (Fig. 4). PFBS did not affect VLDL-TG production (Fig. 4A,B) and modestly reduced VLDL-apoB production (-17%; P=0.055) (Fig. 4C). In contrast, the VLDL-TG production rate was markedly decreased by PFHxS (-74%; P<0.0001) and PFOS (-86%; P<0.0001) (Fig. 4A,B). The VLDL-apoB production rate was decreased to similar extents by PFHxS (-76%; P<0.0001) and PFOS (-87%; P<0.0001) (Fig. 4C), indicating that PFHxS and PFOS both reduce the production of VLDL particles without altering their TG content.

*PFHxS and PFOS increase liver weight and hepatic triglyceride content*

To get further insight into the mechanism how PFHxS and PFOS decrease hepatic VLDL-TG production, we determined the weight and lipid content of the liver (Fig. 5). The liver weight was markedly increased by PFHxS (+110%; P<0.0001) and PFOS (+107%; P<0.0001) (Fig. 5A), accompanied by an increased hepatic TG content (+52%; P<0.05 and +192%; P<0.0001, respectively) (Fig. 5B).

PFOS also markedly increased hepatic cholesteryl esters (+94%; P<0.001) (Fig. 5C) and mildly increased free cholesterol (+16%; P<0.05) (Fig. 5D). PFBS on the other hand decreased both hepatic cholesteryl esters (-36%; P<0.05) and free cholesterol (-19%; P<0.05) (Fig. 5C,D). These data indicate that PFHxS and PFOS decrease VLDL-TG production as a result of impaired TG secretion from the liver, leading to hepatomegaly and hepatic steatosis, rather than being a consequence of reduced hepatic lipids available for VLDL production.



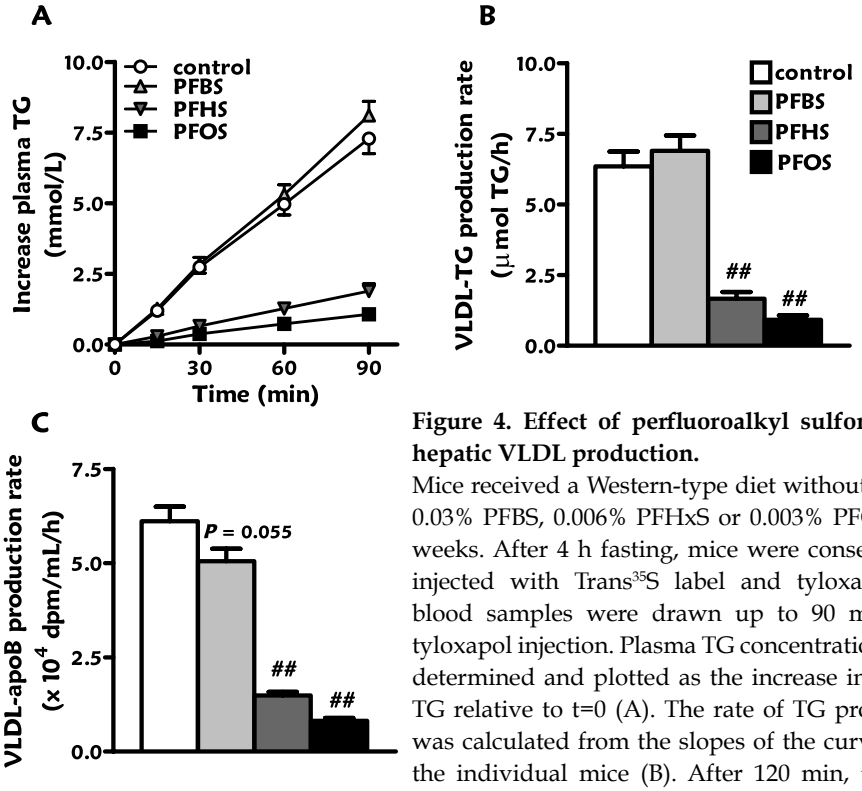


**Figure 4. Effect of perfluoroalkyl sulfonates on hepatic VLDL production.**

Mice received a Western-type diet without or with 0.03% PFBS, 0.006% PFHxS or 0.003% PFOS for 4 weeks. After 4 h fasting, mice were consecutively injected with Trans$^{35}$S label and tyloxapol and blood samples were drawn up to 90 min after tyloxapol injection. Plasma TG concentrations were determined and plotted as the increase in plasma TG relative to t=0 (A). The rate of TG production was calculated from the slopes of the curves from the individual mice (B). After 120 min, the total VLDL fraction was isolated by ultracentrifugation and the rate of newly synthesized VLDL-apoB was determined (C). Data are means ± SEM (n = 7-8). $^{\#\#}$P<0.0001 as compared to the control group.

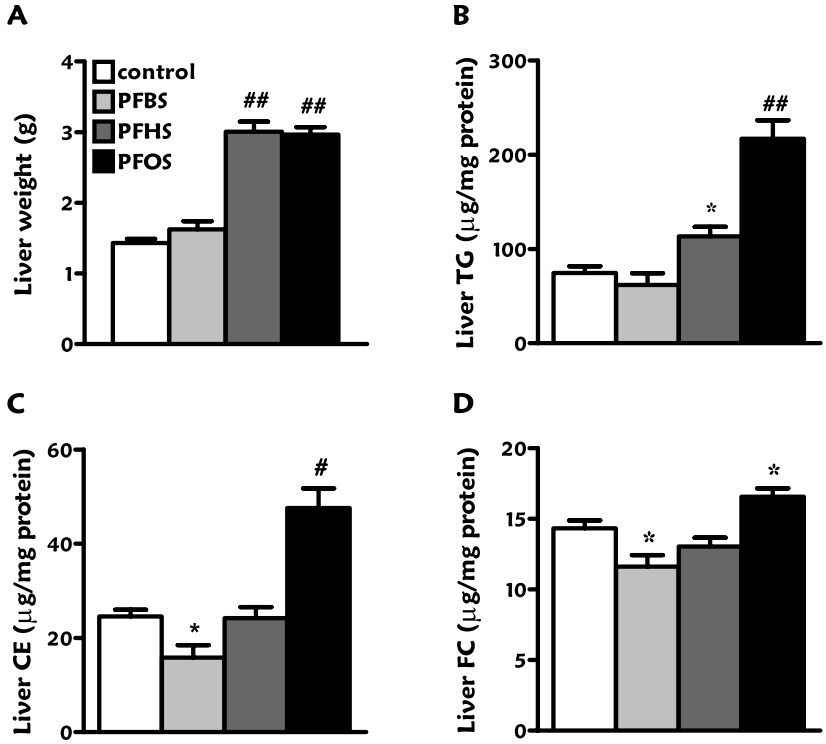


**Figure 5. Effect of perfluoroalkyl sulfonates on liver weight and lipid content.**
Mice received a Western-type diet without or with 0.03% PFBS, 0.006% PFHxS or 0.003% PFOS for 4 weeks. After 6 weeks, livers were collected after a 4 h fast and their weight was determined (A). Liver lipids were extracted and triglycerides (TG) (B), cholesteryl esters (CE) (C) and free cholesterol (FC) (D) were quantified. Data are means ± SEM (n = 6). *P<0.05; #P<0.001; ##P<0.0001 as compared to the control group.



*PFHxS and PFOS decrease white perigonadal fat pad weight, plasma free fatty acids and plasma glycerol*

Since the accumulation of hepatic TG as induced by PFHxS and PFOS, accompanied by a marked reduction in VLDL-TG production, may result in reduced supply of VLDL-TG-derived FA for storage in adipose tissue, we determined the effect of PFAS on perigonadal fat pad weight (Fig. 6A). Indeed, perigonadal fat pad weight was decreased by PFHxS (-28%; P<0.01) and PFOS (-25%; P<0.05), whereas PFBS had no effect. This was accompanied by reduced plasma FA (-41%; P<0.0001 and -37%; P<0.0001) (Fig. 6B) and plasma glycerol (-50%; P<0.0001 and -42%; P<0.0001) (Fig. 6C), both of which are mainly derived from TG lipolysis in adipose tissue.

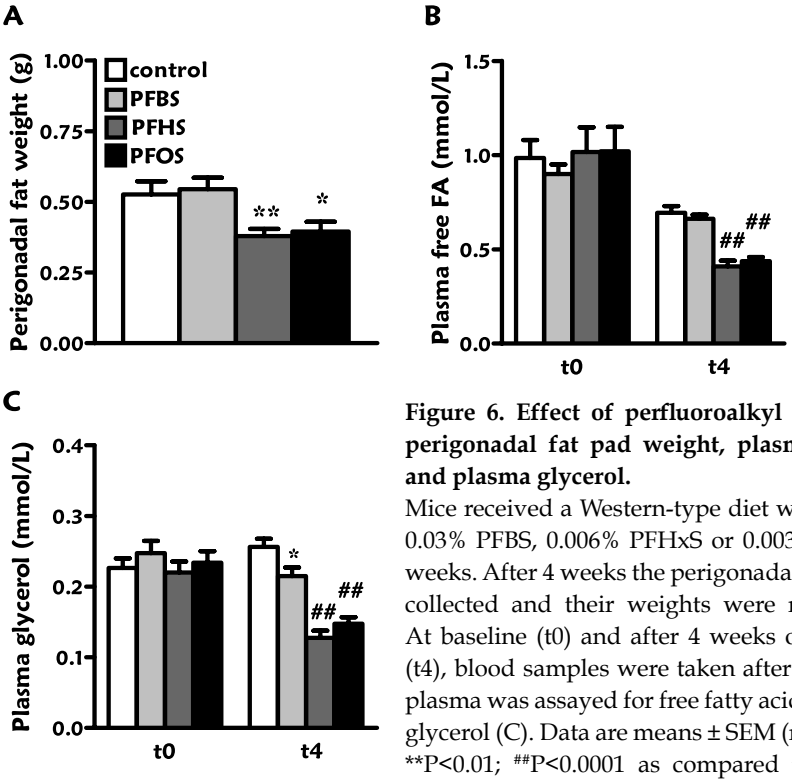


**Figure 6. Effect of perfluoroalkyl sulfonates on perigonadal fat pad weight, plasma fatty acids and plasma glycerol.**
Mice received a Western-type diet without or with 0.03% PFBS, 0.006% PFHxS or 0.003% PFOS for 4 weeks. After 4 weeks the perigonadal fat pads were collected and their weights were measured (A). At baseline (t0) and after 4 weeks of intervention (t4), blood samples were taken after a 4 h fast and plasma was assayed for free fatty acids (FA) (B) and glycerol (C). Data are means ± SEM (n = 6). *P<0.05; **P<0.01; ##P<0.0001 as compared to the control group.



*PFHxS and PFOS decrease fecal bile acid excretion*

To determine whether the changes in hepatic lipid content were accompanied by an effect on cholesterol excretion into feces, the effect of the PFAS on fecal output of neutral sterols and bile acids was determined (Fig. 7). The various PFAS did not affect neutral sterol secretion (Fig. 7A), but excretion of bile acids was decreased by PFHxS (-41%, P<0.05) and PFOS (-50%, P<0.01) (Fig. 7B).

*PFHxS and PFOS decrease HDL-cholesterol clearance*

Since both PFHxS and PFOS decreased plasma levels of HDL-cholesterol and apoAI, we investigated whether this was caused by increased HDL turnover. HDL-cholesterol clearance was determined using autologous [$^3$H]CO-labeled HDL (Fig. 8). Treatment with PFHxS and PFOS increased the clearance of the [$^3$H]CO tracer (Fig. 8A), reflected by an decrease of the half-life of [$^3$H]CO (PFHxS -33%; P<0.001, PFOS -35%; P<0.0001) (Table 2). However, calculation

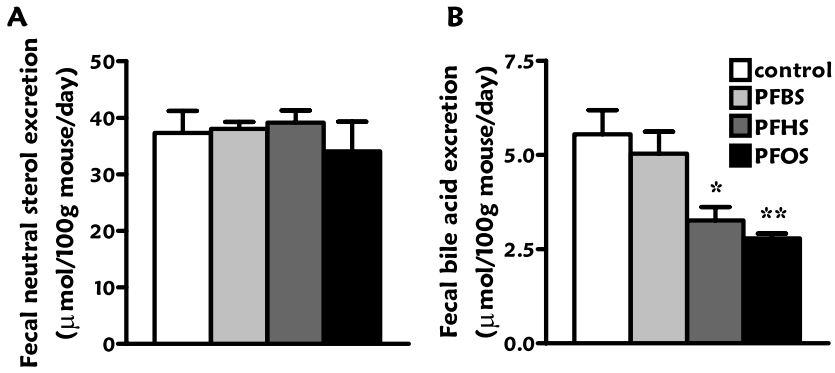


**Figure 7. Effect of perfluoroalkyl sulfonates on fecal bile acid excretion.**
Mice received a Western-type diet without or with 0.03% PFBS, 0.006% PFHxS or 0.003% PFOS for 4 weeks. Feces were collected during a 48-72 h time period at 2 consecutive time points, and neutral sterols (A) and bile acids (B) were quantified by gas chromatographic analysis. Data are means ± SEM (n = 6). *P<0.05; **P<0.01 as compared to the control group.

of the fractional catabolic rate (FCR) of HDL-cholesterol, taking into account the different pool size of HDL-cholesterol after treatment with the various PFAS, showed that the clearance of HDL-cholesterol (calculated as mM HDL-cholesterol cleared per hour) was actually decreased by PFHxS (-48%; P<0.01) and PFOS (-65% P<0.001). The reduction in HDL-cholesterol clearance may be related to a decrease in plasma CETP activity. Indeed, plasma CETP mass was decreased by PFBS (-20%; P<0.01), PFHxS (-36%; P<0.001) and PFOS (-38%; P<0.0001) (Fig. 8B). Collectively, these data indicate that the observed reduction in plasma HDL-cholesterol is likely caused by impaired production and/or maturation of HDL particles rather than enhanced clearance.



**Table 2.** Effect of perfluoroalkyl sulfonates on the fractional catabolic rate of HDL-C.

| | Control | PFBS | PFHxS | PFOS |
|---|---|---|---|---|
| t½ (h) | 3.26 ± 0.11 | 2.89 ± 0.15 | 2.19 ± 0.12 $^{\#}$ | 2.13 ± 0.09 $^{\#\#}$ |
| FCR (pools HDL-C/h) | 0.21 ± 0.01 | 0.24 ± 0.01 | 0.32 ± 0.02 $^{\#}$ | 0.33 ± 0.01 $^{\#\#}$ |
| FCR (mM HDL-C/h) | 0.23 ± 0.02 | 0.25 ± 0.04 | 0.12 ± 0.03 $^{**}$ | 0.08 ± 0.02 $^{\#}$ |

Mice received a Western-type diet without or with 0.03% PFBS, 0.006% PFHxS or 0.003% PFOS for 4 weeks. Mice were injected with autologous [$^{3}$H]CO-labeled HDL. The data from Fig. 8A were used to calculate the plasma half-life and fractional catabolic rate (FCR) as pools or mM of HDL-C cleared per hour. Values are means ± SEM (n=6). **P<0.01, $^{\#}$P<0.001 and $^{\#\#}$P<0.0001.

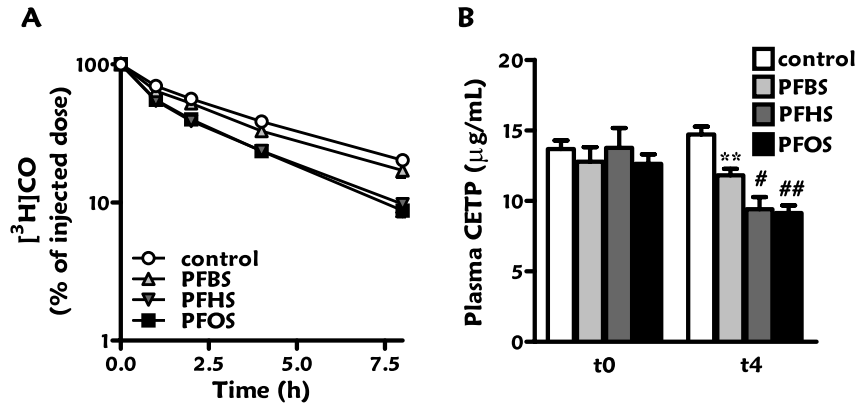


**Figure 8. Effect of perfluoroalkyl sulfonates on the clearance of HDL-cholesterol.**
Mice received a Western-type diet without or with 0.03% PFBS, 0.006% PFHxS or 0.003% PFOS for 4 weeks. Mice were injected with autologous [$^3$H]CO-labeled HDL and plasma samples were taken at indicated time points to determine the plasma clearance of [$^3$H]CO (A). In a separate experiment, 4 h-fasted blood was taken at baseline (t0) and after 4 weeks of intervention (t4) and plasma was assayed for CETP mass (B). Data are means ± SEM (n = 5). **P<0.01; #P<0.001; ##P<0.0001 as compared to control.



*PFHxS and PFOS affect hepatic expression of genes involved in lipid metabolism*

To further investigate the mechanism(s) by which PFAS affect lipid metabolism, we determined the hepatic expression profile of 16331 well characterized mouse genes. As compared to the control group, PFAS resulted in 438 (PFBS), 4230 (PFHxS), and 3986 (PFOS) differentially expressed genes (Supplemental Fig. 1). A selection of genes involved in lipid metabolism is depicted in Table 3. In general, the expression of many of these genes was affected by PFHxS and PFOS, but not by PFBS.

Both PFHxS and PFOS affected genes involved in VLDL metabolism. PFHxS and PFOS largely increased *Lpl* expression, in line with increased VLDL-TG clearance and plasma LPL activity. Despite some differences with respect to the individual effects of both compounds, PFHxS and PFOS both upregulated genes involved in FA uptake and transport (*Slc27a1, Slc27a2, Slc27a4,* and *Cd36*), FA binding and activation (*Fabp4, Acsl1,* and *Acsl3, Acsl4*), and FA oxidation (C*pt1b, Acox1, Acox2, Ehhadh, Acaa1a*, and *Acaa1b*). PFHxS and PFOS also increased important genes involved in TG synthesis and VLDL assembly/secretion (*Dgat1, Scd2,* and *Mttp*). Taken together, these data indicate that the liver attempts to compensate for the large reduction in

VLDL production by increasing FA oxidation, binding and activation, and by mobilisation of FA for TG synthesis and secretion as VLDL. Most likely, these pathways are overshadowed by increased FA uptake and transport resulting in hepatomegaly with hepatic TG accumulation, possibly related to PXR activation[218]. PFHxS and PFOS also affected genes involved in HDL metabolism. They decreased genes involved in HDL synthesis (*Apoa1*) and maturation (*Abca1, Lcat*) and decreased the principle gene involved in HDL clearance (*Scarb1*). These data indicate that the observed large reduction in both HDL-C and apoAI are actually caused by decreased HDL synthesis and maturation, which results in a compensatory increase in SR-BI expression. Finally, PFHxS and PFOS affected genes in hepatic cholesterol metabolism. Both increased *Acat1*, involved in storage of cholesterol as cholesteryl esters, and decreased genes involved in bile acid formation (*Cyp7a1*) and secretion (*Slc10a1, Slc10a2,* and *Abcb11*) as well as cholesterol excretion (*Abcg5, Abcg8*). These data are in line with the observation that PFOS increases the hepatic cholesterol content and that both PFHS and PFOS decrease fecal bile acid secretion.

**Table 3.** Effect of perfluoroalkyl sulfonates on hepatic expression of genes encoding transcription factors and proteins involved in lipid metabolism.

| | | **PFBS** | | **PFHxS** | | **PFOS** | |
|---|---|---|---|---|---|---|---|
| protein | gene | Δ | q-value | Δ | q-value | Δ | q-value |
| **Transcription factors** | | | | | | | |
| LXR alpha | *Nr1h3* | -1.00 | 0.692 | **-1.19** | **0.039** | **-1.27** | **0.008** |
| LXR beta | *Nr1h2* | -1.16 | 0.304 | **-1.24** | **0.046** | -1.08 | 0.277 |
| PPAR alpha | *Ppara* | 1.10 | 0.453 | **-1.40** | **0.002** | **-1.40** | **0.003** |
| PPAR gamma | *Pparg* | 1.07 | 0.619 | 1.25 | 0.179 | **1.52** | **0.042** |
| CAR | *Nr1i3* | -1.13 | 0.546 | -1.01 | 0.443 | **1.82** | **0.007** |
| FXR | *Nr1h4* | -1.01 | 0.676 | **1.19** | **0.035** | **1.21** | **0.028** |
| PXR | *Nr1i2* | -1.03 | 0.622 | **1.28** | **0.006** | **1.59** | **<0.001** |
| PGC1alpha | *Ppargc1a* | -0.18 | 0.547 | **-1.39** | **<0.001** | **-1.27** | **<0.001** |
| PGC1beta | *Ppargc1b* | -0.30 | 0.458 | -0.47 | 0.119 | -0.44 | 0.139 |

| | | PFBS | | PFHxS | | PFOS | |
|---|---|---|---|---|---|---|---|
| protein | gene | Δ | q-value | Δ | q-value | Δ | q-value |
| **Lipolysis** | | | | | | | |
| LPL | *Lpl* | 1.02 | 0.666 | **4.27** | **<0.001** | **2.13** | **<0.001** |
| ApoCI | *Apoc1* | -1.04 | 0.285 | -1.03 | 0.209 | **-1.07** | **0.020** |
| ApoCII | *Apoc2* | 1.01 | 0.672 | -1.16 | 0.056 | **-1.30** | **0.003** |
| ApoCIII | *Apoc3* | -1.00 | 0.683 | -1.04 | 0.139 | -1.01 | 0.370 |
| ApoAV | *Apoa5* | **-1.32** | **0.013** | **-2.01** | **<0.001** | **-1.61** | **<0.001** |
| GPIHBP1 | *Gpihbp1* | -1.25 | 0.189 | 1.19 | 0.103 | **1.36** | **0.012** |
| **FA uptake and transport** | | | | | | | |
| FATPa1 | *Slc27a1* | 1.20 | 0.414 | **2.90** | **<0.001** | **2.33** | **<0.001** |
| FATPa2 | *Slc27a2* | 1.10 | 0.060 | **1.08** | **0.022** | **1.07** | **0.043** |
| FATPa4 | *Slc27a4* | -1.01 | 0.684 | **2.84** | **<0.001** | **2.08** | **<0.001** |
| FATPa5 | *Slc27a5* | -1.00 | 0.683 | **-1.11** | **0.047** | -1.08 | 0.127 |
| CD36 | *Cd36* | **1.62** | **0.001** | **3.48** | **<0.001** | **3.40** | **<0.001** |
| LDLR | *Ldlr* | 1.02 | 0.672 | 1.14 | 0.234 | -1.23 | 0.137 |
| PCSK9 | *Pcsk9* | -1.08 | 0.636 | 1.40 | 0.172 | -1.48 | 0.142 |
| **FA binding and activation** | | | | | | | |
| FABP1 | *Fabp1* | -1.02 | 0.573 | **1.07** | **0.048** | 1.06 | 0.087 |
| FABP2 | *Fabp2* | -1.30 | 0.069 | **-2.04** | **<0.001** | **-2.20** | **<0.001** |
| FABP4 | *Fabp4* | 1.51 | 0.077 | **3.25** | **<0.001** | **2.21** | **<0.001** |
| FABP6 | *Fabp6* | 1.03 | 0.643 | -1.12 | 0.199 | -1.08 | 0.303 |
| FABP7 | *Fabp7* | -1.16 | 0.546 | **-2.20** | **0.004** | -1.35 | 0.169 |
| ACSL1 | *Acsl1* | **1.31** | **0.008** | **1.85** | **<0.001** | **1.73** | **<0.001** |
| ACSL3 | *Acsl3* | 1.19 | 0.482 | **2.98** | **<0.001** | **1.71** | **0.016** |
| ACSL4 | *Acsl4* | 1.19 | 0.170 | **2.08** | **<0.001** | **1.40** | **0.001** |
| ACSL5 | *Acsl5* | -1.10 | 0.437 | **1.42** | **0.002** | 1.03 | 0.407 |
| ACSS1 | *Acss1* | -1.01 | 0.671 | **1.23** | **0.021** | 1.18 | 0.057 |
| ACSS2 | *Acss2* | -1.24 | 0.498 | **1.95** | **0.023** | -1.26 | 0.257 |
| ACSM1 | *Acsm1* | 1.03 | 0.568 | **-1.19** | **0.004** | -1.04 | 0.305 |
| ACSM2 | *Acsm2* | 1.19 | 0.057 | 1.02 | 0.360 | -1.02 | 0.371 |
| ACSM3 | *Acsm3* | -1.27 | 0.080 | **-1.32** | **0.005** | **-1.40** | **0.001** |
| ACSM5 | *Acsm5* | -1.24 | 0.116 | -1.05 | 0.316 | 1.06 | 0.300 |

| | | PFBS | | PFHxS | | PFOS | |
|---|---|---|---|---|---|---|---|
| protein | gene | Δ | q-value | Δ | q-value | Δ | q-value |
| **FA oxidation** | | | | | | | |
| CPT1a | *Cpt1a* | 1.01 | 0.675 | -1.16 | 0.067 | -1.12 | 0.143 |
| CPT1b | *Cpt1b* | 1.04 | 0.645 | **2.91** | **<0.001** | **2.37** | **<0.001** |
| ACO1 | *Acox1* | 1.14 | 0.071 | **1.46** | **<0.001** | **1.39** | **<0.001** |
| ACO2 | *Acox2* | 1.02 | 0.629 | **1.20** | **0.003** | **1.33** | **<0.001** |
| ACO3 | *Acox3* | 1.07 | 0.506 | -1.16 | 0.081 | -1.08 | 0.240 |
| Bifunctional enzyme | *Ehhadh* | **1.37** | **0.008** | **3.19** | **<0.001** | **2.89** | **<0.001** |
| Thiolase 1a | *Acaa1a* | 1.21 | 0.154 | **1.83** | **<0.001** | **1.82** | **<0.001** |
| Thiolase 1b | *Acaa1b* | 1.10 | 0.069 | **1.29** | **<0.001** | **1.24** | **<0.001** |
| Thiolase 2 | *Acaa2* | -1.03 | 0.479 | **1.08** | **0.029** | 1.06 | 0.107 |
| **FA/TG synthesis** | | | | | | | |
| FAS | *Fasn* | -1.42 | 0.403 | 1.53 | 0.135 | -1.13 | 0.374 |
| DGAT1 | *Dgat1* | -1.05 | 0.581 | **1.39** | **0.006** | **1.37** | **0.008** |
| DGAT2 | *Dgat2* | -1.09 | 0.360 | **-1.25** | **0.005** | **-1.16** | **0.042** |
| SCD1 | *Scd1* | -1.54 | 0.109 | 1.18 | 0.226 | -1.03 | 0.420 |
| SCD2 | *Scd2* | 1.14 | 0.282 | **1.65** | **<0.001** | **1.25** | **0.013** |
| ACLY | *Acly* | -1.49 | 0.292 | 1.11 | 0.366 | **-2.47** | **0.003** |
| S14 | *Thrsp* | -1.28 | 0.516 | 1.17 | 0.349 | 1.12 | 0.389 |
| **VLDL assembly** | | | | | | | |
| ApoB | *Apob* | -1.00 | 0.672 | -1.07 | 0.073 | **-1.11** | **0.012** |
| ApoBEC | *Apobec1* | **1.50** | **0.045** | 1.16 | 0.174 | 1.03 | 0.413 |
| MTP | *Mttp* | 1.18 | 0.171 | **1.27** | **0.007** | **1.22** | **0.020** |
| **Cholesterol synthesis** | | | | | | | |
| ACLY | *Acly* | -1.49 | 0.292 | 1.11 | 0.366 | **-2.47** | **0.003** |
| HMG CoA reductase | *Hmgcr* | -1.07 | 0.629 | **1.62** | **0.045** | -1.28 | 0.204 |
| HMG CoA synthase | *Hmgcs2* | 1.03 | 0.573 | -1.03 | 0.337 | 1.05 | 0.244 |
| Squalene synthase | *Fdft1* | -1.25 | 0.342 | **1.78** | **0.003** | -1.08 | 0.360 |
| **Cholesterol storage** | | | | | | | |
| ACAT1 | *Acat1* | -1.06 | 0.370 | **1.17** | **0.002** | **1.10** | **0.034** |
| ACAT2 | *Acat2* | -1.10 | 0.569 | **1.77** | **0.006** | -1.03 | 0.429 |

| | | PFBS | | PFHxS | | PFOS | |
|---|---|---|---|---|---|---|---|
| protein | gene | Δ | q-value | Δ | q-value | Δ | q-value |
| **Cholesterol uptake** | | | | | | | |
| LDLR | *Ldlr* | 1.02 | 0.672 | 1.14 | 0.234 | -1.23 | 0.137 |
| PCSK9 | *Pcsk9* | -1.08 | 0.636 | 1.40 | 0.172 | -1.48 | 0.142 |
| **Cholesterol metabolism** | | | | | | | |
| CYP7A1 | *Cyp7a1* | -1.19 | 0.624 | **-3.20** | **0.037** | **-3.78** | **0.021** |
| IBAT | *Slc10a2* | 1.52 | 0.300 | **-2.45** | **0.005** | **-2.80** | **0.002** |
| BSEP | *Abcb11* | -1.19 | 0.198 | **-1.65** | **<0.001** | **-1.74** | **<0.001** |
| NTCP | *Slc10a1* | -1.24 | 0.191 | **-1.32** | **0.020** | **-1.34** | **0.014** |
| **Cholesterol excretion** | | | | | | | |
| ABCG5 | *Abcg5* | -1.38 | 0.061 | **-2.06** | **<0.001** | **-1.83** | **<0.001** |
| ABCG8 | *Abcg8* | -1.61 | 0.061 | **-2.46** | **<0.001** | **-2.38** | **<0.001** |
| **HDL formation** | | | | | | | |
| ApoAI | *Apoa1* | -1.10 | 0.148 | **-1.35** | **<0.001** | **-1.45** | **<0.001** |
| ApoAII | *Apoa2* | -1.05 | 0.289 | -1.02 | 0.270 | -1.01 | 0.373 |
| **HDL maturation** | | | | | | | |
| ABCA1 | *Abca1* | 1.01 | 0.635 | **-1.14** | **0.024** | -1.09 | 0.092 |
| LCAT | *Lcat* | 1.01 | 0.669 | **-1.43** | **<0.001** | **-1.35** | **<0.001** |
| **HDL remodeling** | | | | | | | |
| PLTP | *Pltp* | -1.07 | 0.629 | **2.28** | **0.002** | 1.31 | 0.171 |
| Endothelial lipase | *Lipg* | -1.15 | 0.457 | -1.04 | 0.398 | -1.19 | 0.185 |
| HL | *Lipc* | -1.17 | 0.081 | **-1.70** | **<0.001** | **-1.40** | **<0.001** |
| **HDL uptake** | | | | | | | |
| SRB1 | *Scarb1* | -1.20 | 0.168 | **-2.31** | **<0.001** | **-1.76** | **<0.001** |

Mice received a Western-type diet without or with perfluoroalkyl sulfonates. Livers were collected after a 4 h fast, total RNA was extracted from livers of individual mice (n=6 per group), and gene expression analysis was performed using Affymetrix GeneChip® mouse genome 430 2.0 arrays. Data represent mean fold change (Δ) as compared to the control group. Q-values are corrected for multiple testing. Values in bold are considered significant (q-value <0.05).



## Discussion

This study investigated the mechanism underlying the effect of PFHxS and PFOS on plasma lipoprotein metabolism, as well as the importance of the alkyl chain length using E3L.CETP mice, a well-established model for human-like lipoprotein metabolism[114, 117, 118, 185, 219]. At high exposure levels, PFHxS and

PFOS lowered plasma TG, VLDL-cholesterol and HDL-cholesterol, which is consistent with previous observations in toxicological studies[207 - 211, 220, 221]. In addition, it was demonstrated that the potency of PFAS to lower plasma lipids decreases with decreasing alkyl chain length (PFOS>PFHxS>PFBS). Mechanistic studies revealed that PFHxS and PFOS decreased lipoprotein levels primarily by severely impairing the production of VLDL and HDL, resulting in hepatomegaly with steatosis as well as combined hypolipidemia.

VLDL levels were decreased by all PFAS tested, albeit with different potency. Considering that the daily intake of PFBS (30 mg/kg/d) was five times that of PFHxS (6 mg/kg/d) and ten times that of PFOS (3 mg/kg/d), PFBS had considerably less effects compared with PFHxS and PFOS. This may, in part, be due to the much lower serum PFBS concentrations than those observed for PFHxS and PFOS. All PFAS tested accelerated VLDL-TG clearance from plasma to a similar extent. PFHxS and PFOS increased plasma LPL activity as well as LPL mRNA in the liver, suggesting LPL activity is increased due to an overall higher LPL expression, which increases the capacity of plasma to enhance VLDL-TG clearance. Accordingly, the uptake of fatty acids was increased in the LPL-expressing organs, skeletal muscle and white adipose tissue (WAT) as well as the liver (i.e. mainly within VLDL remnants). In contrast, PFBS did not increase hepatic LPL mRNA or plasma LPL activity, nor did it differentially affect hepatic gene expression of activators (*apoA5, apoC2*) or inhibitors (*apoC1, apoC3*) of LPL activity as compared to PFHxS and PFOS. This suggests that PFBS accelerates VLDL-TG clearance through a different, as yet unidentified mechanism.

The observation that PFHxS and PFOS were more effective in VLDL lowering than PFBS can be explained by the fact that PFHxS and PFOS, but not PFBS, severely impaired hepatic VLDL-TG production by as much as ~80%. This was a result of reduced VLDL particle production, because PFHxS and PFOS equally decreased the production of VLDL-TG and VLDL-apoB. The decreased VLDL-TG production rate is presumably not explained by reduced availability of liver TG for VLDL synthesis, because both PFHxS and PFOS increased rather than reduced the hepatic TG content, similarly as observed in rats[209]. More likely, PFHxS and PFOS prevent the secretion of VLDL from the liver, resulting in lipid accumulation within the liver. This increase in liver lipid content may have led to upregulation of hepatic genes involved in FA binding and activation and FA

β-oxidation, and in mobilisation of FA for TG synthesis (*Dgat1*) and secretion as VLDL (*Mttp*) in an attempt to lower hepatic FA and thus TG levels.

Collectively, the data suggest that PFHxS and PFOS primarily impair the secretion of VLDL by the liver, leading to hepatic steatosis. The reduced production of VLDL-TG limits substrate availability for LPL on peripheral tissues, leading to less FA delivery to WAT and skeletal muscle. Because LPL-mediated delivery of VLDL-TG-derived FA is a strong determinant of WAT mass and obesity[138], this can explain why PFHxS and PFOS, but not PFBS, reduced gonadal WAT mass accompanied by a reduction of plasma free FA and glycerol that are mainly derived from TG lipolysis in adipose tissue.

PFHxS and PFOS also markedly decreased HDL levels, reflected by a reduction in HDL-C and apoAI. Since PFHxS and PFOS decreased HDL turnover in terms of mM HDL-C cleared per hour, these compounds thus lower HDL levels by reducing the synthesis and maturation of HDL. This is further supported by the fact that PFHxS and PFOS, but not PFBS, decrease the hepatic expression of *Apoa1, Abca1* and *Lcat*, important for the generation of discoidal HDL precursors (apoAI), lipidation of these HDL precursors (ABCA1), and maturation of HDL (LCAT). The mechanism underlying the decrease in HDL turnover may relate to the observed decrease in hepatic *Scarb1* expression and plasma CETP mass.



Nuclear receptors are important regulators of lipid metabolism, and changes in their expression patterns might thus underlie the effects of PFHxS and PFOS on lipid metabolism. PFOS has been demonstrated to trans-activate PPARα[222] and most effects of PFAA have in fact been attributed to activation of the PPARα pathway[208, 209, 223, 224]. Indeed, PFHxS and PFOS increased the hepatic expression of genes involved in both FA uptake and FA β-oxidation, and induced hepatomegaly similar as observed after treatment of E3L.CETP mice with the PPARα agonist fenofibrate[219]. However, PFHxS and PFOS also caused hepatic steatosis, decreased VLDL-TG production and decreased HDL levels, whereas fenofibrate did not induce hepatic steatosis, increased VLDL-TG production and increased HDL levels[219], indicating that additional pathways must be involved.

Xenobiotic metabolism that is provoked by chemical pollutants for detoxification likely represents such an additional pathway. This involves the xenosensor receptors, pregnane X receptor (PXR) and constitutive androstane

receptor (CAR). Initially identified as xenosensors, it is now evident that PXR (and CAR) also trigger pleiotropic effects on liver function[218]. PFOS has been shown to interact with PXR and CAR[85]. In the present study, PFOS increased PXR expression, accompanied by an increase in *Cyp3a11* (1.2-fold) and decrease in *Cyp7a1* (-3.8-fold), both typical for PXR activation. In fact, the effect of PFOS on both liver TG and cholesterol accumulation, and reduction in HDL and fecal bile acids may all be explained by PXR activation. Indeed, specific PXR activation in E3L.CETP mice also reduces HDL accompanied by decreased hepatic expression of apoAI, ABCA1, LCAT and HL[85]. In addition, both PCN[85] and constitutive PXR expression[82] caused accumulation of TG and cholesterol in the liver[218], which is likely explained by the profound induction of FA transport genes including CD36 and FATP as observed in this study. Collectively, our data thus suggest that the effects of PFAS on lipid metabolism are the combined result of activation of nuclear receptors that include at least PPARα and PXR with PFHxS and PFOS as most potent activators.

This study confirms the findings from previous toxicological studies in animal models that PFHxS and PFOS reduce plasma TG and TC[207 - 211, 220, 221], and provides mechanistic explanations. These observations are in seeming contrast with epidemiological studies in humans that have shown modest increases in nonHDL-C. Reductions in TC and TG have not been observed among exposed workers[206] with serum PFOS concentrations as high as 10 μg/mL. On the contrary, recent cross-sectional studies in general population cohorts from the United States even showed positive correlations between PFOS levels and serum cholesterol, due to a positive correlation with nonHDL-C[204, 205]. However, a positive association of PFOS with nonHDL-C in workers with significantly higher serum concentrations than those found in the general population studies was not found[206]. In a recent report, no association of serum PFOS was found for either LDL or nonHDL-C, while a positive association was found for HDL-C in 723 adult Nunavik Inuit[225]. These observations and the mechanistic work reported in our present study suggest that the positive correlation between serum PFOS levels and cholesterol levels that has been found in some general population cohorts is not causal.

Large species differences have been reported with respect to the relative PFOS-induced activation of PPARα, PXR and CAR[85]. Since it is known that

humans are less sensitive to PPARα-related effects than rodents, with approx. 10-fold lower expression of PPARα in liver compared with mice[226], it is possible that in humans PPARα effects do not manifest themselves until higher body burdens are achieved, which would be consistent with the observations in cynomolgus monkeys given daily capsule doses of PFOS[207]. In the latter study, a marker of peroxisome proliferation was increased marginally but with statistical significance in male and female cynomolgus monkeys only in the high-dose group (0.75 mg/kg/d for six months). Serum TC and HDL-C were strongly reduced in this group without a reduction in TG, and hepatic steatosis was clearly apparent. Thus, these findings support the potential of a mixed PPARα and PXR response in the monkey.

In conclusion, we have demonstrated that PFHxS and PFOS reduce plasma TG and TC in E3L.CETP mice, by lowering both VLDL and HDL. Lowering of VLDL was the result of a decreased hepatic VLDL-TG production and increased VLDL-TG clearance. Lowering of HDL was explained by decreased production and maturation. These effects are dependent on the alkyl chain length, as PFBS had negligible effects, and can be explained by the combined action of PPARα and PXR/CAR activation.



**Acknowledgements**

This work was performed within the framework of the Leiden Center for Cardiovascular Research LUMC-TNO and supported by grants from the Nutrigenomics Consortium/Top Institute Food and Nutrition (TiFN), the Center for Medical Systems Biology (CMSB) and the Netherlands Consortium for Systems Biology (NCSB), within the framework of the Netherlands Genomics Initiative (NGI/NWO), the Netherlands Organization for Health Care Research Medical Sciences (ZON-MW project nr. 948 000 04), the Netherlands Organization for Scientific Research (NWO VIDI grant 917.36.351 to PCN Rensen). PCN Rensen is an Established Investigator of the Netherlands Heart Foundation (2009T038). 3M Company, St. Paul, MN, USA, is gratefully acknowledged for its financial support of this study. We thank Marian Bekkers, Simone van der Drift-Droog and Karin Toet for excellent technical assistance.

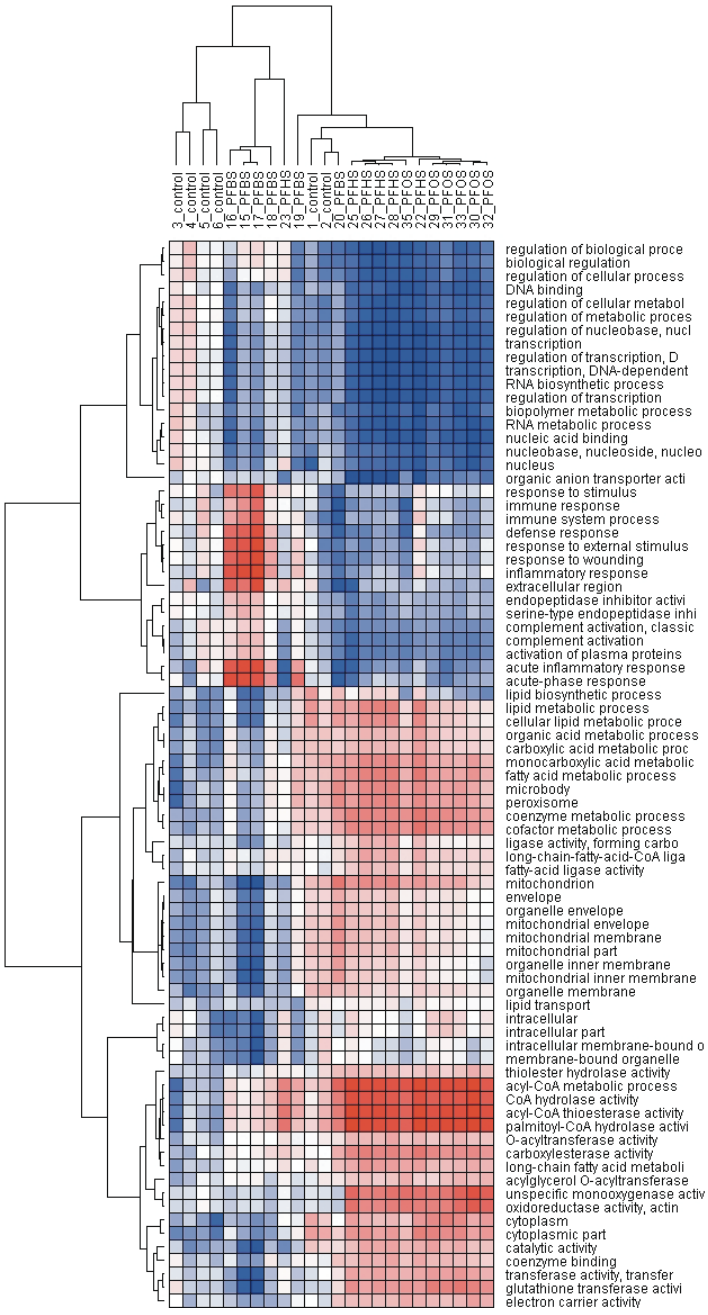


**Supplemental Figure 1. Hierarchical clustering of scores for biological processes.**
T-profiler analysis was performed using expression values corrected for mean expression in the control group. Pathways and biological processes with significant scores (>4 or <-4) in 5 or 6 animals of at least one of the PFAS groups were selected. A hierarchical clustering of these pathways and biological processes and their scores in all samples was generated in GenePattern (Broad Institute, MIT, USA). Red indicates positive score (majority of genes in set are up-regulated), blue indicate negative score (majority of genes in set are down-regulated).

# Chapter 6

## Gene expression profiles distinguish fasting and high-fat diet induced steatosis

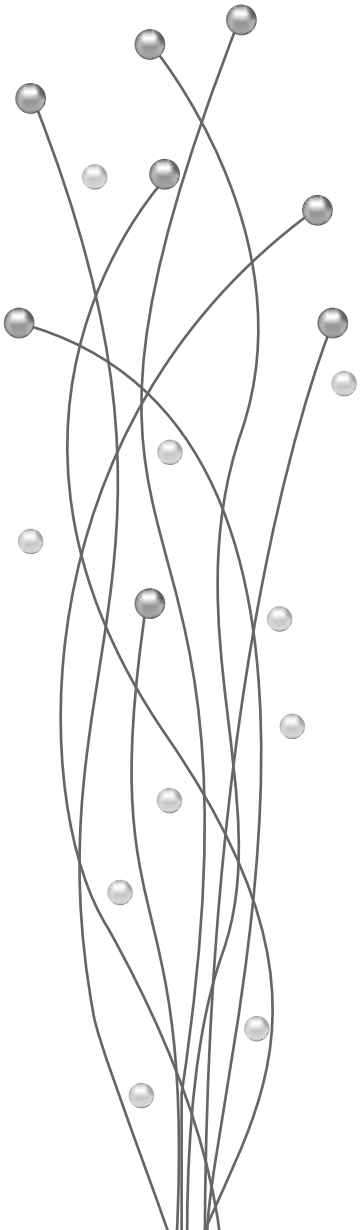

Silvia Bijland*
Anja E Schiel*
Sjoerd AA van den Berg
Peter J Voshol
Louis M Havekes
Rune R Frants
Ko Willems van Dijk

* both authors contributed equally

High-fat diet-induced hepatic triglyceride accumulation or steatosis is associated with hepatic insulin resistance and hypothesized to play a role in the development of the pathology associated with the metabolic syndrome. However, steatosis is also induced by prolonged fasting, which is not associated with hepatic insulin resistance. To investigate whether different pathways lead to steatosis, we performed microarray analysis on livers of mice either fasted for 16 hours or fed a high fat diet for 2 weeks. We analysed expression of 7,500 genes and subsequently performed a pathway analysis to identify changes in hepatic gene expression in both models. Fasting induced a high number of differentially expressed hepatic genes, resulting in a change towards an energy saving phenotype. In contrast, only a small number of genes were differentially expressed after high fat diet. Fasting promoted gluconeogenesis and β-oxidation, strongly suppressed cholesterol synthesis and activated pathways to preserve hepatic function. High fat diet induced steatosis was accompanied by the activation of *Scd1* and the lipogenic transcription factor *Srebp-1c*, both implicated in the development of hepatic insulin resistance. Thus, hepatic lipid overload caused by either prolonged fasting or a high-fat diet activates significantly different gene expression programs.

## Introduction

The metabolic syndrome represents a cluster of well-documented risk factors for the development of type 2 diabetes and cardiovascular disease. In addition to visceral obesity, dyslipidemia and insulin resistance (IR), excessive triglyceride (TG) accumulation in the liver has been implicated to play a role in the development of the metabolic syndrome[227]. Whether hepatic steatosis is primary or secondary to the development of insulin resistance may depend on specific pathology[228]. Numerous studies have shown that high fat diet induces hepatic steatosis, insulin resistance and obesity in rodents. Fasting, on the other hand, also increases hepatic TG content and this is due to the uptake of of adipocyte derived free fatty acids (FA's). This form of hepatic steatosis, in response to a physiological stimulus most living beings are exposed to on a regular basis, develops in the absence of hepatic insulin resistance[229].

This raises the question what the difference is between the development of hepatic steatosis due to increased dietary intake of fat and an increase of available FA's due to release from adipose tissue. Since the liver plays a central role in coordinating the metabolic effects in response to alterations in nutrient availability, we speculated that the control of the expression of key genes involved in metabolism is differently regulated in these distinct forms of hepatic steatosis.

To examine hepatic gene expression in response to hepatic steatosis of different aetiology, we performed a microarray analysis on steatotic livers from mice fed a high fat diet for 2 weeks or fasted for 16 hours. Fasting-induced steatosis is not associated with hepatic insulin resistance[229] while 1 week of high fat diet is enough to induce hepatic insulin resistance[230]. Here, we show that a number of genes that have been proposed to be involved in the development of hepatic insulin resistance are differently regulated in fasting compared to high fat induced steatosis. Furthermore, we show that a number of genes involved in detoxification and regulation of hepatic regeneration are induced in fasted livers while no such activation takes place in high fat diet treated animals. High fat diet on the other hand induces the activation of *Scd1* and *Srebp-1c*, two genes that have been implicated as key factors in the development of hepatic insulin resistance.

## Materials and Methods

*Animals*

Male C57Bl6/J, 12-16 week old mice (n=30) were housed in a 12h light/dark cycle under standard conditions. Animals had free access to food and water. Control mice were fed standard chow. Animals of the high fat group received a diet with 21.5 wt% saturated bovine fat (Hope Farms, Woerden, The Netherlands). Animals were sacrificed at 09:00 h AM after a 16 h fast for the fasted group or 4 h fast for the high fat and control group. Two separate experiments were performed. For each experiment 15 mice were randomly assigned to the different experimental groups (n=5 per group). Livers from experiment 1 were extracted at day 15 and used for RNA isolation and subsequent microarray and RT-PCR analysis. From animals of experiment 2, blood was collected at day 0, day 10 and day 15. All experiments were approved by the Animal Ethics Committee of the Leiden University Medical Center.



*Plasma parameters*

Plasma was obtained via tail vein bleeding in chilled paraxonized capillary tubes to prevent *ex vivo* lypolysis[231], and assayed for glucose, insulin, TG, and total cholesterol using commercially available Kits (glucose hexokinase method (Instruchemie, Delfzijl, The Netherlands), ultra sensitive mouse insulin ELISA (Mercodia, Uppsala, Sweden), 1488872 and 236691 Roche Molecular Biochemicals, (Indianapolis, IN, USA), respectively).

*Isolation, amplification and labelling of RNA*

Total RNA was isolated from livers of mice fed a high fat diet or chow for 2 weeks or an overnight fast (16 h). RNA was isolated with the NucleoSpin RNA® II-kit (Machery-Nagel, Düren, Germany). The RNA concentration was determined by absorbency at 260 nm with a NanoDrop (Isogen Life Science, Ijsselstein, The Netherlands), and RNA integrity was verified by use of the RNA 6000 Nano assay on the Agilent 2100 Bioanalyzer (Agilent Technologies, Amstelveen, The Netherlands). RNA was reverse transcribed with incorporation of amino-allyl-UTP (aa-UTP) using the MessageAmp™ aRNA kit, according to the manufacturer's instructions, then column purified and eluted in nuclease-free

water. A total of 3.75 mg column-purified aRNA of each liver was labelled with both monofunctional dyes, cyanine-3 (Cy3) and cyanine-5 (Cy5) (Amersham Biosciences, GE Healthcare, Diegem, Belgium), as previously described[232] to allow all experiments to be performed as dye-swaps. Cy3 labelled aRNA of one experimental group was combined with Cy5 labelled aRNA of the other experimental group and vice versa. Combined probes were concentrated with Montage PCR columns (Millipore, Amsterdam, The Netherlands), recovered in TE and dye incorporation efficiency was then determined by wave-scan with the NanoDrop.

*Hybridization of glass oligonucleotide microarrays*

Murine oligonucleotide microarrays were produced in the Leiden Genome Technology Center by spotting the Sigma-Genosys mouse 7.5K oligonucleotide library (v. 1.0) (65mer, 20 µl in 50% DMSO) in duplicate on poly-L-lysine-coated slides[232]. Hybridization was done as described previously[232] with minor modifications. To the combined aRNA's hybridization mix was added (final concentrations, 0.15 mg/ml yeast tRNA, 0.15 mg/ml poly(A)+ RNA, 3 x SSC and 0.3% SDS), probes were denatured at 95°C for 2 min and centrifuged for 10 min at 13 000g. Hybridizations were performed overnight in Corning Hybridization chambers at 55°C in a water bath. Slides were washed with increasing stringency and then dehydrated by short washes in 70, 90 and 100% ethanol. After drying arrays were scanned with the Agilent G2565BA microarray scanner. Feature analysis was done with GenePix Pro 5.0 (Axon, Molecular Devices, Sunnyvale, U.S.A). Fluorescence intensities were normalized to median array densities to generate normalized measurements for each gene across all samples.



*Quantitative real-time PCR*

One microgram of total RNA of individual animals was reverse transcribed into cDNA with the RevertAid™ H Minus first strand Kit (Fermentas, St.Leon-Rot, Germany) primed with random hexamers. Thirty nanogram cDNA were amplified with gene specific primers in a 15 µl reaction containing 1 x SYBR-green mix (BioRad, Veenendaal, The Netherlands). All primers were tested to have efficiency between 90 and 110%. All samples were amplified in duplicates on a MyiQ machine (BioRad). Values were normalized to the amount of two

endogenous control genes (Cyclophilin B and β-2-microglobulin) and relative changes in gene expression were then calculated with the iQ5-software version 2.0 (BioRad). Three animals of each experimental group were analysed.

*Statistical Analysis*

All data are expressed as mean ± SD. Statistical analysis was performed by one-way ANOVA with post hoc using Newmann-Keuls test. Microarray data were analysed with the limma-package[233] from the Bioconductor software project (http://bioconductor.org) in the R environment for statistical computing (http://www.R-project.org). Only genes with an average expression level exceeding 1.5 times the background over all arrays and channels and a P-value < 0.05 were included in the pathway analysis. Associations with GO biological process, molecular function, cellular component groups, and biological pathways were obtained with the Web-based integrated data mining system WebGestalt[234]. A hypergeometric test was performed with the whole list of genes as the reference.



**Results**

*Plasma parameters*

Plasma TG, total cholesterol, insulin and glucose were determined in 16 hour fasted, high fat fed and control animals. Table 1 summarizes plasma parameters at day 0, day 10 and day 15. Cholesterol was elevated in animals receiving the high fat diet at day 10 and increased further until day 15. TG was slightly decreased in 16 hour fasted mice at day 15 compared to controls. Glucose levels did not differ between controls and high fat diet fed mice at any time point. As expected, glucose was significantly reduced after 16 hours of fasting compared to controls at day 15. Insulin levels were not altered by high fat feeding and dropped bellow detection limits after 16 hours of fasting (data not shown).

*Gene expression changes induced by 16 hours of fasting or high fat diet*

We performed three comparisons by microarray analysis. A comparison was made between individual mice of the control and high fat fed or 16 hour fasted groups of mice. In addition, a direct comparison was made between high fat fed and 16 hour fasted animals. Based on the performed microarray experiments,

we could identify 390 differentially expressed genes comparing livers from high fat fed animals with livers from 16 hour fasted mice, 407 differentially expressed genes comparing 16 hour fasted animals to control animals and 65 differentially expressed genes comparing high fat fed animals to control mice. Only 23 genes showed overlap in gene expression between the 16 hours fasted animals compared to control and high fat fed animals compared to control mice as is shown in figure 1.

**Table 1.** Plasma values measured in control, high fat fed and 16 hour fasted mice.

| | control | high fat | 16 hour fasted |
|---|---|---|---|
| Triglycerides (mmol/L) | | | |
| day 0 | 0.8 ± 0.2 | 0.7 ± 0.1 | n.d. |
| day 10 | 0.8 ± 0.1 | 0.7 ± 0.1 | n.d. |
| day 15 | 0.9 ± 0.1 | 0.8 ± 0.2 | 0.5 ± 0.1 |
| Cholesterol (mmol/L) | | | |
| day 0 | 2.8 ± 0.2 | 2.2 ± 0.2 | n.d. |
| day 10 | 2.9 ± 0.3 | 4.0 ± 0.8 ***/a | n.d. |
| day 15 | 2.5 ± 0.3 | 4.8 ± 0.5 ***/a | 2.4 ± 0.1 |
| Glucose (mmol/L) | | | |
| day 0 | 6.4 ± 0.9 | 6.3 ± 0.6 | n.d. |
| day 10 | 6.2 ± 0.8 | 7.1 ± 1.0 | n.d. |
| day 15 | 6.2 ± 1.0 | 6.1 ± 1.1 | 4.1 ± 1.0 ** |

Values are expressed as means ± SD (n=5 in each group). *p<0.05, **p<0.01, ***p<0.001 compared to controls and a <0.001 compared to day 0 of the same treatment group. Significance was determined by ANOVA followed by Newman-Keuls post-hoc test. n.d. not determined.



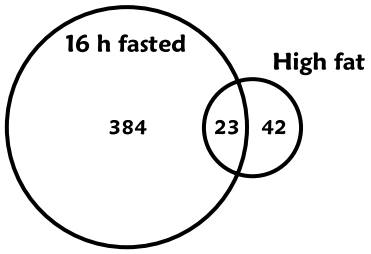


**Figure 1 Venn diagram of differentially expressed genes**
Hepatic expression of genes in 16 hour fasted mice compared to control and high fat fed mice compared to control and the overlap in gene expression between both groups.

To get a better understanding of coordinated changes in their biological context we performed an analysis with the web-based tool "WebGestalt" to group genes according to their Gene Ontology (GO) categories. Table 2 summarizes pathways enriched with differentially expressed genes of the comparisons of high fat fed versus fasted, 16 hour fasted versus controls and high fat fed versus control. 16 hours of fasting induced the majority of differentially expressed genes detected as is implied by the overlap of affected pathways in the comparisons of high fat fed versus 16 hour fasted and 16 hour fasted versus controls. Only a relative small number of genes were differentially expressed in high fat fed animals compared to control. This small number of differentially expressed genes clearly hampered the pathway analysis. This is reflected by the higher P-values calculated by the hypergeometric test as well as the fact that only very general GO terms were relatively enriched (Table 2).

**Table 2.** Gene expression pathway analysis



| | **16 fasted vs control** | | **16h fasted vs high fat** | | **high fat vs control** | |
|---|---|---|---|---|---|---|
| GO-term | # genes observed | P-value | # genes observed | P-value | # genes observed | P-value |
| alcohol catabolism | | | | | 3 | 4.20E-03 |
| alcohol metabolism | 27 | 4.99E-09 | 20 | 2.67E-05 | 5 | 5.96E-03 |
| carbohydrate catabolism | | | | | 3 | 7.50E-03 |
| carbohydrate metabolism | 31 | 1.25E-06 | | | | |
| carbon-oxygen lyase activity | 11 | 1.86E-06 | | | | |
| carboxylic acid metabolism | 40 | 6.75E-11 | 34 | 3.37E-08 | | |
| cellular carbohydrate metabolism | 22 | 8.54E-05 | | | 3 | 7.50E-03 |
| cellular catabolism | | | | | 7 | 3.13E-03 |
| cellular lipid metabolism | 49 | 2.58E-16 | 38 | 4.23E-10 | | |
| cholesterol biosynthesis | 5 | 9.01E-05 | | | | |
| cholesterol metabolism | 10 | 1.36E-05 | | | | |
| cofactor metabolism | | | 16 | 1.53E-05 | | |
| complement activation | 9 | 6.81E-06 | | | | |
| complement activation, classical pathway | 8 | 5.00E-06 | | | | |
| electron transport | 30 | 7.97E-09 | 22 | 5.97E-05 | 9 | 9.91E-06 |

| | 16 fasted vs control | | 16h fasted vs high fat | | high fat vs control | |
|---|---|---|---|---|---|---|
| GO-term | # genes observed | P-value | # genes observed | P-value | # genes observed | P-value |
| endopeptidase inhibitor activity | | | | | 4 | 3.81E-03 |
| endoplasmic reticulum | 42 | 8.72E-10 | | | 9 | 5.31E-04 |
| energy derivation by oxidation of organic compounds | 17 | 1.71E-06 | | | | |
| fatty acid metabolism | 19 | 6.20E-08 | 14 | 7.50E-05 | | |
| generation of precursor metabolites and energy | 47 | 4.15E-13 | 34 | 9.15E-07 | 12 | 1.60E-06 |
| glucose catabolism | | | | | 3 | 3.86E-03 |
| glucose metabolism | | | | | 4 | 1.93E-03 |
| glutathione transferase activity | | | | | 3 | 2.61E-04 |
| glycolysis | | | | | 3 | 2.96E-03 |
| hexose catabolism | | | | | 3 | 3.86E-03 |
| hexose metabolism | | | | | 4 | 4.31E-03 |
| humoral defense mechanism (sensu Vertebrata) | 9 | 9.38E-05 | | | | |
| hydro-lyase activity | 10 | 3.90E-06 | | | | |
| lipid biosynthesis | 26 | 3.43E-11 | 18 | 5.94E-06 | | |
| lipid binding | | | | | 7 | 3.28E-03 |
| lipid metabolism | 53 | 1.08E-15 | 42 | 5.19E-10 | | |
| lipid transport | | | | | 4 | 1.41E-04 |
| lipid transporter activity | | | | | 3 | 3.61E-03 |
| lipoprotein metabolism | | | | | 3 | 1.77E-03 |
| mitochondrial envelope | 23 | 1.80E-07 | 19 | 2.99E-05 | 23 | 1.97E-03 |
| mitochondrial inner membrane | 18 | 1.18E-05 | | | | |
| mitochondrial membrane | 18 | 2.67E-05 | | | | |
| mitochondrion | 58 | 2.75E-16 | 46 | 1.03E-09 | | |
| monooxygenase activity | 17 | 1.37E-08 | | | 6 | 1.82E-05 |
| monosaccharide catabolism | | | | | 3 | 3.86E-03 |
| monosaccharide metabolism | | | | | 4 | 4.31E-03 |
| organelle envelope | 24 | 4.32E-06 | | | | |

| | 16 fasted vs control | | 16h fasted vs high fat | | high fat vs control | |
|---|---|---|---|---|---|---|
| GO-term | # genes observed | P-value | # genes observed | P-value | # genes observed | P-value |
| organelle inner membrane | 19 | 7.09E-06 | 17 | 7.51E-05 | | |
| organelle membrane | 28 | 7.23E-05 | | | | |
| organic acid metabolism | 40 | 6.75E-11 | 34 | 3.37E-08 | | |
| peroxisome | 14 | 2.29E-07 | 14 | 1.83E-07 | | |
| protease inhibitor activity | | | | | 4 | 3.81E-03 |
| steroid biosynthesis | 16 | 1.07E-12 | 10 | 2.95E-06 | | |
| steroid dehydrogenase activity | 6 | 7.75E-06 | 6 | 6.81E-06 | | |
| steroid metabolism | 22 | 1.41E-11 | 20 | 3.03E-10 | | |
| sterol biosynthesis | 7 | 1.97E-06 | | | | |
| sterol metabolism | 12 | 4.12E-07 | | | | |

Pathways with a P-value <0.01 determined by hypergeometric test in the comparison of 16 hour fasted versus controls, 16 hour fasted versus high fat fed and high fat fed versus controls.



*Expression of key genes involved in energy homeostasis by RT-PCR*

We confirmed the changes detected with the microarray analysis by performing RT-PCR on a number of differentially expressed genes. We selected five up- (*Pcx*, *Cpt1a*, *Crat1*, *Cyp8b1* and *Cyp3a13*) and four down-regulated genes (*Cyp51*, *Elovl3*, *Gck*, and *Sqle*) from the 16 hour fasted versus control and high fat versus control comparison to confirm our array findings. Table 3 summarizes the results of the RT-PCR experiments. We could confirm the findings of the microarray experiment with the exception that 3 genes reached statistical significance in the RT-PCR experiment in the high fat fed group that had not been significant in the microarray experiment.

A number of genes known from the literature to be involved in the development of obesity and the metabolic syndrome did not pass the technical selection threshold or were not present on the microarray at all. We therefore decided to extend the analysis with additional RT-PCR experiments to analyze the expression of a selected set of transcription factors and genes suspected to play a role in the development of obesity and the metabolic syndrome (Fig. 2). Compared to control, the Farnesoid X receptor (*Fxr*, gene name: *Nr1h4*) was

increased in both groups, but more pronounced in 16 hour fasted animals. The same was true for the Liver X receptor alpha (*Lxrα, Nr1h3*), Pregnane X receptor (*Pxr, Nr1i2*) and the Hepatic Nuclear Factor 4 alpha (*Hnf4α, Nr2a1*) (Fig. 2a). In contrast, we detected an increase in hepatic peroxisome proliferate activated receptor alpha *(Pparα, Nr1c1*) expression in high fat fed mice which was absent in 16 hour fasted livers and was not detected on microarray. The PPAR delta isoform (*Pparδ, Nr1c2*) was not altered in either group while the PPAR gamma isoform (*Pparγ, Nr1c3*) was up-regulated in livers of 16 hour fasted animals but not in those fed a high fat diet. This up-regulation of *Pparγ* in 16 hour fasted animals was accompanied by a concomitant increase in PPAR gamma co-activation factor 1a (*Pparγc1a)* expression which was absent in high fat fed mice while no change in *Pparγc1b* expression was detectable in either group (Fig. 2b). For the sterol regulatory element binding proteins family (*Srebp's*), *Srebp-1a* showed the same pattern as *Pparα* with only an increase in expression in high fat fed mice. *Srebp-1c* on the other hand, was upregulated in high fat fed animals but downregulated in 16 hour fasted animals, compared to control. This same pattern of expression was seen for stearoyl-CoA desaturase (*Scd1*). The constitutive androstane receptor (*Car*) was exclusively up-regulated in livers of 16 hour fasted animals.

Table 3. Validation of microarray gene expression data with RT-PCR

| | **16 hr fasted vs control** | | **high fat vs control** | |
|---|---|---|---|---|
| Gene | Array, Ratio | PCR, relative expression | Array, Ratio | PCR, relative expression |
| *Pcx* | + 1.56** | 3.43*** | + 1.16 | 1.43 |
| *Cpt1a* | + 1.46* | 3.85*** | + 1.16 | 1.82* |
| *Crat1* | + 1.53** | 5.87*** | + 1.04 | 1.20 |
| *Cyp8b1* | + 2.42*** | 4.39*** | - 1.18 | 1.14 |
| *Cyp3a13* | + 1.66** | 3.45*** | - 1.12 | 0.90 |
| *Cyp51* | - 2.47*** | 0.33** | + 1.10 | 1.06 |
| *Elovl3* | - 4.10*** | 0.26** | - 1.19 | 1.34** |
| *Gck* | - 3.60*** | 0.35** | + 1.12 | 2.30** |
| *Sqle* | - 1.37* | 0.24* | - 1.05 | 1.18 |

Relative expression to controls as determined with the ΔΔCt-method. PCR Values are means of 3 animals per group. *p<0.05, **p<0.01, ***p<0.001 as determined by ANOVA followed by Newman-Keuls post-hoc test.

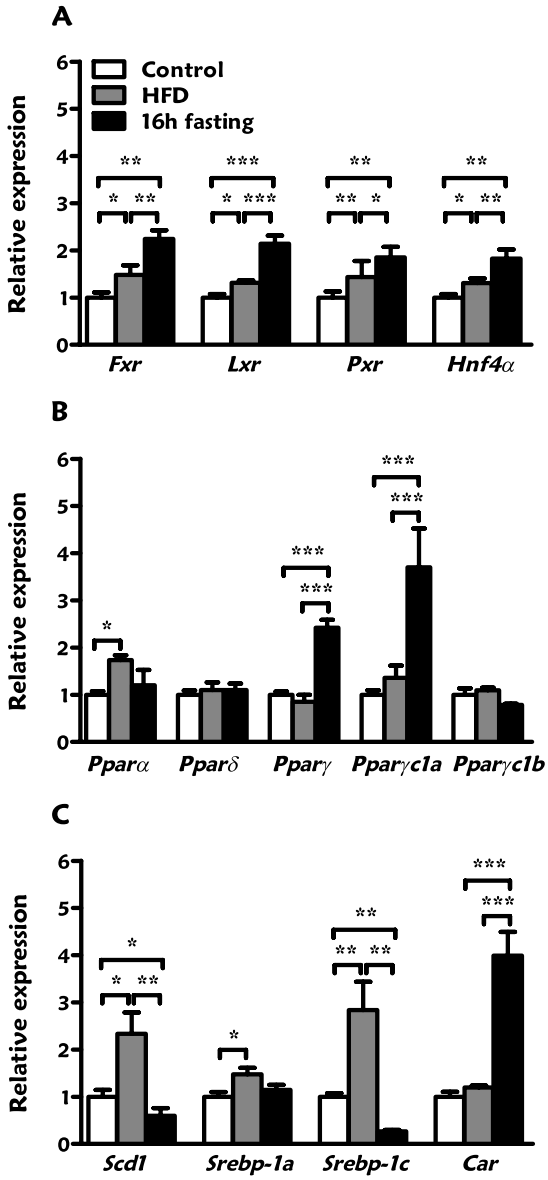


**Figure 2 Expression levels of selected transcription factors determined by real-time PCR in livers from high fat fed or fasted mice relative to controls.**
Relative expression to controls as determined with the ΔΔCt-method. Data represent means of 3 animals per group. *p<0.05, **p<0.01, ***p<0.001 as determined by ANOVA followed by Newman-Keuls post-hoc test.

**Discussion**

Hepatic steatosis can be induced in mice by fasting for 16 hours and is accompanied by an increase in hepatic TG content comparable to that induced after two weeks of high fat diet[230]. In contrast to steatosis induced by high fat diet, the fasting response does not result in the development of hepatic insulin resistance. We have investigated the alterations in hepatic gene expression induced by 16 hour fasting or two week high fat diet exposure to identify genes that are differentially expressed in these distinct forms of steatosis. Fasting had a profound effect on pathways involved in lipid metabolism, fatty acid metabolism, steroid metabolism and biosynthesis, carbohydrate metabolism as well as on energy generation related genes. These changes reflected the expected shift from glucose utilization towards energy generation derived from fatty acid oxidation. Interestingly, we also detected the up-regulation of a number of genes involved in hepatic detoxification.

Fasting induces a shift in fuel utilization for energy generation from glucose to FA's. This was reflected by significant changes in enzymes involved in glycolysis: glucokinase (*Gck*) was down-regulated and aldolase A (*AldoA*) was up-regulated in fasted liver, which was detected in the microarray experiments. We further detected the up-regulation of the lactate dehydrogenases A (*Ldha*) and B (*Ldhb*) (microarray) together with pyruvate carboxylase (*Pcx*) (both microarray and RT-PCR (Table 3)). *Pcx* encodes the mitochondrial enzyme that converts pyruvate to oxaloacetate and thus provides intermediates for the citric acid cycle[235].

The shift towards FA utilization upon fasting was further reflected by an up-regulation of several genes involved in mitochondrial FA β-oxidation. With microarray analysis, we detected up-regulation of acyl-CoA synthetase long-chain family member 1 (*Acsl1*), carnitine palmitoyltransferase 1a (*Cpt1a*), solute carrier family 25 (*Slc25a20*), acyl-Coenzyme A dehydrogenase very long chain (*Acadvl*), acyl-Coenzyme A dehydrogenase long-chain (*Acadl*), acyl-Coenzyme A dehydrogenase, medium chain (*Acadm*), dodecenoyl-Coenzyme A delta isomerase (*Dci*) and enoyl-Coenzyme A, hydratase/3-hydroxyacyl Coenzyme A dehydrogenase (*Ehhadh*). Interestingly, we saw a down-regulation of peroxisomal trans-2-enoyl-CoA reductase (*Pecr*), the hepatic microsomal enzyme that catalyses the reduction of trans-2-enoyl-

CoAs of varying chain lengths from 6:1 to 16:1. None of these genes were identified as differentially expressed in livers from mice fed a high fat diet (data not shown). The change in the expression of *Cpt1* was also confirmed with RT-PCR (Table 3).

One of the most prominently affected pathways in fasted livers was cholesterol biosynthesis. The SREBP family of transcription factors is known to represent the master regulators of lipogenesis and cholesterogenesis. They are able to directly activate genes involved in the synthesis and uptake of cholesterol, fatty acids, TG's and phopsholipids[236]. Of the three isoforms SREBP-1a, -1c and -2 it is known that SREBP-2 is the main regulator of cholesterol synthesis if expressed at physiological levels. We did not detect a change in the microarray experiments and only a minor decrease in SREBP-2 transcript with PCR in the fasted livers, but this was not significant. One of the known target genes of SREBP-2, HMG-CoA reductase (*Hmgcr*) was also not changed. However, both SREBP-2 and HMG-CoA reductase have been shown to be subject to post-transcriptional regulation[237, 238]. Since we have not measured activated protein levels of SREBP-2, we can not exclude that these might be diminished in the situation of fasting. Nonetheless, even in the absence of changes in gene expression levels of SREBP-2, we did see reduced expression levels of the SREBP-2 regulated genes *Mevalonate kinase (Mvk), farnesyl diphosphate farnesyl transferase (Fdft1), Squalene epoxidase (Sqle), cytochrome P450 family 51 (Cyp51), sterol C5 desaturase (Sc5d) and 7-dehydrocholesterol reductase (Dhcr7)*[78] in fasted livers compared to control mice fed chow diet (data not shown). The down-regulation of *Cyp51* and *Sqle* was also confirmed by RT-PCR (Table 3). Overall, these data confirm previous results showing that fasting results in downregulation of the cholesterol biosynthesis pathway[239].



Another pathway affected by fasting included the regulators of hepatic detoxification processes, pregnane X receptor (*Pxr*) and constitutive androstane receptor (*Car*). Car was exclusively up-regulated in livers of fasted animals as detected by microarray and RT-PCR while Pxr was up-regulated in livers of fasted animals and also modestly increased in high fat fed mice (Fig. 2). Target genes regulated by these lipid-activated nuclear transcription factors include, among others, the family of cytochrome P-450 enzymes and

cytosolic binding proteins[240]. We could detect up-regulation of 8 Cyp-family members (*Cyp3a13, Cyp3a25, Cyp4a10, Cyp4a14*, *Cyp8b1*, *Cyp17a1*, *Cyp26a1* and *Cyp39a1*) and down-regulation of 3 members (*Cyp2f2*, *Cyp2j6* and *Cyp4f14*) in our microarray experiments when we compared fasted livers with those of controls. In livers of high fat fed mice all 6 detected Cyp-family members (*Cyp2a4, Cyp2f2*, *Cyp3a25, Cyp4a10, Cyp4a14* and *Cyp4a41*) were down-regulated when compared to controls. Two of these, Cyp4a10 and Cyp4a14, appear to be regulated diametrically opposed in fasted and high fat fed mice, which makes them potential target genes of Car. The activation of hepatic detoxification was further supported by the up-regulation of two members of the sulfotransferase family of phase-II conjugation enzymes, *Sult1a1* and *Sult1d1*. These enzymes help to conjugate endo- and xenobiotics with a sulfonate group to render them water soluble and excretable. Interestingly, it has recently been demonstrated that CAR and PXR also play a role in the regulation of hepatic energy metabolism by influencing gluconeogenesis, beta-oxidation, ketogenesis, lipogenesis and thyroid hormone activity via crosstalk with transcription factors such as FOXO1[241].

As can be seen in Figure 2a, changes in the expression of nuclear transcription factors belonging to the PPAR family were mainly seen in fasted livers. High fat diet did induce a mild up-regulation of Pparγ. Pparγ activation stimulates FA transport, FA oxidation, ketogenesis and gluconeogenesis. Pparγ is a regulator of adipogenesis and induces FA uptake and storage when activated. It has therefore been proposed that the up-regulation of Pparγ is a mechanism that allows hepatocytes to facilitate storage of excess FA's in a way that will not cause damage to the cell[242]. There are several mouse models of obesity in which the development of hepatic steatosis was correlated with increased hepatic levels of Pparγ[243, 244]. The transcription of *Pparγc1a* is a co-activator of FOXO-1 and has been shown to be intimately involved in the regulation of energy metabolism in response to fasting[245].

We have not found direct evidence of altered insulin signalling, but two genes, *Scd1* and *Srebp-1c,* which have been associated with the development of hepatic steatosis and IR, were inversely regulated in fasting and high fat diet. We detected a significant down-regulation of *Srebp-1c*, the main regulator of the fatty acid biosynthesis pathway in fasted livers and a significant

up-regulation in livers of high fat fed mice (Fig. 2). There is evidence that hepatic steatosis and IR is associated with an up-regulation of Srebp-1c, which is increased in response to the elevated insulin levels as seen in the leptin deficient *ob/ob* mice[78]. Furthermore, hepatic overexpression of Srebp-1c in transgenic mice leads to an increased *de novo* synthesis of TG which can cause hepatic steatosis [246]. A potential mechanism for the role of SREBPs in the development of IR is a direct interaction with the promoter of the insulin receptor substrate 2 (IRS-2). The IRS-2 promoter contains an insulin response element and is regulated by the forkhead proteins. It has been shown that this binding site can be occupied by all three SREBP isoforms and results in decreased IRS-2 transcription and protein, providing a potential molecular mechanism that explains the switch to increased lipogenesis and decreased hepatic glycogen synthesis seen in obesity and the metabolic syndrome[247].

Scd1 was exclusively regulated in response to high fat diet and has been shown to be modulated in response to dietary, physiological and hormonal stimuli, including insulin and polyunsaturated FA's[248]. Absence of Scd1 has been associated with the resistance to diet induced obesity and IR[248, 249]. Experiments with anti-sense oligo (ASO) treatment confirmed a role of Scd1 in IR. In these experiments, severe hepatic insulin resistance as determined by insulin clamp studies was reversed by 5 day treatment with a ASO against Scd1 which resulted in a 80% reduction of hepatic mRNA levels of Scd1, comparable to the reduction seen in livers of fasted mice (Fig. 2c).



The most striking difference comparing livers from fasted mice with high fat diet fed mice was the number of differentially expressed genes. While fasting induced changes in the expression of more than 400 hepatic genes compared to chow fed mice, only a small number of differentially expressed genes could be detected in response to a two week period of high fat diet feeding. Apparently, the metabolic adaptation induced by high fat feeding does not represent a strong adaptive signal and can be achieved without all too dramatic changes in the hepatic transcriptional program. Since prolonged fasting endangers survival and fertility and thus survival of the species, selective evolutionary pressure for a strong adaptive response upon fasting would have been beneficial.

**Acknowledgements**

This study was supported by; the NutriGenomics Consortium, Top Institute Food and Nutrition with financial support by the Dutch government; by the Netherlands Heart Foundation (project nr. 2001.141); and by the Netherlands Organisation for Health Care Research Medical Sciences (ZON-MW project nr. 948 000 04).

# Chapter 7

## General discussion

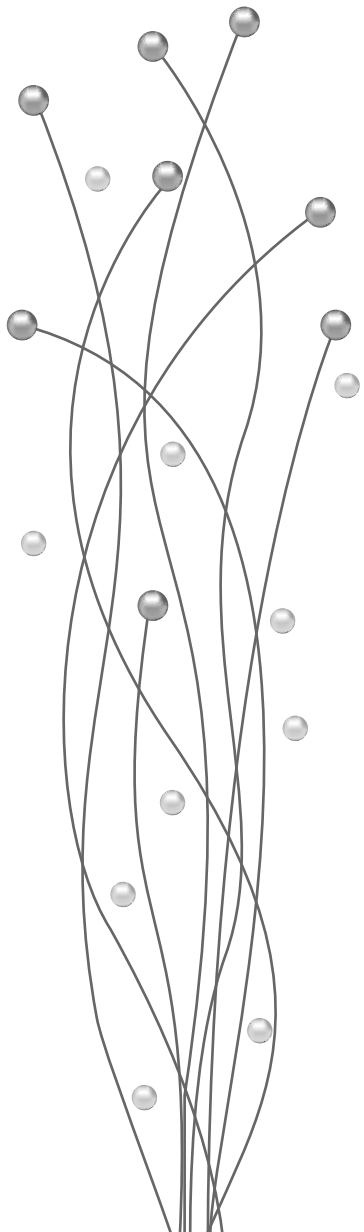

Nowadays, our energy intake chronically exceeds the energy we use, and therefore fat accumulates resulting in overweight and obesity. The energy in our diet is stored as carbohydrates and fat. Since the storage of carbohydrates in the body is limited, excess energy is stored as fat and mobilized again during fasting to provide energy. This mobilization occurs by the release of fatty acids (FA) by adipose tissue into the circulation. Part of the FA are used directly for ATP supply following oxidation, but a large fraction of the FA enters the liver where FA are re-esterified into triglycerides (TG) that are secreted as part of the core of VLDL particles by the liver. These VLDL particles deliver FA to peripheral tissues where they can be used to generate energy. The cycling of FA and TG enables us to adapt to changes in energy demand, but the western daily energy intake exceeds our ability to maintain homeostasis.

Obesity is strongly associated with metabolic dyslipidemia, which is characterized by low levels of HDL-cholesterol (C) and high levels of TG. Additional pathologies associated with obesity include high blood pressure and systemic inflammation and, collectively, these abnormalities are known as the metabolic syndrome (MetS). MetS is probably the most prevalent cause for the current increase in patients with diabetes mellitus type 2 (DM2) and cardiovascular disease (CVD). The studies described in this thesis evaluated several aspects of the regulation of VLDL-TG metabolism and the main conclusion and implications of our findings are discussed in this chapter.



**CETP and VLDL metabolism**

Cholesteryl ester transfer protein (CETP) transfers TG and cholesteryl esters between lipoproteins and has a major impact on cholesterol metabolism by decreasing HDL-C and increasing LDL-C. Although CETP also transfers TG, it was not clear whether and to what extent CETP would affect TG metabolism. In a small study with three heterozygous CETP deficient persons, it was shown that the postprandial TG response after an oral fat load was decreased compared to normal persons, suggesting that CETP may retard TG clearance from plasma[250]. In naturally CETP-deficient mice, it was shown that expression of human CETP increased the postprandial TG response after an oral fat load

by reducing the clearance rate of chylomicron-like lipoprotein particles, due to reduced LPL activity[140]. Thus, CETP may have the capacity to affect TG metabolism.

In **chapter 2**, we studied the role of CETP on VLDL metabolism in ApoE*3-Leiden (E3L) mice. E3L mice have a more human-like VLDL metabolism than wild type mice and have been extensively used to dissect the effects of diets and drugs on lipoprotein metabolism[114, 115, 117, 118]. The expression of human CETP, under control of its natural flanking regions, in the E3L background enables us to study both VLDL and HDL metabolism in a more human-like setting. Our experiments in **chapter 2** indicate that CETP mainly affects cholesterol metabolism and not TG metabolism. In addition, expression of CETP did not affect high fat diet-induced obesity. This suggests that also under conditions where TG/FA metabolism is stressed, CETP does not affect TG metabolism. The major implication of these findings is that it is unlikely that pharmaceutical modulation of CETP activity affects TG metabolism and obesity in humans. Although this does require validation in human studies, it indicates that potential negative side-effects of CETP inhibitors in relation to obesity and related diseases are less likely to occur.

Recently, several drugs have been developed to inhibit CETP, thereby increasing HDL-C and reducing the risk for CVD. Of these CETP inhibitors, torcetrapib was the first drug used in large clinical trials (RADIANCE[251], ILLUSTRATE[252], and ILLUMINATE[122]). Although the outcome of these trials were negative, probably related to off-target side-effects of torcetrapib, combination therapy of atorvastatin and torcetrapib for 2 years increased HDL-C by almost 60% compared to patients receiving atorvastatin alone. In these studies, torcetrapib caused only a minor reduction in plasma TG (-16%). Short-term treatment with anacetrapib, a more recent CETP inhibitor, had no effect on plasma TG levels[253]. These data support our findings that CETP inhibition does not evoke major effects of plasma TG metabolism.

Our data also indicate that CETP does not affect the development of diet induced obesity. However, obese subjects do present with increased circulating levels of CETP, indicating that obesity per se does affect CETP level and activity. It is likely that this is a direct consequence of the increase in adipose tissue, which has been demonstrated to be an important source of plasma CETP[254, 255, 256].

This is further supported by the reduction in CETP mass and activity after marked weight loss[257, 258, 259]. However, since obesity is associated with multiple metabolic abnormalities, it cannot be excluded that alternative mechanisms explain the association of obesity with increased CETP activity.

Plasma CETP activity is dependent on CETP levels, protein levels of activators and inhibitors, as well as on the presence and composition of donor and acceptor particles for lipid exchange. Variations in the CETP gene, characterized by single point mutations (called single nucleotide polymorphisms, SNPs), are related to changes in CETP plasma levels and activity. The most studied SNP in the CETP gene is the so-called Taq1B polymorphism. CETP mass and activity are higher in carriers of the Taq1B1 allele compared to carriers of the Taq1B2 allele, which is associated with lower HDL-C levels in B1 carriers[260]. Most meta-analyses show that high TG levels are causal to the interaction of the Taq1B polymorphism with HDL-C in obese subjects by providing more acceptors for the transfer of cholesterol from HDL to apoB containing lipoproteins[261]. Low levels of HDL-C and high levels of TG are risk factors for the development of CVD. Therefore it appears that although CETP does not directly affect TG metabolism, TG levels do determine the effect of genetic variation in CETP on cholesterol metabolism thereby increasing the risk to develop CVD.



**Nuclear receptor ligands and VLDL metabolism**

Nuclear receptors play an important role in the orchestration of energy metabolism and are important targets for drug development for diseases associated with the MetS. Nuclear receptors regulate the expression of genes involved in energy homeostasis and numerous other processes by binding to specific DNA regulatory elements. The natural ligands of nuclear receptors include hormones and lipid intermediates. One of the physiological roles of a subset of nuclear receptors is to function as sensors of energy status by activating or inhibiting specific target genes and pathways to maintain homeostasis.

Various drugs act by functioning as synthetic ligands for specific nuclear receptors and thus affect energy metabolism. For example, the fibrate class of

compounds activate peroxisome proliferator-activated receptor alpha (PPARα) and are prescribed to lower plasma TG levels. Thiazolidinediones (TZDs) activate PPARγ and are prescribed to lower plasma glucose and lipid levels in DM2 patients. However, TZDs also lower FA turnover, thereby effectively lowering hepatic fat content[262]. More drugs that target nuclear receptors do also influence lipid and energy metabolism as a side effect. For example, rifampicin is an antibiotic drug that activates pregnane X receptor (PXR) and can cause hepatic lipid accumulation and steatosis[86, 180, 181]. In this thesis, a number of compounds that act via nuclear receptors have been investigated to determine the precise mechanism by which they affect VLDL-TG metabolism.

*Fenofibrate*

In **chapter 3** we focussed on the effect of the TG-lowering drug and PPARα activator fenofibrate on VLDL-TG metabolism. In the past, it has been shown that activation of PPARα lowers plasma TG levels by increasing the clearance of VLDL-TG. However, it was also suggested that PPARα reduces VLDL-TG production. First, in vitro experiments showed that incubation of cultured hepatocytes with fenofibrate reduced TG secretion[153]. Second, experiments using the strong PPARα agonists Wy14643 also showed a reduction of VLDL secretion in vivo[152]. In addition, mice lacking PPARα show increased VLDL production[150, 151]. However, the effect of fibrates on VLDL secretion in humans remains inconclusive as either decreased or no changes in apoB production were observed whereas no effects on VLDL-TG production have been reported[263, 149].

To dissect the effect of PPARα modulation on VLDL-TG metabolism in a more human-like setting, we used E3L.CETP mice receiving a clinically relevant dose of fenofibrate. In **chapter 3** we showed that fenofibrate actually increases rather than decreases VLDL-TG secretion without altering the rate of VLDL-apoB production. Furthermore, VLDL-TG clearance was strongly enhanced explaining the overall reduction in plasma TG, which can be explained by an increase in of lipoprotein lipase (LPL) activity. Part of the FA liberated by lipolysis are not directly taken up by the underlying tissue but add to the plasma pool of albumin-bound FA, which is taken up by the liver. The increased hepatic uptake of albumin-bound FA contributed to the increased

flux of FA through the liver, resulting in higher VLDL-TG production and an increased particle size of nascent VLDL particles. This implies that PPARα activation by fenofibrate increases FA turnover.

In MetS, and especially obesity, FA overflow also occurs and it is believed that the increased FA turnover plays a role in the development of DM2. However, treatment with fenofibrate in diet-induced obese mice showed that activation of PPARα actually prevented severe obesity, adipocyte hypertrophy and maintained normal glycaemia[264, 265]. Together these data suggest that the increased FA turnover per se is not sufficient to induce pathology associated with MetS and is likely compensated by the regulation of additional pathways affected by PPARα activation.

Systemic inflammation is another feature of MetS that might trigger pathology in obese people. PPARs have been shown to play a role in macrophage activation in the vasculature thereby reducing atherosclerosis[266]. PPARα has been shown to have a more general effect on inflammation by inhibiting the activation of peritoneal macrophages by lipopolysaccharide (LPS)[267]. Activation of PPARα inhibits the expression of genes involved in the acute phase response and inflammatory cytokines including interleukin-6 (IL-6) and tumor necrosis factor alpha (TNF-α)[268]. Patients with dyslipidemia indeed show reduced levels of IL-6 and TNF-α when treated with fenofibrate[269]. Therefore the suppression of inflammation might be the reason why increased FA turnover by fenofibrate does not induce pathology. This is supported by a study in mice showing that hepatic PPARα activation suppresses expression of hepatic TNF-α and reduces hepatic fat accumulation during the development of fatty liver disease[270]. Small studies in humans showed no reduction of hepatic TG content upon treatment with fenofibrate[263, 271]. However in one of these studies, patients with NAFLD treated with fenofibrate did show improvement of MetS and liver function[271]. It would therefore be interesting to determine whether this anti-inflammatory effect of PPARα activation is sufficient to prevent pathology associated with increased FA turnover.

Since side-effects have been reported for fenofibrate including gastrointestinal disorders and skin reactions, new PPARα therapeutics are being developed that exhibit tissue- and gene-selective activities. Collectively, such agonists are known as selective PPAR modulators (SPPARMs). These

SSPARMs may provide novel insight in the role of specific PPARα-induced pathways in specific tissues in the development of MetS.

*Rifampicin*

Rifampicin is an antibiotic prescribed for the treatment of tuberculosis and is also a ligand for the nuclear receptor pregnane X receptor (PXR). Activation of PXR is associated with alterations in lipid metabolism and hepatic steatosis[85, 86, 180, 181, 182, 272]. Furthermore, rifampicin might also directly affect lipoprotein metabolism since its metabolites (known as ansamycins) can directly bind lipoproteins which might influence lipoprotein clearance[273, 274]. In **chapter 4** we determined the effect of rifampicin on VLDL-TG metabolism. Treatment with rifampicin induced hepatic steatosis and strongly reduced plasma cholesterol levels whereas plasma TG levels were unaltered. The reduction of cholesterol was mainly confined to the VLDL-sized fraction and due to reduced VLDL-particle production by the liver. However, this was not reflected by a reduction in plasma TG levels. This could be explained by TG enrichment of secreted VLDL itself.

Rifampicin treatment in obese people should be critically considered. In obesity, insulin resistance of the liver and adipose tissues is associated with hypertriglyceridemia due to increased VLDL-TG production. This can be attributed to the failure of insulin to suppress the FA flux from adipose tissue to the liver and the failure of insulin to inhibit VLDL production. Increased levels of VLDL-TG result in increased CETP activity and reduced HDL-C levels. Treating obese patients with rifampicin might further reduce HDL-C levels in a CETP-independent manner by reducing the formation of HDL. Overall this may further increase their risk to develop CVD.

Liver insulin resistance in obesity is also associated with hepatic steatosis. Similar to our findings in mice, rifampicin treatment has been reported to cause hepatic steatosis, especially in patients that consumed large amounts of alcohol. People consuming more than 6 alcoholic drinks per day are at great risk to develop alcoholic hepatic steatosis since alcohol affects multiple steps in hepatic FA metabolism. Thus, care should be taken in the administration of rifampicin to heavy drinkers as well as patients with the MetS, since this might exacerbate the exisiting hepatic steatosis.

*Perfluoroalkyl sulfonates*

Chemical pollutants such as pesticides, industrial solvents and plasticizers can disrupt energy homeostasis by interfering with nuclear receptor-mediated gene expression. We are exposed to these pollutants via water, air and our diet and they mimic lipids or hormones due to their chemical structure. However, how and to what extent FA/TG metabolism is affected by these pollutants is hardly known.

Perfluoroalkyl sulfonates (PFAS) are widely used as repellents, surfactants and fire-retardant foams[195, 199]. They are extremely resistant to metabolic and environmental degradation and therefore bio-accumulate. Studies in animal models have shown that PFAS affect plasma lipid parameters although the exact mechanism is not known. In **chapter 5**, we show that PFAS activate multiple nuclear receptors and mainly PPARα and the xenobiotic receptors Constitutive Androstane Receptor (CAR) and PXR. This results in an almost complete blockade of both VLDL-TG and VLDL-apoB production, whereas VLDL-TG clearance is increased.



In addition to PFAS, there are various chemical pollutants present in our environment that can affect energy homeostasis of which some have recently been shown to cause obesity (called obesogens). Obesogens can be functionally defined as chemical agents that promote lipid accumulation and adipogenesis[275, 276]. These obesogens include bisphenol A, various xenoestrogens, organotins and phthalates, many of which end up in the human due to their use as, for example, surfactants or due to the ubiquitous use of pesticides and plastics from which they are derived. In addition to influencing energy homeostasis by activating multiple nuclear receptors, these pollutants might also affect inflammatory gene expression via the same nuclear receptors. However, the net effect of these compounds on the various pathways that are regulated via nuclear receptors are largely unexplored.

**Role of nuclear receptors in metabolic stress**

Whole body energy homeostasis is tightly regulated. During fasting or excessive caloric intake, energy balance is disrupted and adaptations in energy metabolism are necessary to maintain homeostasis. Both PPARα and CAR

are involved in the metabolic adaptations that occur during fasting. PPARα regulates the uptake and transport of FA in the cell, activates β-oxidation, and activates ketone body synthesis. CAR on the other hand inhibits β-oxidation by competing with PPARα for its binding site in the 3-hydroxyacyl-CoA dehydrogenase gene promoter, an important enzyme of peroxisomal FA β-oxidation. CAR also inhibits gluconeogenesis[79, 277]. There are reports indicating that PPARα ligands such as Wy14643 and ciprofibrate induce CAR expression[278, 279]. However, activation of CAR was not seen in our fenofibrate study in **chapter 3**. It is more than likely that under physiological conditions subtle changes in the activation of multiple nuclear receptors regulate the response of TG and energy metabolism. It is interesting to study if these nuclear receptor mediated changes in energy homeostasis are associated with pathology. We therefore compared the effect of fasting and high fat diet feeding on the expression of genes involved in lipid metabolism in the liver as shown in **chapter 6**.

Since the liver plays an important role in adjusting lipid and energy homeostasis, we investigated the changes in liver gene expression after prolonged fasting and 2 weeks of high fat feeding in mice. One of the major findings in **chapter 6** is the level of gene regulation involved in the adaptation of energy homeostasis. During fasting, over 400 genes were differently expressed compared to control, whereas during high fat feeding, only 65 genes were differently expressed compared to control. This suggests a very complex transcriptional regulation of energy homeostasis during fasting

Both during fasting and high fat feeding, the liver switches to lipid metabolism thereby increasing β-oxidation. One of the major differences between fasting and high fat feeding includes the up-regulation of genes involved in FA biosynthesis upon high fat feeding, while these genes are down-regulated after prolonged fasting. During both fasting and high fat feeding, the liver becomes steatotic. However, only after high fat feeding the accumulation of liver lipid is associated with the development of insulin resistance[230]. The origin of this difference may reside in the fate of the TG pool in response to fasting, which is oxidation. Whereas the fate of the TG pool in response to high fat feeding is ectopic storage. The exact mechanism involved in the development of insulin resistance in response to high fat feeding requires

further investigation.

It is believed that metabolic inflexibility plays a role in the pathology of the MetS. Both during fasting but also in obesity and insulin resistance, FA oxidation increases[280, 281, 282, 283]. However, when glucose becomes available again, for example during re-feeding, the body switches from FA to glucose oxidation. In obese and DM2 subjects switching between fat and glucose oxidation is impaired, a phenomenon described as metabolic inflexibility[284, 285]. PPARα plays a dominant role in lipid oxidation and therefore likely plays a key role in metabolic flexibility[286].

However, it has become apparent that in obese subjects lipogenesis is activated in addition to increased β-oxidation by PPARα activation. This increased lipogenesis has been attributed to activation of SREBP-1c[78]. In obese rodents, liver lipogenesis is associated with the activation of forkhead box O1 (FOXO1) signalling[287]. Recently, activation of FOXO1 has been identified to influence VLDL metabolism by increasing the expression of microsomal triglyceride transfer protein (MTTP) and the secretion of VLDL-TG[288]. It has long been known that, under fasting conditions, FOXO1 expression is increased and promotes hepatic gluconeogenesis, whereas under fed conditions, insulin inhibits the effects of FOXO1 on hepatic gluconeogenesis[289, 290]. The effect of FOXO1 on promoting VLDL production shows that FOXO1 plays a critical role in the metabolic adaptations necessary to respond to fasting and refeeding and influences metabolic flexibility. In insulin resistant obese subjects, the regulation of FOXO1 activity by insulin is impaired thereby causing both hyperglycemia and hypertriglyceridemia[291].



Another feature of the MetS is systemic low-grade inflammation. In obese individuals, adipose tissue expands resulting in the release of less anti-inflammatory and more pro-inflammatory adipokines from adipocytes[292]. As a result, the adipose tissue becomes inflamed and this is believed to play a role in the low grade systemic inflammation seen in obese subjects. Several studies have shown that pro-inflammatory cytokines can induce insulin resistance[293, 294], which may be reversed by anti-inflammatory medication[295, 296]. It seems likely that the double role of nuclear receptors in both energy/lipid metabolism and inflammation is central to the pathology associated with the MetS. Since nuclear receptors play a key role in metabolic flexibility it is interesting to

determine to what extent they also modulate our inflammatory responsiveness. In fact, while the prevalence of obesity increases in our population so does the incidence of allergy. Although there is controversy about the relation between obesity and allergy symptoms[297, 298, 299, 300], it is suggested that obesity is associated with predisposition to allergy, especially allergy for food, and that systemic inflammation plays a key role in this association[301]. It would be interesting to determine whether allergy increases the risk to develop obesity or obesity increases the risk to develop allergy.

**Concluding remarks**

Regulation of VLDL-TG metabolism plays a role in energy homeostasis which is disturbed in obesity and associated pathology. Nuclear receptors are important in the regulation of VLDL-TG metabolism and therefore interesting targets for the development of drugs to treat MetS. The overall focus of this thesis was on the effects of several nuclear receptors on VLDL-TG metabolism, but these nuclear receptors clearly also affect inflammation. Since the MetS is a multifactorial disease, targeting both energy homeostasis and inflammation with nuclear receptors agonists may be an excellent approach to treat obesity related diseases. Unfortunately, most studies neglect the pleiotropic effects of nuclear receptors and therefore more integrated research focussed on both lipid metabolism and inflammation is necessary.

# Chapter 8

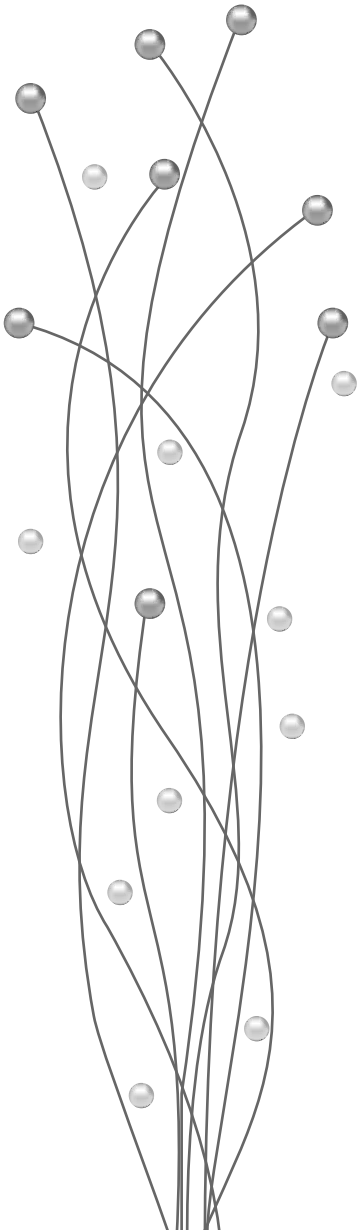

References

Summary

Nederlandse samenvatting
voor niet-ingewijden

List of publications

Curriculum vitae

1. Caballero, B. *The global epidemic of obesity: an overview.* Epidemiol. Rev. 29, 1-5 (2007).
2. Haslam, D. W. and James, W. P. *Obesity.* Lancet 366, 1197-1209 (2005).
3. Malhi, H. and Gores, G. J. *Molecular mechanisms of lipotoxicity in nonalcoholic fatty liver disease.* Semin. Liver Dis. 28, 360-369 (2008).
4. Yki-Jarvinen, H. *Fat in the liver and insulin resistance.* Ann. Med. 37, 347-356 (2005).
5. Capeau, J. *Insulin resistance and steatosis in humans.* Diabetes Metab 34, 649-657 (2008).
6. Mahley, R. W., Innerarity, T. L., Rall, S. C., Jr. *et al. Plasma lipoproteins: apolipoprotein structure and function.* J. Lipid Res. 25, 1277-1294 (1984).
7. Mu, H. and Hoy, C. E. *The digestion of dietary triacylglycerols.* Prog. Lipid Res. 43, 105-133 (2004).
8. Hussain, M. M., Kancha, R. K., Zhou, Z. *et al. Chylomicron assembly and catabolism: role of apolipoproteins and receptors.* Biochim. Biophys. Acta 1300, 151-170 (1996).
9. Green, P. H. and Riley, J. W. *Lipid absorption and intestinal lipoprotein formation.* Aust. N. Z. J. Med. 11, 84-90 (1981).
10. Ginsberg, H. N. *Lipoprotein physiology.* Endocrinol. Metab Clin. North Am. 27, 503-519 (1998).
11. Mahley, R. W., Hui, D. Y., Innerarity, T. L. *et al. Chylomicron remnant metabolism. Role of hepatic lipoprotein receptors in mediating uptake.* Arteriosclerosis 9, I14-I18 (1989).
12. Mahley, R. W. and Ji, Z. S. *Remnant lipoprotein metabolism: key pathways involving cell-surface heparan sulfate proteoglycans and apolipoprotein E.* J. Lipid Res. 40, 1-16 (1999).
13. Lusis, A. J. *Atherosclerosis.* Nature 407, 233-241 (2000).
14. Glass, C. K. and Witztum, J. L. *Atherosclerosis. the road ahead.* Cell 104, 503-516 (2001).
15. Zannis, V. I., Chroni, A., and Krieger, M. *Role of apoA-I, ABCA1, LCAT, and SR-BI in the biogenesis of HDL.* J. Mol. Med. 84, 276-294 (2006).
16. Huuskonen, J., Olkkonen, V. M., Jauhiainen, M. *et al. The impact of phospholipid transfer protein (PLTP) on HDL metabolism.* Atherosclerosis 155, 269-281 (2001).
17. Tall, A. R. *An overview of reverse cholesterol transport.* Eur. Heart J. 19 Suppl A, A31-A35 (1998).
18. O'Brien, P. J., Alborn, W. E., Sloan, J. H. *et al. The novel apolipoprotein A5 is present in human serum, is associated with VLDL, HDL, and chylomicrons, and circulates at very low concentrations compared with other apolipoproteins.* Clin. Chem. 51, 351-359 (2005).

19. Out, R., Hoekstra, M., Spijkers, J. A. *et al. Scavenger receptor class B type I is solely responsible for the selective uptake of cholesteryl esters from HDL by the liver and the adrenals in mice.* J. Lipid Res. 45, 2088-2095 (2004).

20. Acton, S., Rigotti, A., Landschulz, K. T. *et al. Identification of scavenger receptor SR-BI as a high density lipoprotein receptor.* Science 271, 518-520 (1996).

21. Krieger, M. *Scavenger receptor class B type I is a multiligand HDL receptor that influences diverse physiologic systems.* J. Clin. Invest 108, 793-797 (2001).

22. Chiang, J. Y. *Regulation of bile acid synthesis: pathways, nuclear receptors, and mechanisms.* J. Hepatol. 40, 539-551 (2004).

23. Morton, R. E. and Zilversmit, D. B. *Inter-relationship of lipids transferred by the lipid-transfer protein isolated from human lipoprotein-deficient plasma.* J. Biol. Chem. 258, 11751-11757 (1983).

24. Drayna, D., Jarnagin, A. S., McLean, J. *et al. Cloning and sequencing of human cholesteryl ester transfer protein cDNA.* Nature 327, 632-634 (1987).

25. Gibbons, G. F. *Assembly and secretion of hepatic very-low-density lipoprotein.* Biochem. J. 268, 1-13 (1990).

26. Tietge, U. J., Bakillah, A., Maugeais, C. *et al. Hepatic overexpression of microsomal triglyceride transfer protein (MTP) results in increased in vivo secretion of VLDL triglycerides and apolipoprotein B.* J. Lipid Res. 40, 2134-2139 (1999).

27. Fisher, E. A. and Ginsberg, H. N. *Complexity in the secretory pathway: the assembly and secretion of apolipoprotein B-containing lipoproteins.* J. Biol. Chem. 277, 17377-17380 (2002).

28. Barrows, B. R. and Parks, E. J. *Contributions of different fatty acid sources to very low-density lipoprotein-triacylglycerol in the fasted and fed states.* J. Clin. Endocrinol. Metab 91, 1446-1452 (2006).

29. Donnelly, K. L., Smith, C. I., Schwarzenberg, S. J. *et al. Sources of fatty acids stored in liver and secreted via lipoproteins in patients with nonalcoholic fatty liver disease.* J. Clin. Invest 115, 1343-1351 (2005).

30. Minahk, C., Kim, K. W., Nelson, R. *et al. Conversion of low density lipoprotein-associated phosphatidylcholine to triacylglycerol by primary hepatocytes.* J. Biol. Chem. 283, 6449-6458 (2008).

31. Vance, D. E. *Role of phosphatidylcholine biosynthesis in the regulation of lipoprotein homeostasis.* Curr. Opin. Lipidol. 19, 229-234 (2008).

32. Wiggins, D. and Gibbons, G. F. *Origin of hepatic very-low-density lipoprotein triacylglycerol: the contribution of cellular phospholipid.* Biochem. J. 320 ( Pt 2), 673-679 (1996).

33. Zechner, R. *The tissue-specific expression of lipoprotein lipase: implications for energy and lipoprotein metabolism.* Curr. Opin. Lipidol. 8, 77-88 (1997).

34. Goldberg, I. J. *Lipoprotein lipase and lipolysis: central roles in lipoprotein metabolism and atherogenesis.* J. Lipid Res. 37, 693-707 (1996).

35. Beigneux, A. P., Weinstein, M. M., Davies, B. S. *et al. GPIHBP1 and lipolysis: an update.* Curr. Opin. Lipidol. 20, 211-216 (2009).

36. Sugden, M. C., Holness, M. J., and Howard, R. M. *Changes in lipoprotein lipase activities in adipose tissue, heart and skeletal muscle during continuous or interrupted feeding.* Biochem. J. 292 ( Pt 1), 113-119 (1993).

37. Ruge, T., Wu, G., Olivecrona, T. *et al. Nutritional regulation of lipoprotein lipase in mice.* Int. J. Biochem. Cell Biol. 36, 320-329 (2004).

38. Wang, C. S. *Structure and functional properties of apolipoprotein C-II.* Prog. Lipid Res. 30, 253-258 (1991).

39. Schaap, F. G., Rensen, P. C., Voshol, P. J. *et al. ApoAV reduces plasma triglycerides by inhibiting very low density lipoprotein-triglyceride (VLDL-TG) production and stimulating lipoprotein lipase-mediated VLDL-TG hydrolysis.* J. Biol. Chem. 279, 27941-27947 (2004).

40. Merkel, M., Loeffler, B., Kluger, M. *et al. Apolipoprotein AV accelerates plasma hydrolysis of triglyceride-rich lipoproteins by interaction with proteoglycan-bound lipoprotein lipase.* J. Biol. Chem. 280, 21553-21560 (2005).

41. Ginsberg, H. N., Le, N. A., Goldberg, I. J. *et al. Apolipoprotein B metabolism in subjects with deficiency of apolipoproteins CIII and AI. Evidence that apolipoprotein CIII inhibits catabolism of triglyceride-rich lipoproteins by lipoprotein lipase in vivo.* J. Clin. Invest 78, 1287-1295 (1986).



42. Havel, R. J., Fielding, C. J., Olivecrona, T. *et al. Cofactor activity of protein components of human very low density lipoproteins in the hydrolysis of triglycerides by lipoproteins lipase from different sources.* Biochemistry 12, 1828-1833 (1973).

43. Lichtenstein, L. and Kersten, S. *Modulation of plasma TG lipolysis by Angiopoietin-like proteins and GPIHBP1.* Biochim. Biophys. Acta 1801, 415-420 (2010).

44. Medh, J. D., Bowen, S. L., Fry, G. L. *et al. Lipoprotein lipase binds to low density lipoprotein receptors and induces receptor-mediated catabolism of very low density lipoproteins in vitro.* J. Biol. Chem. 271, 17073-17080 (1996).

45. Zimmermann, R., Strauss, J. G., Haemmerle, G. *et al. Fat mobilization in adipose tissue is promoted by adipose triglyceride lipase.* Science 306, 1383-1386 (2004).

46. Zimmermann, R., Lass, A., Haemmerle, G. *et al. Fate of fat: the role of adipose triglyceride lipase in lipolysis.* Biochim. Biophys. Acta 1791, 494-500 (2009).

47. Watt, M. J. and Steinberg, G. R. *Regulation and function of triacylglycerol lipases in cellular metabolism.* Biochem. J. 414, 313-325 (2008).

48. Su, X. and Abumrad, N. A. *Cellular fatty acid uptake: a pathway under construction.* Trends Endocrinol. Metab 20, 72-77 (2009).

49. Stremmel, W., Pohl, L., Ring, A. *et al. A new concept of cellular uptake and intracellular trafficking of long-chain fatty acids.* Lipids 36, 981-989 (2001).

50. van der Vusse, G. J., van Bilsen, M., Glatz, J. F. *et al. Critical steps in cellular fatty acid uptake and utilization.* Mol. Cell Biochem. 239, 9-15 (2002).

51. Briscoe, C. P., Tadayyon, M., Andrews, J. L. *et al. The orphan G protein-coupled receptor GPR40 is activated by medium and long chain fatty acids.* J. Biol. Chem. 278, 11303-11311 (2003).

52. Brown, A. J., Goldsworthy, S. M., Barnes, A. A. *et al. The Orphan G protein-coupled receptors GPR41 and GPR43 are activated by propionate and other short chain carboxylic acids.* J. Biol. Chem. 278, 11312-11319 (2003).

53. Itoh, Y., Kawamata, Y., Harada, M. *et al. Free fatty acids regulate insulin secretion from pancreatic beta cells through GPR40.* Nature 422, 173-176 (2003).

54. Oh Da, Y., Talukdar, S., Bae, E. J. *et al. GPR120 is an omega-3 fatty acid receptor mediating potent anti-inflammatory and insulin-sensitizing effects.* Cell 142, 687-698 (2010).

55. Xiong, Y., Miyamoto, N., Shibata, K. *et al. Short-chain fatty acids stimulate leptin production in adipocytes through the G protein-coupled receptor GPR41.* Proc. Natl. Acad. Sci. U. S. A 101, 1045-1050 (2004).

56. Hirasawa, A., Tsumaya, K., Awaji, T. *et al. Free fatty acids regulate gut incretin glucagon-like peptide-1 secretion through GPR120.* Nat. Med. 11, 90-94 (2005).

57. Le Poul, E., Loison, C., Struyf, S. *et al. Functional characterization of human receptors for short chain fatty acids and their role in polymorphonuclear cell activation.* J. Biol. Chem. 278, 25481-25489 (2003).

58. Sina, C., Gavrilova, O., Forster, M. *et al. G protein-coupled receptor 43 is essential for neutrophil recruitment during intestinal inflammation.* J. Immunol. 183, 7514-7522 (2009).

59. Glass, C. K. *Going nuclear in metabolic and cardiovascular disease.* J. Clin. Invest 116, 556-560 (2006).

60. Germain, P., Staels, B., Dacquet, C. *et al. Overview of nomenclature of nuclear receptors.* Pharmacol. Rev. 58, 685-704 (2006).

61. Daynes, R. A. and Jones, D. C. *Emerging roles of PPARs in inflammation and immunity.* Nat. Rev. Immunol. 2, 748-759 (2002).

62. Lefebvre, P., Chinetti, G., Fruchart, J. C. *et al. Sorting out the roles of PPAR alpha in energy metabolism and vascular homeostasis.* J. Clin. Invest 116, 571-580 (2006).

63. Staels, B., Vu-Dac, N., Kosykh, V. A. *et al. Fibrates downregulate apolipoprotein C-III expression independent of induction of peroxisomal acyl coenzyme A oxidase. A potential mechanism for the hypolipidemic action of fibrates.* J. Clin. Invest 95, 705-712 (1995).

64. Schoonjans, K., Peinado-Onsurbe, J., Lefebvre, A. M. *et al. PPARalpha and PPARgamma activators direct a distinct tissue-specific transcriptional response via a PPRE in the lipoprotein lipase gene.* EMBO J. 15, 5336-5348 (1996).

65. Martin, G., Schoonjans, K., Lefebvre, A. M. *et al. Coordinate regulation of the expression of the fatty acid transport protein and acyl-CoA synthetase genes by PPARalpha and PPARgamma activators.* J. Biol. Chem. 272, 28210-28217 (1997).

66. Motojima, K., Passilly, P., Peters, J. M. *et al. Expression of putative fatty acid transporter genes are regulated by peroxisome proliferator-activated receptor alpha and gamma activators in a tissue- and inducer-specific manner.* J. Biol. Chem. 273, 16710-16714 (1998).

67. Brandt, J. M., Djouadi, F., and Kelly, D. P. *Fatty acids activate transcription of the muscle carnitine palmitoyltransferase I gene in cardiac myocytes via the peroxisome proliferator-activated receptor alpha.* J. Biol. Chem. 273, 23786-23792 (1998).

68. Barak, Y., Nelson, M. C., Ong, E. S. *et al. PPAR gamma is required for placental, cardiac, and adipose tissue development.* Mol. Cell 4, 585-595 (1999).

69. Rosen, E. D., Sarraf, P., Troy, A. E. *et al. PPAR gamma is required for the differentiation of adipose tissue in vivo and in vitro.* Mol. Cell 4, 611-617 (1999).

70. Vidal-Puig, A., Jimenez-Linan, M., Lowell, B. B. *et al. Regulation of PPAR gamma gene expression by nutrition and obesity in rodents.* J. Clin. Invest 97, 2553-2561 (1996).

71. Olswang, Y., Cohen, H., Papo, O. *et al. A mutation in the peroxisome proliferator-activated receptor gamma-binding site in the gene for the cytosolic form of phosphoenolpyruvate carboxykinase reduces adipose tissue size and fat content in mice.* Proc. Natl. Acad. Sci. U. S. A 99, 625-630 (2002).

72. Kliewer, S. A., Forman, B. M., Blumberg, B. *et al. Differential expression and activation of a family of murine peroxisome proliferator-activated receptors.* Proc. Natl. Acad. Sci. U. S. A 91, 7355-7359 (1994).



73. Wang, Y. X., Lee, C. H., Tiep, S. *et al. Peroxisome-proliferator-activated receptor delta activates fat metabolism to prevent obesity.* Cell 113, 159-170 (2003).

74. Tanaka, T., Yamamoto, J., Iwasaki, S. *et al. Activation of peroxisome proliferator-activated receptor delta induces fatty acid beta-oxidation in skeletal muscle and attenuates metabolic syndrome.* Proc. Natl. Acad. Sci. U. S. A 100, 15924-15929 (2003).

75. Brown, A. J., Sun, L., Feramisco, J. D. *et al. Cholesterol addition to ER membranes alters conformation of SCAP, the SREBP escort protein that regulates cholesterol metabolism.* Mol. Cell 10, 237-245 (2002).

76. Repa, J. J., Liang, G., Ou, J. *et al. Regulation of mouse sterol regulatory element-binding protein-1c gene (SREBP-1c) by oxysterol receptors, LXRalpha and LXRbeta.* Genes Dev. 14, 2819-2830 (2000).

77. Watanabe, M., Houten, S. M., Wang, L. *et al. Bile acids lower triglyceride levels via a pathway involving FXR, SHP, and SREBP-1c.* J. Clin. Invest 113, 1408-1418 (2004).

78. Horton, J. D., Goldstein, J. L., and Brown, M. S. *SREBPs: activators of the complete program of cholesterol and fatty acid synthesis in the liver.* J. Clin. Invest 109, 1125-1131 (2002).

79. Ueda, A., Hamadeh, H. K., Webb, H. K. *et al. Diverse roles of the nuclear orphan receptor CAR in regulating hepatic genes in response to phenobarbital.* Mol. Pharmacol. 61, 1-6 (2002).

80. Kassam, A., Winrow, C. J., Fernandez-Rachubinski, F. *et al. The peroxisome proliferator response element of the gene encoding the peroxisomal beta-oxidation enzyme enoyl-CoA hydratase/3-hydroxyacyl-CoA dehydrogenase is a target for constitutive androstane receptor beta/9-cis-retinoic acid receptor-mediated transactivation.* J. Biol. Chem. 275, 4345-4350 (2000).

81. Nakamura, K., Moore, R., Negishi, M. *et al. Nuclear pregnane X receptor cross-talk with FoxA2 to mediate drug-induced regulation of lipid metabolism in fasting mouse liver.* J. Biol. Chem. 282, 9768-9776 (2007).

82. Zhou, J., Zhai, Y., Mu, Y. *et al. A novel pregnane X receptor-mediated and sterol regulatory element-binding protein-independent lipogenic pathway.* J. Biol. Chem. 281, 15013-15020 (2006).

83. Rezen, T., Tamasi, V., Lovgren-Sandblom, A. *et al. Effect of CAR activation on selected metabolic pathways in normal and hyperlipidemic mouse livers.* BMC. Genomics 10, 384- (2009).

84. Maglich, J. M., Lobe, D. C., and Moore, J. T. *The nuclear receptor CAR (NR1I3) regulates serum triglyceride levels under conditions of metabolic stress.* J. Lipid Res. 50, 439-445 (2009).

85. de Haan, W., de Vries-van der Weij, Mol, I. M. *et al. PXR agonism decreases plasma HDL levels in ApoE3-Leiden.CETP mice.* Biochim. Biophys. Acta 1791, 191-197 (2009).

86. Morere, P., Nouvet, G., Stain, J. P. *et al. [Information obtained by liver biopsy in 100 tuberculous patients].* Sem. Hop. 51, 2095-2102 (1975).

87. Grieco, A., Forgione, A., Miele, L. *et al. Fatty liver and drugs.* Eur. Rev. Med. Pharmacol. Sci. 9, 261-263 (2005).

88. Vega, R. B., Huss, J. M., and Kelly, D. P. *The coactivator PGC-1 cooperates with peroxisome proliferator-activated receptor alpha in transcriptional control of nuclear genes encoding mitochondrial fatty acid oxidation enzymes.* Mol. Cell Biol. 20, 1868-1876 (2000).

89. Bhalla, S., Ozalp, C., Fang, S. *et al. Ligand-activated pregnane X receptor interferes with HNF-4 signaling by targeting a common coactivator PGC-1alpha. Functional implications in hepatic cholesterol and glucose metabolism.* J. Biol. Chem. 279, 45139-45147 (2004).

90. Shiraki, T., Sakai, N., Kanaya, E. *et al. Activation of orphan nuclear constitutive androstane receptor requires subnuclear targeting by peroxisome proliferator-activated receptor gamma coactivator-1 alpha. A possible link between xenobiotic response and nutritional state.* J. Biol. Chem. 278, 11344-11350 (2003).

91. Lin, J., Yang, R., Tarr, P. T. *et al. Hyperlipidemic effects of dietary saturated fats mediated through PGC-1beta coactivation of SREBP.* Cell 120, 261-273 (2005).

92. Puigserver, P., Rhee, J., Donovan, J. *et al. Insulin-regulated hepatic gluconeogenesis through FOXO1-PGC-1alpha interaction.* Nature 423, 550-555 (2003).

93. Yoon, J. C., Puigserver, P., Chen, G. *et al. Control of hepatic gluconeogenesis through the transcriptional coactivator PGC-1.* Nature 413, 131-138 (2001).

94. Saltiel, A. R. and Kahn, C. R. *Insulin signalling and the regulation of glucose and lipid metabolism.* Nature 414, 799-806 (2001).

95. Bollen, M., Keppens, S., and Stalmans, W. *Specific features of glycogen metabolism in the liver.* Biochem. J. 336 ( Pt 1), 19-31 (1998).

96. Exton, J. H. and Park, C. R. *Control of gluconeogenesis in liver. I. General features of gluconeogenesis in the perfused livers of rats.* J. Biol. Chem. 242, 2622-2636 (1967).

97. Reaven, G. M. *The insulin resistance syndrome: definition and dietary approaches to treatment.* Annu. Rev. Nutr. 25, 391-406 (2005).

98. Dekker, J. M., Girman, C., Rhodes, T. *et al. Metabolic syndrome and 10-year cardiovascular disease risk in the Hoorn Study.* Circulation 112, 666-673 (2005).

99. Jeppesen, J., Hansen, T. W., Rasmussen, S. *et al. Metabolic syndrome, low-density lipoprotein cholesterol, and risk of cardiovascular disease: a population-based study.* Atherosclerosis 189, 369-374 (2006).

100. Manninen, V., Tenkanen, L., Koskinen, P. *et al. Joint effects of serum triglyceride and LDL cholesterol and HDL cholesterol concentrations on coronary heart disease risk in the Helsinki Heart Study. Implications for treatment.* Circulation 85, 37-45 (1992).

101. Kim, J. K., Fillmore, J. J., Chen, Y. *et al. Tissue-specific overexpression of lipoprotein lipase causes tissue-specific insulin resistance.* Proc. Natl. Acad. Sci. U. S. A 98, 7522-7527 (2001).

102. Seppala-Lindroos, A., Vehkavaara, S., Hakkinen, A. M. *et al. Fat accumulation in the liver is associated with defects in insulin suppression of glucose production and serum free fatty acids independent of obesity in normal men.* J. Clin. Endocrinol. Metab 87, 3023-3028 (2002).

103. Virkamaki, A., Korsheninnikova, E., Seppala-Lindroos, A. *et al. Intramyocellular lipid is associated with resistance to in vivo insulin actions on glucose uptake, antilipolysis, and early insulin signaling pathways in human skeletal muscle.* Diabetes 50, 2337-2343 (2001).

104. den Boer, M. A., Voshol, P. J., Kuipers, F. *et al. Hepatic glucose production is more sensitive to insulin-mediated inhibition than hepatic VLDL-triglyceride production.* Am. J. Physiol Endocrinol. Metab 291, E1360-E1364 (2006).

105. den Boer, M., Voshol, P. J., Kuipers, F. *et al. Hepatic steatosis: a mediator of the metabolic syndrome. Lessons from animal models.* Arterioscler. Thromb. Vasc. Biol. 24, 644-649 (2004).

106. Rader, D. J. *Effect of insulin resistance, dyslipidemia, and intra-abdominal adiposity on the development of cardiovascular disease and diabetes mellitus.* Am. J. Med. 120, S12-S18 (2007).

107. Getz, G. S. and Reardon, C. A. *Diet and murine atherosclerosis.* Arterioscler. Thromb. Vasc. Biol. 26, 242-249 (2006).

108. van den Maagdenberg, A. M., Hofker, M. H., Krimpenfort, P. J. *et al. Transgenic mice carrying the apolipoprotein E3-Leiden gene exhibit hyperlipoproteinemia.* J. Biol. Chem. 268, 10540-10545 (1993).

109. de Knijff, P., van den Maagdenberg, A. M., Stalenhoef, A. F. *et al. Familial dysbetalipoproteinemia associated with apolipoprotein E3-Leiden in an extended multigeneration pedigree.* J. Clin. Invest 88, 643-655 (1991).

110. van Vlijmen, B. J., van den Maagdenberg, A. M., Gijbels, M. J. *et al. Diet-induced hyperlipoproteinemia and atherosclerosis in apolipoprotein E3-Leiden transgenic mice.* J. Clin. Invest 93, 1403-1410 (1994).

111. Verschuren, L., Kleemann, R., Offerman, E. H. *et al. Effect of low dose atorvastatin versus diet-induced cholesterol lowering on atherosclerotic lesion progression and inflammation in apolipoprotein E*3-Leiden transgenic mice.* Arterioscler. Thromb. Vasc. Biol. 25, 161-167 (2005).

112. Kleemann, R., Princen, H. M., Emeis, J. J. *et al. Rosuvastatin reduces atherosclerosis development beyond and independent of its plasma cholesterol-lowering effect in APOE*3-Leiden transgenic mice: evidence for antiinflammatory effects of rosuvastatin.* Circulation 108, 1368-1374 (2003).

113. Delsing, D. J., Post, S. M., Groenendijk, M. *et al. Rosuvastatin reduces plasma lipids by inhibiting VLDL production and enhancing hepatobiliary lipid excretion in ApoE*3-leiden mice.* J. Cardiovasc. Pharmacol. 45, 53-60 (2005).

114. van der Hoogt, C. C., de Haan, W., Westerterp, M. *et al. Fenofibrate increases HDL-cholesterol by reducing cholesteryl ester transfer protein expression.* J. Lipid Res. 48, 1763-1771 (2007).

115. Zadelaar, S., Kleemann, R., Verschuren, L. *et al. Mouse models for atherosclerosis and pharmaceutical modifiers.* Arterioscler. Thromb. Vasc. Biol. 27, 1706-1721 (2007).

116. Westerterp, M., van der Hoogt, C. C., de Haan, W. *et al. Cholesteryl ester transfer protein decreases high-density lipoprotein and severely aggravates atherosclerosis in APOE*3-Leiden mice.* Arterioscler. Thromb. Vasc. Biol. 26, 2552-2559 (2006).

117. van der Hoorn, J. W., de Haan, W., Berbee, J. F. *et al. Niacin increases HDL by reducing hepatic expression and plasma levels of cholesteryl ester transfer protein in APOE*3Leiden.CETP mice.* Arterioscler. Thromb. Vasc. Biol. 28, 2016-2022 (2008).

118. de Haan, W., van der Hoogt, C. C., Westerterp, M. *et al. Atorvastatin increases HDL cholesterol by reducing CETP expression in cholesterol-fed APOE*3-Leiden. CETP mice.* Atherosclerosis 197, 57-63 (2008).

119. de Vries-van der Weij, de Haan, W., Hu, L. *et al. Bexarotene induces dyslipidemia by increased very low-density lipoprotein production and cholesteryl ester transfer protein-mediated reduction of high-density lipoprotein.* Endocrinology 150, 2368-2375 (2009).

120. Boden, W. E. *High-density lipoprotein cholesterol as an independent risk factor in cardiovascular disease: assessing the data from Framingham to the Veterans Affairs High--Density Lipoprotein Intervention Trial.* Am. J. Cardiol. 86, 19L-22L (2000).

121. Nordestgaard, B. G., Benn, M., Schnohr, P. *et al. Nonfasting triglycerides and risk of myocardial infarction, ischemic heart disease, and death in men and women.* JAMA 298, 299-308 (2007).

122. Barter, P. J., Caulfield, M., Eriksson, M. *et al. Effects of torcetrapib in patients at high risk for coronary events.* N. Engl. J. Med. 357, 2109-2122 (2007).

123. Bloomfield, D., Carlson, G. L., Sapre, A. *et al. Efficacy and safety of the cholesteryl ester transfer protein inhibitor anacetrapib as monotherapy and coadministered with atorvastatin in dyslipidemic patients.* Am. Heart J. 157, 352-360 (2009).

124. Rennings, A. J. and Stalenhoef, A. F. *JTT-705: is there still future for a CETP inhibitor after torcetrapib?* Expert. Opin. Investig. Drugs 17, 1589-1597 (2008).

125. Clark, R. W., Sutfin, T. A., Ruggeri, R. B. *et al. Raising high-density lipoprotein in humans through inhibition of cholesteryl ester transfer protein: an initial multidose study of torcetrapib.* Arterioscler. Thromb. Vasc. Biol. 24, 490-497 (2004).

126. de Grooth, G. J., Kuivenhoven, J. A., Stalenhoef, A. F. *et al. Efficacy and safety of a novel cholesteryl ester transfer protein inhibitor, JTT-705, in humans: a randomized phase II dose-response study.* Circulation 105, 2159-2165 (2002).

127. Hermann, F., Enseleit, F., Spieker, L. E. *et al. Cholesterylestertransfer protein inhibition and endothelial function in type II hyperlipidemia.* Thromb. Res. 123, 460-465 (2009).

128. Rashid, S., Trinh, D. K., Uffelman, K. D. *et al. Expression of human hepatic lipase in the rabbit model preferentially enhances the clearance of triglyceride-enriched versus native high-density lipoprotein apolipoprotein A-I.* Circulation 107, 3066-3072 (2003).

129. Jiang, X. C., Agellon, L. B., Walsh, A. *et al. Dietary cholesterol increases transcription of the human cholesteryl ester transfer protein gene in transgenic mice. Dependence on natural flanking sequences.* J. Clin. Invest 90, 1290-1295 (1992).

130. Berbee, J. F., van der Hoogt, C. C., Sundararaman, D. *et al. Severe hypertriglyceridemia in human APOC1 transgenic mice is caused by apoC-I-induced inhibition of LPL.* J. Lipid Res. 46, 297-306 (2005).

131. Aalto-Setala, K., Fisher, E. A., Chen, X. *et al. Mechanism of hypertriglyceridemia in human apolipoprotein (apo) CIII transgenic mice. Diminished very low density lipoprotein fractional catabolic rate associated with increased apo CIII and reduced apo E on the particles.* J. Clin. Invest 90, 1889-1900 (1992).

132. Pietzsch, J., Subat, S., Nitzsche, S. *et al. Very fast ultracentrifugation of serum lipoproteins: influence on lipoprotein separation and composition.* Biochim. Biophys. Acta 1254, 77-88 (1995).

133. Li, X., Catalina, F., Grundy, S. M. *et al. Method to measure apolipoprotein B-48 and B-100 secretion rates in an individual mouse: evidence for a very rapid turnover of VLDL and preferential removal of B-48- relative to B-100-containing lipoproteins.* J. Lipid Res. 37, 210-220 (1996).

134. Egusa, G., Brady, D. W., Grundy, S. M. *et al. Isopropanol precipitation method for the determination of apolipoprotein B specific activity and plasma concentrations during metabolic studies of very low density lipoprotein and low density lipoprotein apolipoprotein B.* J. Lipid Res. 24, 1261-1267 (1983).

135. Rensen, P. C., Herijgers, N., Netscher, M. H. *et al. Particle size determines the specificity of apolipoprotein E-containing triglyceride-rich emulsions for the LDL receptor versus hepatic remnant receptor in vivo.* J. Lipid Res. 38, 1070-1084 (1997).

136. Teusink, B., Voshol, P. J., Dahlmans, V. E. *et al. Contribution of fatty acids released from lipolysis of plasma triglycerides to total plasma fatty acid flux and tissue-specific fatty acid uptake.* Diabetes 52, 614-620 (2003).

137. Rensen, P. C., Jong, M. C., van Vark, L. C. *et al. Apolipoprotein E is resistant to intracellular degradation in vitro and in vivo. Evidence for retroendocytosis.* J. Biol. Chem. 275, 8564-8571 (2000).

138. Voshol, P. J., Rensen, P. C., van Dijk, K. W. *et al. Effect of plasma triglyceride metabolism on lipid storage in adipose tissue: studies using genetically engineered mouse models.* Biochim. Biophys. Acta 1791, 479-485 (2009).

139. Escola-Gil, J. C., Julve, J., Marzal-Casacuberta, A. *et al. ApoA-II expression in CETP transgenic mice increases VLDL production and impairs VLDL clearance.* J. Lipid Res. 42, 241-248 (2001).

140. Salerno, A. G., Patricio, P. R., Berti, J. A. *et al. Cholesteryl ester transfer protein (CETP) increases postprandial triglyceridemia and delays triglyceride plasma clearance in transgenic mice.* Biochem. J. 419, 629-634 (2009).

141. Harada, L. M., Amigo, L., Cazita, P. M. *et al. CETP expression enhances liver HDL-cholesteryl ester uptake but does not alter VLDL and biliary lipid secretion.* Atherosclerosis 191, 313-318 (2007).

142. Lamarche, B., Uffelman, K. D., Carpentier, A. *et al. Triglyceride enrichment of HDL enhances in vivo metabolic clearance of HDL apo A-I in healthy men.* J. Clin. Invest 103, 1191-1199 (1999).

143. Melchior, G. W., Castle, C. K., Murray, R. W. *et al. Apolipoprotein A-I metabolism in cholesteryl ester transfer protein transgenic mice. Insights into the mechanisms responsible for low plasma high density lipoprotein levels.* J. Biol. Chem. 269, 8044-8051 (1994).

144. Rashid, S., Barrett, P. H., Uffelman, K. D. *et al. Lipolytically modified triglyceride-enriched HDLs are rapidly cleared from the circulation.* Arterioscler. Thromb. Vasc. Biol. 22, 483-487 (2002).

145. Chapman, M. J. *Fibrates in 2003: therapeutic action in atherogenic dyslipidaemia and future perspectives.* Atherosclerosis 171, 1-13 (2003).

146. Schoonjans, K., Staels, B., and Auwerx, J. *The peroxisome proliferator activated receptors (PPARS) and their effects on lipid metabolism and adipocyte differentiation.* Biochim. Biophys. Acta 1302, 93-109 (1996).

147. Staels, B., Dallongeville, J., Auwerx, J. *et al. Mechanism of action of fibrates on lipid and lipoprotein metabolism.* Circulation 98, 2088-2093 (1998).

148. Hogue, J. C., Lamarche, B., Deshaies, Y. *et al. Differential effect of fenofibrate and atorvastatin on in vivo kinetics of apolipoproteins B-100 and B-48 in subjects with type 2 diabetes mellitus with marked hypertriglyceridemia.* Metabolism 57, 246-254 (2008).

149. Watts, G. F., Ji, J., Chan, D. C. *et al. Relationships between changes in plasma lipid transfer proteins and apolipoprotein B-100 kinetics during fenofibrate treatment in the metabolic syndrome.* Clin. Sci. (Lond) 111, 193-199 (2006).

150. Linden, D., Alsterholm, M., Wennbo, H. *et al. PPARalpha deficiency increases secretion and serum levels of apolipoprotein B-containing lipoproteins.* J. Lipid Res. 42, 1831-1840 (2001).

151. Tordjman, K., Bernal-Mizrachi, C., Zemany, L. *et al. PPARalpha deficiency reduces insulin resistance and atherosclerosis in apoE-null mice.* J. Clin. Invest 107, 1025-1034 (2001).

152. Kersten, S. *Peroxisome proliferator activated receptors and lipoprotein metabolism.* PPAR. Res. 2008, 132960- (2008).

153. Hahn, S. E. and Goldberg, D. M. *Modulation of lipoprotein production in Hep G2 cells by fenofibrate and clofibrate.* Biochem. Pharmacol. 43, 625-633 (1992).

154. Lamb, R. G., Koch, J. C., and Bush, S. R. *An enzymatic explanation of the differential effects of oleate and gemfibrozil on cultured hepatocyte triacylglycerol and phosphatidylcholine biosynthesis and secretion.* Biochim. Biophys. Acta 1165, 299-305 (1993).

155. Zechner, R. *Rapid and simple isolation procedure for lipoprotein lipase from human milk.* Biochim. Biophys. Acta 1044, 20-25 (1990).

156. Bligh, E. G. and Dyer, W. J. *A rapid method of total lipid extraction and purification.* Can. J. Biochem. Physiol 37, 911-917 (1959).

157. de Groot, P. J., Reiff, C., Mayer, C. *et al. NuGO contributions to GenePattern.* Genes Nutr. 3, 143-146 (2008).

158. Storey, J. D. and Tibshirani, R. *Statistical significance for genomewide studies.* Proc. Natl. Acad. Sci. U. S. A 100, 9440-9445 (2003).

159. Boorsma, A., Foat, B. C., Vis, D. *et al. T-profiler: scoring the activity of predefined groups of genes using gene expression data.* Nucleic Acids Res. 33, W592-W595 (2005).

160. Reich, M., Liefeld, T., Gould, J. *et al. GenePattern 2.0.* Nat. Genet. 38, 500-501 (2006).

161. Adiels, M., Taskinen, M. R., Packard, C. *et al. Overproduction of large VLDL particles is driven by increased liver fat content in man.* Diabetologia 49, 755-765 (2006).

162. Guerin, M., Bruckert, E., Dolphin, P. J. *et al. Fenofibrate reduces plasma cholesteryl ester transfer from HDL to VLDL and normalizes the atherogenic, dense LDL profile in combined hyperlipidemia.* Arterioscler. Thromb. Vasc. Biol. 16, 763-772 (1996).

163. Heller, F. and Harvengt, C. *Effects of clofibrate, bezafibrate, fenofibrate and probucol on plasma lipolytic enzymes in normolipaemic subjects.* Eur. J. Clin. Pharmacol. 25, 57-63 (1983).

164. Malmendier, C. L., Lontie, J. F., Delcroix, C. *et al. Apolipoproteins C-II and C-III metabolism in hypertriglyceridemic patients. Effect of a drastic triglyceride reduction by combined diet restriction and fenofibrate administration.* Atherosclerosis 77, 139-149 (1989).

165. Aoyama, T., Peters, J. M., Iritani, N. *et al. Altered constitutive expression of fatty acid-metabolizing enzymes in mice lacking the peroxisome proliferator-activated receptor alpha (PPARalpha).* J. Biol. Chem. 273, 5678-5684 (1998).

166. Gulick, T., Cresci, S., Caira, T. *et al. The peroxisome proliferator-activated receptor regulates mitochondrial fatty acid oxidative enzyme gene expression.* Proc. Natl. Acad. Sci. U. S. A 91, 11012-11016 (1994).

167. Shiri-Sverdlov, R., Wouters, K., van Gorp, P. J. *et al. Early diet-induced non-alcoholic steatohepatitis in APOE2 knock-in mice and its prevention by fibrates.* J. Hepatol. 44, 732-741 (2006).

168. Ameen, C., Edvardsson, U., Ljungberg, A. *et al. Activation of peroxisome proliferator-activated receptor alpha increases the expression and activity of microsomal triglyceride transfer protein in the liver.* J. Biol. Chem. 280, 1224-1229 (2005).

169. Duval, C., Muller, M., and Kersten, S. *PPARalpha and dyslipidemia.* Biochim. Biophys. Acta 1771, 961-971 (2007).

170. Watts, G. F., Barrett, P. H., Ji, J. *et al. Differential regulation of lipoprotein kinetics by atorvastatin and fenofibrate in subjects with the metabolic syndrome.* Diabetes 52, 803-811 (2003).

171. Duivenvoorden, I., Teusink, B., Rensen, P. C. *et al. Acute inhibition of hepatic beta-oxidation in APOE*3Leiden mice does not affect hepatic VLDL secretion or insulin sensitivity.* J. Lipid Res. 46, 988-993 (2005).

172. Linden, D., Lindberg, K., Oscarsson, J. *et al. Influence of peroxisome proliferator-activated receptor alpha agonists on the intracellular turnover and secretion of apolipoprotein (Apo) B-100 and ApoB-48.* J. Biol. Chem. 277, 23044-23053 (2002).

173. Srivastava, R. A., Jahagirdar, R., Azhar, S. *et al. Peroxisome proliferator-activated receptor-alpha selective ligand reduces adiposity, improves insulin sensitivity and inhibits atherosclerosis in LDL receptor-deficient mice.* Mol. Cell Biochem. 285, 35-50 (2006).

174. Hall, R. G., Leff, R. D., and Gumbo, T. *Treatment of active pulmonary tuberculosis in adults: current standards and recent advances. Insights from the Society of Infectious Diseases Pharmacists.* Pharmacotherapy 29, 1468-1481 (2009).

175. Austerhoff, A., Kindler, U., Knop, P. *et al. [Liver toxicity of combined rifampicin-isoniazid-ethambutol medication (author's transl)].* Dtsch. Med. Wochenschr. 99, 1182- (1974).

176. Pilheu, J. A., De Salvo, M. C., and Barcat, J. A. *[Effect of isoniazid and rifampicin regimens on the liver of tuberculosis patients].* Medicina (B Aires) 39, 298-304 (1979).

177. Taranger, J., Girbal, J. P., and Giacchero, G. *[Rifampicin and liver function (72 punctures biopsies)].* Rev. Tuberc. Pneumol. (Paris) 34, 717-720 (1970).

178. Khogali, A. M., Chazan, B. I., Metcalf, V. J. *et al. Hyperlipidaemia as a complication of rifampicin treatment.* Tubercle. 55, 231-233 (1974).

179. Lehmann, J. M., McKee, D. D., Watson, M. A. *et al. The human orphan nuclear receptor PXR is activated by compounds that regulate CYP3A4 gene expression and cause drug interactions.* J. Clin. Invest 102, 1016-1023 (1998).

180. Piriou, A., Warnet, J. M., Jacqueson, A. *et al. Fatty liver induced by high doses of rifampicin in the rat: possible relation with an inhibition of RNA polymerases in eukariotic cells.* Arch. Toxicol. Suppl 333-337 (1979).

181. Piriou, A., Maissiat, R., Jacqueson, A. *et al. Ultrastructural changes in the parenchymal liver cells of rats treated with high doses of rifampicin.* Br. J. Exp. Pathol. 68, 201-207 (1987).

182. Hoekstra, M., Lammers, B., Out, R. *et al. Activation of the nuclear receptor PXR decreases plasma LDL-cholesterol levels and induces hepatic steatosis in LDL receptor knockout mice.* Mol. Pharm. 6, 182-189 (2009).

183. Berbee, J. F., Havekes, L. M., and Rensen, P. C. *Apolipoproteins modulate the inflammatory response to lipopolysaccharide.* J. Endotoxin. Res. 11, 97-103 (2005).

184. Speijer, H., Groener, J. E., van, Ramshorst E. *et al. Different locations of cholesteryl ester transfer protein and phospholipid transfer protein activities in plasma.* Atherosclerosis 90, 159-168 (1991).

185. de Haan, W., de Vries-van der Weij, J., van der Hoorn, J. W. *et al. Torcetrapib does not reduce atherosclerosis beyond atorvastatin and induces more proinflammatory lesions than atorvastatin.* Circulation 117, 2515-2522 (2008).

186. Gautier, T., Tietge, U. J., Boverhof, R. *et al. Hepatic lipid accumulation in apolipoprotein C-I-deficient mice is potentiated by cholesteryl ester transfer protein.* J. Lipid Res. 48, 30-40 (2007).

187. van Eck, M., Twisk, J., Hoekstra, M. *et al. Differential effects of scavenger receptor BI deficiency on lipid metabolism in cells of the arterial wall and in the liver.* J. Biol. Chem. 278, 23699-23705 (2003).

188. Williamson, R., Lee, D., Hagaman, J. *et al. Marked reduction of high density lipoprotein cholesterol in mice genetically modified to lack apolipoprotein A-I.* Proc. Natl. Acad. Sci. U. S. A 89, 7134-7138 (1992).

189. Sporstol, M., Tapia, G., Malerod, L. *et al. Pregnane X receptor-agonists down-regulate hepatic ATP-binding cassette transporter A1 and scavenger receptor class B type I.* Biochem. Biophys. Res. Commun. 331, 1533-1541 (2005).

190. Sakai, N., Vaisman, B. L., Koch, C. A. *et al. Targeted disruption of the mouse lecithin:cholesterol acyltransferase (LCAT) gene. Generation of a new animal model for human LCAT deficiency.* J. Biol. Chem. 272, 7506-7510 (1997).

191. Jiang, X. C., Bruce, C., Mar, J. *et al. Targeted mutation of plasma phospholipid transfer protein gene markedly reduces high-density lipoprotein levels.* J. Clin. Invest 103, 907-914 (1999).

192. Le Goff, W., Guerin, M., and Chapman, M. J. *Pharmacological modulation of cholesteryl ester transfer protein, a new therapeutic target in atherogenic dyslipidemia.* Pharmacol. Ther. 101, 17-38 (2004).

193. Rigotti, A., Trigatti, B. L., Penman, M. *et al. A targeted mutation in the murine gene encoding the high density lipoprotein (HDL) receptor scavenger receptor class B type I reveals its key role in HDL metabolism.* Proc. Natl. Acad. Sci. U. S. A 94, 12610-12615 (1997).

194. Kissa E. *Fluorinated surfactants and repellents.* (2001).

195. Calafat, A. M., Wong, L. Y., Kuklenyik, Z. *et al. Polyfluoroalkyl chemicals in the U.S. population: data from the National Health and Nutrition Examination Survey (NHANES) 2003-2004 and comparisons with NHANES 1999-2000.* Environ. Health Perspect. 115, 1596-1602 (2007).

196. Xu, L., Krenitsky, D. M., Seacat, A. M. *et al. Biotransformation of N-ethyl-N-(2-hydroxyethyl)perfluorooctanesulfonamide by rat liver microsomes, cytosol, and slices and by expressed rat and human cytochromes P450.* Chem. Res. Toxicol. 17, 767-775 (2004).

197. Xu, L., Krenitsky, D. M., Seacat, A. M. *et al. N-glucuronidation of perfluorooctanesulfonamide by human, rat, dog, and monkey liver microsomes and by expressed rat and human UDP-glucuronosyltransferases.* Drug Metab Dispos. 34, 1406-1410 (2006).

198. D'eon, J. C., Hurley, M. D., Wallington, T. J. *et al. Atmospheric chemistry of N-methyl perfluorobutane sulfonamidoethanol, C4F9SO2N(CH3)CH2CH2OH: kinetics and mechanism of reaction with OH.* Environ. Sci. Technol. 40, 1862-1868 (2006).

199. Giesy, J. P. and Kannan, K. *Global distribution of perfluorooctane sulfonate in wildlife.* Environ. Sci. Technol. 35, 1339-1342 (2001).

200. Hansen, K. J., Clemen, L. A., Ellefson, M. E. *et al. Compound-specific, quantitative characterization of organic fluorochemicals in biological matrices.* Environ. Sci. Technol. 35, 766-770 (2001).

201. Olsen, G. W., Burris, J. M., Ehresman, D. J. *et al. Half-life of serum elimination of perfluorooctanesulfonate,perfluorohexanesulfonate, and perfluorooctanoate in retired fluorochemical production workers.* Environ. Health Perspect. 115, 1298-1305 (2007).

202. Lau, C., Anitole, K., Hodes, C. *et al. Perfluoroalkyl acids: a review of monitoring and toxicological findings.* Toxicol. Sci. 99, 366-394 (2007).

203. Olsen, G. W., Chang, S. C., Noker, P. E. *et al. A comparison of the pharmacokinetics of perfluorobutanesulfonate (PFBS) in rats, monkeys, and humans.* Toxicology 256, 65-74 (2009).

204. Nelson, J. W., Hatch, E. E., and Webster, T. F. *Exposure to polyfluoroalkyl chemicals and cholesterol, body weight, and insulin resistance in the general U.S. population.* Environ. Health Perspect. 118, 197-202 (2010).

205. Steenland, K., Tinker, S., Frisbee, S. *et al. Association of perfluorooctanoic acid and perfluorooctane sulfonate with serum lipids among adults living near a chemical plant.* Am. J. Epidemiol. 170, 1268-1278 (2009).

206. Olsen, G. W., Burris, J. M., Burlew, M. M. *et al. Epidemiologic assessment of worker serum perfluorooctanesulfonate (PFOS) and perfluorooctanoate (PFOA) concentrations and medical surveillance examinations.* J. Occup. Environ. Med. 45, 260-270 (2003).

207. Seacat, A. M., Thomford, P. J., Hansen, K. J. *et al. Subchronic toxicity studies on perfluorooctanesulfonate potassium salt in cynomolgus monkeys.* Toxicol. Sci. 68, 249-264 (2002).

208. Curran, I., Hierlihy, S. L., Liston, V. *et al. Altered fatty acid homeostasis and related toxicologic sequelae in rats exposed to dietary potassium perfluorooctanesulfonate (PFOS).* J. Toxicol. Environ. Health A 71, 1526-1541 (2008).

209. Haughom, B. and Spydevold, O. *The mechanism underlying the hypolipemic effect of perfluorooctanoic acid (PFOA), perfluorooctane sulphonic acid (PFOSA) and clofibric acid.* Biochim. Biophys. Acta 1128, 65-72 (1992).

210. Martin, M. T., Brennan, R. J., Hu, W. *et al. Toxicogenomic study of triazole fungicides and perfluoroalkyl acids in rat livers predicts toxicity and categorizes chemicals based on mechanisms of toxicity.* Toxicol. Sci. 97, 595-613 (2007).

211. Manal, A., Abd El-Nasser, M. A., Shaaban, A. A. *et al. Toxicological efects of perfluoroalkyl acids on pregnant female mice.* Ass. Univ. Environ. Res. 12, 23-39 (2009).

212. Butenhoff, J. L., Chang, S. C., Ehresman, D. J. *et al. Evaluation of potential reproductive and developmental toxicity of potassium perfluorohexanesulfonate in Sprague Dawley rats.* Reprod. Toxicol. 27, 331-341 (2009).



213. Lieder, P. H., Chang, S. C., York, R. G. *et al. Toxicological evaluation of potassium perfluorobutanesulfonate in a 90-day oral gavage study with Sprague-Dawley rats.* Toxicology 255, 45-52 (2009).

214. Ehresman, D. J., Froehlich, J. W., Olsen, G. W. *et al. Comparison of human whole blood, plasma, and serum matrices for the determination of perfluorooctanesulfonate (PFOS), perfluorooctanoate (PFOA), and other fluorochemicals.* Environ. Res. 103, 176-184 (2007).

215. Post, S. M., Groenendijk, M., Solaas, K. *et al. Cholesterol 7alpha-hydroxylase deficiency in mice on an APOE*3-Leiden background impairs very-low-density lipoprotein production.* Arterioscler. Thromb. Vasc. Biol. 24, 768-774 (2004).

216. Post, S. M., de Roos, B., Vermeulen, M. *et al. Cafestol increases serum cholesterol levels in apolipoprotein E*3-Leiden transgenic mice by suppression of bile acid synthesis.* Arterioscler. Thromb. Vasc. Biol. 20, 1551-1556 (2000).

217. Post, S. M., de Crom, R., van Haperen, R. *et al. Increased fecal bile acid excretion in transgenic mice with elevated expression of human phospholipid transfer protein.* Arterioscler. Thromb. Vasc. Biol. 23, 892-897 (2003).

218. Moreau, A., Vilarem, M. J., Maurel, P. *et al. Xenoreceptors CAR and PXR activation and consequences on lipid metabolism, glucose homeostasis, and inflammatory response.* Mol. Pharm. 5, 35-41 (2008).

219. Bijland, S., Pieterman, E. J., Maas, A. C. *et al. Fenofibrate increases very low density lipoprotein-triglyceride production despite reducing plasma triglyceride levels in APOE*3-Leiden.CETP mice.* J. Biol. Chem. 285, 25168-25175 (2010).

220. Berthiaume, J. and Wallace, K. B. *Perfluorooctanoate, perflourooctanesulfonate, and N-ethyl perfluorooctanesulfonamido ethanol; peroxisome proliferation and mitochondrial biogenesis.* Toxicol. Lett. 129, 23-32 (2002).

221. Seacat, A. M., Thomford, P. J., Hansen, K. J. *et al. Sub-chronic dietary toxicity of potassium perfluorooctanesulfonate in rats.* Toxicology 183, 117-131 (2003).

222. Shipley, J. M., Hurst, C. H., Tanaka, S. S. *et al. Trans-activation of PPARalpha and induction of PPARalpha target genes by perfluorooctane-based chemicals.* Toxicol. Sci. 80, 151-160 (2004).

223. Bjork, J. A., Lau, C., Chang, S. C. *et al. Perfluorooctane sulfonate-induced changes in fetal rat liver gene expression.* Toxicology 251, 8-20 (2008).

224. Ikeda, T., Aiba, K., Fukuda, K. *et al. The induction of peroxisome proliferation in rat liver by perfluorinated fatty acids, metabolically inert derivatives of fatty acids.* J. Biochem. 98, 475-482 (1985).

225. Chateau-Degat, M. L., Pereg, D., Dallaire, R. *et al. Effects of perfluorooctanesulfonate exposure on plasma lipid levels in the Inuit population of Nunavik (Northern Quebec).* Environ. Res. (2010).

226. Tilton, S. C., Orner, G. A., Benninghoff, A. D. *et al. Genomic profiling reveals an alternate mechanism for hepatic tumor promotion by perfluorooctanoic acid in rainbow trout.* Environ. Health Perspect. 116, 1047-1055 (2008).

227. Alberti, K. G., Zimmet, P., and Shaw, J. *International Diabetes Federation: a consensus on Type 2 diabetes prevention.* Diabet. Med. 24, 451-463 (2007).

228. Lonardo, A., Lombardini, S., Scaglioni, F. *et al. Hepatic steatosis and insulin resistance: does etiology make a difference?* J. Hepatol. 44, 190-196 (2006).

229. Heijboer, A. C., Donga, E., Voshol, P. J. *et al. Sixteen hours of fasting differentially affects hepatic and muscle insulin sensitivity in mice.* J. Lipid Res. 46, 582-588 (2005).

230. Heijboer, A. C., Voshol, P. J., Donga, E. *et al. High fat diet induced hepatic insulin resistance is not related to changes in hypothalamic mRNA expression of NPY, AgRP, POMC and CART in mice.* Peptides 26, 2554-2558 (2005).

231. Zambon, A., Hashimoto, S. I., and Brunzell, J. D. *Analysis of techniques to obtain plasma for measurement of levels of free fatty acids.* J. Lipid Res. 34, 1021-1028 (1993).

232. 't Hoen, P. A., de Kort, F., van Ommen, G. J. *et al. Fluorescent labelling of cRNA for microarray applications.* Nucleic Acids Res. 31, e20- (2003).

233. Smyth, G. K. *Linear models and empirical bayes methods for assessing differential expression in microarray experiments.* Stat. Appl. Genet. Mol. Biol. 3, Article3- (2004).

234. Zhang, B., Kirov, S., and Snoddy, J. *WebGestalt: an integrated system for exploring gene sets in various biological contexts.* Nucleic Acids Res. 33, W741-W748 (2005).

235. Newgard, C. B., Lu, D., Jensen, M. V. *et al. Stimulus/secretion coupling factors in glucose-stimulated insulin secretion: insights gained from a multidisciplinary approach.* Diabetes 51 Suppl 3, S389-S393 (2002).

236. Brown, M. S. and Goldstein, J. L. *The SREBP pathway: regulation of cholesterol metabolism by proteolysis of a membrane-bound transcription factor.* Cell 89, 331-340 (1997).

237. Eberle, D., Hegarty, B., Bossard, P. *et al. SREBP transcription factors: master regulators of lipid homeostasis.* Biochimie 86, 839-848 (2004).

238. Goldstein, J. L. and Brown, M. S. *Regulation of the mevalonate pathway.* Nature 343, 425-430 (1990).

239. Tomkins, G. M. and Chaikoff, I. L. *Cholesterol synthesis by liver. I. Influence of fasting and of diet.* J. Biol. Chem. 196, 569-573 (1952).

240. Chawla, A., Repa, J. J., Evans, R. M. *et al. Nuclear receptors and lipid physiology: opening the X-files.* Science 294, 1866-1870 (2001).

241. Konno, Y., Negishi, M., and Kodama, S. *The roles of nuclear receptors CAR and PXR in hepatic energy metabolism.* Drug Metab Pharmacokinet. 23, 8-13 (2008).

242. Yu, S., Matsusue, K., Kashireddy, P. *et al. Adipocyte-specific gene expression and adipogenic steatosis in the mouse liver due to peroxisome proliferator-activated receptor gamma1 (PPARgamma1) overexpression.* J. Biol. Chem. 278, 498-505 (2003).



243. Heikkinen, S., Auwerx, J., and Argmann, C. A. *PPARgamma in human and mouse physiology.* Biochim. Biophys. Acta 1771, 999-1013 (2007).

244. Tanaka, T., Masuzaki, H., Ebihara, K. *et al. Transgenic expression of mutant peroxisome proliferator-activated receptor gamma in liver precipitates fasting-induced steatosis but protects against high-fat diet-induced steatosis in mice.* Metabolism 54, 1490-1498 (2005).

245. Gross, D. N., van den Heuvel, A. P., and Birnbaum, M. J. *The role of FoxO in the regulation of metabolism.* Oncogene 27, 2320-2336 (2008).

246. Shimomura, I., Bashmakov, Y., and Horton, J. D. *Increased levels of nuclear SREBP-1c associated with fatty livers in two mouse models of diabetes mellitus.* J. Biol. Chem. 274, 30028-30032 (1999).

247. Ide, T., Shimano, H., Yahagi, N. *et al. SREBPs suppress IRS-2-mediated insulin signalling in the liver.* Nat. Cell Biol. 6, 351-357 (2004).

248. Ntambi, J. M., Miyazaki, M., Stoehr, J. P. *et al. Loss of stearoyl-CoA desaturase-1 function protects mice against adiposity.* Proc. Natl. Acad. Sci. U. S. A 99, 11482-11486 (2002).

249. Sampath, H., Miyazaki, M., Dobrzyn, A. *et al. Stearoyl-CoA desaturase-1 mediates the pro-lipogenic effects of dietary saturated fat.* J. Biol. Chem. 282, 2483-2493 (2007).

250. Inazu, A., Nakajima, K., Nakano, T. *et al. Decreased post-prandial triglyceride response and diminished remnant lipoprotein formation in cholesteryl ester transfer protein (CETP) deficiency.* Atherosclerosis 196, 953-957 (2008).

251. Kastelein, J. J., van Leuven, S. I., Burgess, L. *et al. Effect of torcetrapib on carotid atherosclerosis in familial hypercholesterolemia.* N. Engl. J. Med. 356, 1620-1630 (2007).

252. Nicholls, S. J., Tuzcu, E. M., Brennan, D. M. *et al. Cholesteryl ester transfer protein inhibition, high-density lipoprotein raising, and progression of coronary atherosclerosis: insights from ILLUSTRATE (Investigation of Lipid Level Management Using Coronary Ultrasound to Assess Reduction of Atherosclerosis by CETP Inhibition and HDL Elevation).* Circulation 118, 2506-2514 (2008).

253. Krishna, R., Anderson, M. S., Bergman, A. J. *et al. Effect of the cholesteryl ester transfer protein inhibitor, anacetrapib, on lipoproteins in patients with dyslipidaemia and on 24-h ambulatory blood pressure in healthy individuals: two double-blind, randomised placebo-controlled phase I studies.* Lancet 370, 1907-1914 (2007).

254. Arai, T., Yamashita, S., Hirano, K. *et al. Increased plasma cholesteryl ester transfer protein in obese subjects. A possible mechanism for the reduction of serum HDL cholesterol levels in obesity.* Arterioscler. Thromb. 14, 1129-1136 (1994).

255. Dullaart, R. P., Sluiter, W. J., Dikkeschei, L. D. *et al. Effect of adiposity on plasma lipid transfer protein activities: a possible link between insulin resistance and high density lipoprotein metabolism.* Eur. J. Clin. Invest 24, 188-194 (1994).

256. Magkos, F., Mohammed, B. S., and Mittendorfer, B. *Plasma lipid transfer enzymes in non-diabetic lean and obese men and women.* Lipids 44, 459-464 (2009).

257. Ebenbichler, C. F., Laimer, M., Kaser, S. *et al. Relationship between cholesteryl ester transfer protein and atherogenic lipoprotein profile in morbidly obese women.* Arterioscler. Thromb. Vasc. Biol. 22, 1465-1469 (2002).

258. Laimer, M. W., Engl, J., Tschoner, A. *et al. Effects of weight loss on lipid transfer proteins in morbidly obese women.* Lipids 44, 1125-1130 (2009).

259. Ritsch, A. and Patsch, J. R. *Cholesteryl ester transfer protein: gathering momentum as a genetic marker and as drug target.* Curr. Opin. Lipidol. 14, 173-179 (2003).

260. Boekholdt, S. M. and Thompson, J. F. *Natural genetic variation as a tool in understanding the role of CETP in lipid levels and disease.* J. Lipid Res. 44, 1080-1093 (2003).

261. Borggreve, S. E., Hillege, H. L., Wolffenbuttel, B. H. *et al. The effect of cholesteryl ester transfer protein -629C->A promoter polymorphism on high-density lipoprotein cholesterol is dependent on serum triglycerides.* J. Clin. Endocrinol. Metab 90, 4198-4204 (2005).

262. Yki-Jarvinen, H. *Thiazolidinediones and the liver in humans.* Curr. Opin. Lipidol. 20, 477-483 (2009).

263. Fabbrini, E., Mohammed, B. S., Korenblat, K. M. *et al. Effect of fenofibrate and niacin on intrahepatic triglyceride content, very low-density lipoprotein kinetics, and insulin action in obese subjects with nonalcoholic fatty liver disease.* J. Clin. Endocrinol. Metab 95, 2727-2735 (2010).

264. Jeong, S. and Yoon, M. *Fenofibrate inhibits adipocyte hypertrophy and insulin resistance by activating adipose PPARalpha in high fat diet-induced obese mice.* Exp. Mol. Med. 41, 397-405 (2009).

265. Guerre-Millo, M., Gervois, P., Raspe, E. *et al. Peroxisome proliferator-activated receptor alpha activators improve insulin sensitivity and reduce adiposity.* J. Biol. Chem. 275, 16638-16642 (2000).

266. Duan, S. Z., Usher, M. G., and Mortensen, R. M. *PPARs: the vasculature, inflammation and hypertension.* Curr. Opin. Nephrol. Hypertens. 18, 128-133 (2009).

267. Babaev, V. R., Ishiguro, H., Ding, L. *et al. Macrophage expression of peroxisome proliferator-activated receptor-alpha reduces atherosclerosis in low-density lipoprotein receptor-deficient mice.* Circulation 116, 1404-1412 (2007).

268. Marx, N., Kehrle, B., Kohlhammer, K. *et al. PPAR activators as antiinflammatory mediators in human T lymphocytes: implications for atherosclerosis and transplantation-associated arteriosclerosis.* Circ. Res. 90, 703-710 (2002).

269. Madej, A., Okopien, B., Kowalski, J. *et al. Effects of fenofibrate on plasma cytokine concentrations in patients with atherosclerosis and hyperlipoproteinemia IIb.* Int. J. Clin. Pharmacol. Ther. 36, 345-349 (1998).

270. Ip, E., Farrell, G. C., Robertson, G. *et al. Central role of PPARalpha-dependent hepatic lipid turnover in dietary steatohepatitis in mice.* Hepatology 38, 123-132 (2003).

271. Fernandez-Miranda, C., Perez-Carreras, M., Colina, F. *et al. A pilot trial of fenofibrate for the treatment of non-alcoholic fatty liver disease.* Dig. Liver Dis. 40, 200-205 (2008).

272. Zhou, C., King, N., Chen, K. Y. *et al. Activation of pregnane X receptor induces hypercholesterolemia in wild-type and accelerates atherosclerosis in apolipoprotein E deficient mice.* J. Lipid Res. (2009).

273. Gibson, J. C., Lee, W. H., and Piccolo, J. R. *The ansamycins: hypolipidemic agents stimulating cholesterol removal by nonclassical mechanisms.* J. Lipid Res. 35, 1524-1534 (1994).

274. Gibson, J. C., Lee, W. H., and Stephan, Z. F. *The ansamycins: a novel class of hypolipidemic agents with a high affinity for lipoproteins.* Atherosclerosis 112, 47-57 (1995).

275. Grun, F. and Blumberg, B. *Perturbed nuclear receptor signaling by environmental obesogens as emerging factors in the obesity crisis.* Rev. Endocr. Metab Disord. 8, 161-171 (2007).

276. Grun, F. and Blumberg, B. *Endocrine disrupters as obesogens.* Mol. Cell Endocrinol. 304, 19-29 (2009).

277. Miao, J., Fang, S., Bae, Y. *et al. Functional inhibitory cross-talk between constitutive androstane receptor and hepatic nuclear factor-4 in hepatic lipid/glucose metabolism is mediated by competition for binding to the DR1 motif and to the common coactivators, GRIP-1 and PGC-1alpha.* J. Biol. Chem. 281, 14537-14546 (2006).

278. Guo, D., Sarkar, J., Suino-Powell, K. *et al. Induction of nuclear translocation of constitutive androstane receptor by peroxisome proliferator-activated receptor alpha synthetic ligands in mouse liver.* J. Biol. Chem. 282, 36766-36776 (2007).

279. Wieneke, N., Hirsch-Ernst, K. I., Kuna, M. *et al. PPARalpha-dependent induction of the energy homeostasis-regulating nuclear receptor NR1i3 (CAR) in rat hepatocytes: potential role in starvation adaptation.* FEBS Lett. 581, 5617-5626 (2007).

280. Randle, P. J., Garland, P. B., Hales, C. N. *et al. The glucose fatty-acid cycle. Its role in insulin sensitivity and the metabolic disturbances of diabetes mellitus.* Lancet 1, 785-789 (1963).

281. Randle, P. J., Garland, P. B., Newsholme, E. A. *et al. The glucose fatty acid cycle in obesity and maturity onset diabetes mellitus.* Ann. N. Y. Acad. Sci. 131, 324-333 (1965).

282. Randle, P. J. *Regulatory interactions between lipids and carbohydrates: the glucose fatty acid cycle after 35 years.* Diabetes Metab Rev. 14, 263-283 (1998).

283. Peterson, L. R., Herrero, P., Schechtman, K. B. *et al. Effect of obesity and insulin resistance on myocardial substrate metabolism and efficiency in young women.* Circulation 109, 2191-2196 (2004).

284. Kelley, D. E. and Mandarino, L. J. *Fuel selection in human skeletal muscle in insulin resistance: a reexamination.* Diabetes 49, 677-683 (2000).

285. Kelley, D. E., Goodpaster, B. H., and Storlien, L. *Muscle triglyceride and insulin resistance.* Annu. Rev. Nutr. 22, 325-346 (2002).

286. Sugden, M. C., Zariwala, M. G., and Holness, M. J. *PPARs and the orchestration of metabolic fuel selection.* Pharmacol. Res. 60, 141-150 (2009).

287. Tremblay, F., Gagnon, A., Veilleux, A. *et al. Activation of the mammalian target of rapamycin pathway acutely inhibits insulin signaling to Akt and glucose transport in 3T3-L1 and human adipocytes.* Endocrinology 146, 1328-1337 (2005).

288. Kamagate, A., Qu, S., Perdomo, G. *et al. FoxO1 mediates insulin-dependent regulation of hepatic VLDL production in mice.* J. Clin. Invest 118, 2347-2364 (2008).

289. Accili, D. and Arden, K. C. *FoxOs at the crossroads of cellular metabolism, differentiation, and transformation.* Cell 117, 421-426 (2004).

290. Barthel, A., Schmoll, D., and Unterman, T. G. *FoxO proteins in insulin action and metabolism.* Trends Endocrinol. Metab 16, 183-189 (2005).

291. Kamagate, A. and Dong, H. H. *FoxO1 integrates insulin signaling to VLDL production.* Cell Cycle 7, 3162-3170 (2008).

292. Maury, E. and Brichard, S. M. *Adipokine dysregulation, adipose tissue inflammation and metabolic syndrome.* Mol. Cell Endocrinol. 314, 1-16 (2010).

293. Hotamisligil, G. S. *Inflammatory pathways and insulin action.* Int. J. Obes. Relat Metab Disord. 27 Suppl 3, S53-S55 (2003).

294. Moller, D. E. *Potential role of TNF-alpha in the pathogenesis of insulin resistance and type 2 diabetes.* Trends Endocrinol. Metab 11, 212-217 (2000).

295. Hundal, R. S., Petersen, K. F., Mayerson, A. B. *et al. Mechanism by which high-dose aspirin improves glucose metabolism in type 2 diabetes.* J. Clin. Invest 109, 1321-1326 (2002).

296. Yuan, M., Konstantopoulos, N., Lee, J. *et al. Reversal of obesity- and diet-induced insulin resistance with salicylates or targeted disruption of Ikkbeta.* Science 293, 1673-1677 (2001).

297. Jarvis, D., Chinn, S., Potts, J. *et al. Association of body mass index with respiratory symptoms and atopy: results from the European Community Respiratory Health Survey.* Clin. Exp. Allergy 32, 831-837 (2002).

298. Schachter, L. M., Peat, J. K., and Salome, C. M. *Asthma and atopy in overweight children.* Thorax 58, 1031-1035 (2003).

299. Tantisira, K. G., Litonjua, A. A., Weiss, S. T. *et al. Association of body mass with pulmonary function in the Childhood Asthma Management Program (CAMP).* Thorax 58, 1036-1041 (2003).

300. Xu, B., Jarvelin, M. R., and Pekkanen, J. *Body build and atopy.* J. Allergy Clin. Immunol. 105, 393-394 (2000).

301. Visness, C. M., London, S. J., Daniels, J. L. *et al. Association of obesity with IgE levels and allergy symptoms in children and adolescents: results from the National Health and Nutrition Examination Survey 2005-2006.* J. Allergy Clin. Immunol. 123, 1163-9, 1169 (2009).

**Summary**

Obesity is characterized by excessive fat storage and is associated with various diseases like cardiovascular disease (CVD) and type 2 diabetes (DM2), thereby being a serious problem of public health. Excessive energy intake is an important cause of obesity since excess energy is primarily stored as fat. The stored fat is mobilized again during fasting in the form of fatty acids (FA). These FA are re-esterified in the liver in triglycerides (TG) that are secreted in VLDL particles to deliver FA to peripheral tissues where they can be used for energy.

One of the current views of the cause of diseases related to obesity is the (mis) handling of TG derived FA. Therefore it is important to understand pathways involved in the uptake, distribution, oxidation and storage of TG. In this thesis we have evaluated the effect of different interventions on VLDL-TG metabolism to gain a better understanding of its complex regulation. For these studies we used APOE*3-Leiden (E3L) and E3L.CETP transgenic mice that have a human-like lipoprotein metabolism and respond to lipid-modifying drugs in a ways similar to humans.



The first part of this thesis focuses on the effect of cholesteryl ester transfer protein (CETP) on VLDL-TG metabolism. CETP transfers cholesteryl esters and TG between lipoproteins and has been shown to have a major impact on cholesterol metabolism. Previous studies in E3L mice have shown that expression of CETP reduces HDL-C, increases LDL-C and thereby increases the risk to develop atherosclerosis. Whether CETP also has impact on TG metabolism was explored in **chapter 2**. Expression of CETP hardly affected VLDL-TG metabolism and did not influence high fat diet induced obesity in E3L mice. We concluded that CETP inhibitors are not likely to have adverse health effects related to TG metabolism.

The second part of this thesis addressed the effect of different pharmaceutical interventions on the regulation of VLDL-TG metabolism by nuclear receptors. Intermediates of lipid metabolism and hormones activate nuclear receptors after which they are transported to the nucleus where they regulate amongst other the expression of genes involved in energy homeostasis. These nuclear receptors include peroxisome proliferators activated receptors (PPARs) and the xenobiotic receptors pregnane X receptor (PXR) and constitutive androstane receptor (CAR).

In **chapter 3** we investigated the effect of the pharmacologic PPARα activator

fenofibrate on VLDL-TG metabolism. To this end, E3L.CETP mice were fed a western-type diet without or with fenofibrate. Treatment with fenofibrate lowered total plasma TG levels by increasing lipolysis of VLDL-TG. Unexpectedly, fenofibrate increased VLDL-TG production which is partly explained by increased FA turnover.

The effect of rifampicin on VLDL metabolism was studied in **chapter 4**. E3L.CETP mice were treated with the PXR agonist rifampicin, an antibiotic prescribed for the treatment of tuberculosis. Treatment with this drug is associated with hepatic steatosis and dyslipidemia. E3L.CETP mice were fed a western-type diet for 3 weeks followed by an additional 3 weeks diet without or with increasing doses of rifampicin. The highest dose of rifampicin used (0.10%) showed a decrease of both HDL and VLDL cholesterol levels whereas total TG levels were unaltered. This decrease in cholesterol was mainly explained by lowering of both HDL and VLDL particle production by the liver. However, the VLDL particles secreted were enriched in TG explaining why total TG levels were not affected by rifampicin.

In addition to drugs affecting nuclear receptors and lipid metabolism, chemical pollutants might also act as agonists for nuclear receptors. In **chapter 5** we describe the hypolipidemic effects of perfluoroakyl sulfonates (PFAS), a group of chemicals used for stain repellence and coatings. These compounds are higly resistant to degradation and bioaccumulate. PFAS activate PPARα as well as the xenobiotic receptors PXR and CAR, altogether reducing HDL and VLDL production by the liver as well as increasing VLDL-TG clearance by increasing lipolysis.

In **chapter 6** we examined the differences in hepatic gene expression in response to fasting or a high fat diet, both known to induce hepatic steatosis. However, only after high fat diet feeding this steatosis is associated with hepatic insulin resistance. To gain insight in the transcriptional processes leading to steatosis associated insulin resistance, C57Bl6/J mice were fed standard chow diet or a high fat diet for 2 weeks. After 2 weeks half of the mice fed chow were fasted for 16 hours whereas the other part of the chow fed mice and the high fat diet fed mice were fasted for 4 hours. Strikingly, fasting affected far more genes compared to control than feeding a high fat diet. Furthermore, hardly any overlap in gene expression profile was seen between fasting and a high

fat diet, suggesting completely different gene programmes are activated. High fat diet feeding was especially associated with activation of PPARα whereas fasting activated xenobiotic receptors PXR and CAR.

**Chapter 7** discusses the observation that nuclear receptors have a major impact on lipoprotein metabolism and play a key role in the pathology associated with obesity. Nuclear receptors are used as targets for the development of drugs to treat the metabolic syndrome. However, although we only focussed on the effect of nuclear receptors on lipoprotein metabolism in this thesis, inflammation is also regulated by these nuclear receptors. Development of new drugs that target nuclear receptors focuses on organ-specificity as well as gene-specificity. However, a focus on dyslipidemia only might neglect the anti-inflammatory effects of novel potential drugs that could provide added benefit.

8

## Nederlandse samenvatting voor niet-ingewijden

### Ongezond overgewicht

Zwaarlijvigheid (**obesitas**) is het overmatig opslaan van vet in ons lichaam en leidt tot ziektes als hart- en vaatziekten en suikerziekte en is daarom een groot probleem in de gezondheidszorg. Of iemand obees is wordt bepaald aan de hand van je Body Mass Index (**BMI**): het lichaamsgewicht in kilogram, gedeeld door de lichaamslengte in meters in het kwadraat ($kg/m^2$). Een BMI tussen 18,5 en 25 wordt beschouwd als ideaal voor een gezond individu; een BMI van meer dan 25 wordt beschouwd als te zwaar (overgewicht); een BMI van meer dan 30 wordt beschouwd als obesitas. Overmatige inname van calorieën is één van de belangrijkste oorzaken van obesitas omdat de extra calorieën voornamelijk als vet worden opgeslagen. Wanneer we vasten wordt dit vet weer vrijgemaakt in de vorm van **vetzuren** zodat we het vet kunnen gebruiken als energie bron. De meeste van deze vetzuren gaan direct naar de lever waar ze worden omgezet in **triglyceriden** (TG). Deze TG bestaan uit een glycerol keten met drie vetzuren. TG worden vanuit de lever vervolgens weer vrijgelaten in de bloedbaan.



### Transport van vet in ons lichaam

Omdat vet slecht oplost in water en bloed, moet vet 'oplosbaar' verpakt worden om getransporteerd te worden in ons lichaam. De verpakking van vet wordt ook wel een **lipoproteïne** genoemd. Afhankelijk van hun samenstelling hebben deze lipoproteïnen een ander dichtheid en worden ze als volgt ingedeeld: zeer lage dichtheid lipoproteïnen (**VLDL**) met voornamelijk TG, lage dichtheid lipoproteïnen (**LDL**) met TG en cholesterol en hoge dichtheid lipoproteïnen (**HDL**) met voornamelijk cholesterol. Het hebben van veel LDL is een risicofactor voor het ontstaan van aderverkalking terwijl HDL er juist voor beschermd. LDL is in de volksmond ook wel bekend als slecht cholesterol en HDL als goed cholesterol.

TG uit de lever komen in de bloedbaan terecht in VLDL om bij andere weefsels vetzuren af te leveren die als energie bron gebruikt kunnen worden. Omdat TG zeer groot is moeten deze eerst weer omgezet worden in losse vetzuren voordat ze door de weefsels opgenomen kunnen worden. Dit proces heet **lipolyse**. De reden dat vetzuren eerst via de lever in TG worden omgezet heeft te maken met het feit dat vetzuren zelf toxisch zijn. In weefsels worden ze daarom zo snel mogelijk óf verbrand óf weer omgezet in TG zodat ze geen schade kunnen aanrichten.

**Verstoring TG transport in obesitas**

Er wordt momenteel heel veel onderzoek gedaan naar de reden waarom mensen met obesitas een hoog risico lopen om hart- en vaatziekten en suikerziekte te ontwikkelen. Men denkt dat één van de oorzaken hiervoor is dat het lichaam verkeerd omgaat met TG en de vetzuren hiervan. Daarom is het belangrijk dat we meer inzicht krijgen in de stofwisseling processen betrokken bij de opname, het transport, de verbranding en de opslag van TG en vetzuren (**TG metabolisme**). In dit proefschrift onderzoeken we het effect van verschillende interventies op het metabolisme van VLDL-TG om zo beter inzicht te krijgen in de regulatie hiervan.

In het eerste deel van dit proefschrift hebben we gekeken naar het effect van cholesteryl ester transfer proteïne (**CETP**) op het VLDL-TG metabolisme. CETP is betrokken bij het verplaatsen van cholesteryl esters en TG tussen lipoproteïnen en we hebben eerder al laten zien dat CETP een grote invloed heeft op het cholesterol metabolisme. De werking van CETP leidt tot verlaagde niveaus van HDL cholesterol (goed cholesterol) en een toename van LDL cholesterol (slecht cholesterol) waardoor de kans op aderverkalking toeneemt. Of CETP ook effect heeft op TG is onderzocht in **hoofdstuk 2**. De werking van CETP heeft nauwelijks effect op het VLDL-TG metabolisme en heeft geen effect op de ontwikkeling van obesitas door het aangeboden dieet. Omdat CETP cholesterol verplaatst van HDL naar LDL en het goede cholesterol hierdoor afneemt, worden er medicijnen ontwikkeld om CETP te remmen en zo het goede cholesterol te verhogen. Het is belangrijk dat het remmen van CETP geen negatieve bijwerkingen heeft omdat CETP ook TG verplaatst tussen lipoproteïnen. We concluderen dan ook dat CETP remmers waarschijnlijk geen negatieve bijwerkingen zullen hebben met betrekking tot het TG metabolisme.

**Regulatie van TG metabolisme**

In het tweede deel van dit proefschrift hebben we gekeken naar de effecten van verschillende farmacologische interventies op de regulatie van het VLDL-TG metabolisme. **Nucleaire receptoren** spelen hierbij een grote rol. Dit zijn eiwitten in de cel die zijn betrokken bij de communicatie in de cel. Nucleaire receptoren herkennen specifieke moleculen in de cel, bijvoorbeeld vetzuren, en verplaatsen zich vervolgens naar de kern van de cel waar ze de **werking (expressie) van genen** beïnvloeden. Genen zijn onderdeel van ons DNA en bevatten de receptuur om 'machines' te maken. Deze machines zijn de werktuigen in onze cellen en hebben allemaal een eigen functie. Wanneer

de expressie van een gen toeneemt wordt er meer van die machine gemaakt. Op deze manier worden processen in onze cellen, en dus in ons lichaam, beïnvloed. Andere moleculen die herkend kunnen worden door nucleaire receptoren zijn hormonen en xenobiotica. Xenobiotica zijn moleculen die van nature niet in het lichaam voorkomen, bijvoorbeeld medicijnen die we slikken. Tot de nucleaire receptoren behoren de peroxisoom proliferator geactiveerde receptoren (**PPAR**), en de xenobioticum receptoren pregnaan X receptor (**PXR**) en constitutieve androstaan receptor (**CAR**).

In **hoofdstuk 3** hebben we het effect van de farmacologische PPARα activator fenofibraat op het VLDL-TG metabolisme onderzocht. Fenofibraat behoort tot de groep van de fibraten en hebben als belangrijkste functie het verlaging van TG in het bloed. Er werd altijd vanuit gegaan dat deze verlaging wordt veroorzaakt door minder productie van VLDL-TG én meer opname van VLDL-TG. Onze studie laat zien dat de verlaging van TG door fenofibraat geheel wordt verklaard door meer opname van VLDL-TG. Onverwacht veroorzaakt fenofibraat zelfs een verhoging van de productie van VLDL-TG door de lever. Deze toename wordt deels veroorzaakt door een toename in de omvorming en verplaatsing van vetzuren, oftewel meer **vetzuur omzet**. Verhoogde omzetting van vetzuren in het lichaam wordt als één van de oorzaken beschouwd voor het ontstaan van ziekten gerelateerd aan obesitas. Het is dus belangrijk dat we niet alleen weten wat medicijnen op totale niveau's doen van TG en cholesterol maar ook hoe medicijnen dit doen. Waarschijnlijk is de verhoogde omzetting van vetzuren met fenofibraat niet schadelijk omdat fenofibraat ook ontsteking remt. Ontsteking is ook belangrijk bij het ontstaan van hart- en vaatziekten en suikerziekte in mensen met obesitas.



Het effect van rifampicine op het VLDL metabolisme is onderzocht in **hoofdstuk 4**. Rifampicine is een antibioticum dat wordt voorgeschreven voor de behandeling van tuberculose. Maar rifampicine activeert ook PXR. Bij behandeling met dit medicijn zijn bijwerkingen als vervetting van de lever en verstoring van TG en cholesterol in het bloed bekend. In onze studie laten we zien dat rifampicine inderdaad PXR activeert en leidt tot een verlaging zowel HDL als VLDL cholesterol terwijl de TG niveau's onveranderd blijven. De afname van het cholesterol wordt veroorzaakt door minder productie van voornamelijk VLDL door de lever. Omdat de VLDL deeltjes uitgescheiden door de lever meer TG bevatten heeft rifampicine geen effect op het totale TG niveau.

Chemische verontreinigende stoffen hebben ook invloed op nucleaire receptoren. In **hoofdstuk 5** beschrijven we het effect van perfluoroakyl sulfonaten (**PFAS**) op het TG en cholesterol metabolisme. PFAS zijn chemische stoffen die worden gebruikt in anti-vlek middelen en in coatings. Nadeel van deze stoffen is dat ze biologisch slecht afbreekbaar zijn en daardoor ophopen in het milieu. We laten zien dat PFAS de nucleaire receptoren PPARα, PXR en CAR activeren, wat leidt tot remming van zowel de HDL als VLDL productie door de lever. Daarnaast stimuleren PFAS de lipolyse van VLDL-TG. Bij elkaar verklaart dit waarom cholesterol en TG sterk verlagen in onze studie.

In **hoofdstuk 6** hebben we gekeken naar de verschillen in lever gen expressie in reactie op langdurig vasten of een hoog vet dieet. Zowel langdurig vasten als een hoog vet dieet leiden tot vervetting van de lever maar alleen bij een hoog vet dieet is er ook sprake van dat de lever niet langer reageert op insuline. Dit wordt ook wel insuline resistentie genoemd en kan leiden tot suikerziekte. We hebben deze studie uitgevoerd om meer inzicht te krijgen in de regulatie van het vet metabolisme bij zowel lever vervetting als insuline resistentie. Opvallend is dat vasten de werking van veel meer genen beïnvloed vergeleken met controle dieren dan een hoog vet dieet. Daarnaast was er ook nauwelijks overlap in de genen die tot werking kwamen vergeleken tussen vasten en hoog vet dieet. Dit suggereert dat er compleet andere gen expressie programma's betrokken zijn bij het ontstaan van een vette lever tussen vasten en een hoog vet dieet. Hoog vet dieet geïnduceerde vette levers waren geassocieerd met activatie van PPARα terwijl na vasten vooral de xenobioticum receptoren PXR en CAR werden geactiveerd.

In dit proefschrift laten we zien dat nucleaire receptoren een grote invloed hebben op het VLDL-TG metabolisme en ook betrokken zijn bij het ontstaan van ziektes gerelateerd aan obesitas. Momenteel wordt er veel aandacht besteed aan het ontwikkelen van medicijnen die nucleaire receptoren beïnvloeden om zo ziekten in obese mensen te behandelen. Onze onderzoeken laten vooral zien wat het effect is van nucleaire receptoren op VLDL-TG maar ze hebben vaak ook invloed op ontsteking. Bij het ontstaan van ziektes bij obesitas zijn vaak vele verschillende processen betrokken waaronder het TG metabolisme en ontsteking. Door geïntegreerd onderzoek te doen naar deze verschillende processen kunnen we een beter beeld krijgen waarom mensen met obesitas ziek worden en goede medicijnen ontwikkelen.

**List of publications**

Bijland S, van den Berg SAA, Voshol PJ, van den Hoek AM, Princen HM, Havekes LM, Rensen PCN, Willems van Dijk K. CETP does not affect triglyceride production or clearance in APOE*3-Leiden mice.
Journal of Lipid Research 2010;51(1):97-102

van den Berg SAA, Guigas B, Bijland S, Ouwens M, Voshol PJ, Frants RR, Havekes LM, Romijn JA, Willems van Dijk K. High levels of dietary stearate promote adiposity and deteriorate hepatic insulin sensitivity.
Nutrition & Metabolism 2010;7:24

van den Berg SAA*, Nabben M*, Bijland S, Voshol PJ, van Klinken JB, Havekes LM, Romijn JA, Hoeks J, Hesselink MK, Schrauwen P, Willems van Dijk K. High levels of whole body energy expenditure are associated with skeletal muscle mitochondrial uncoupling in C57Bl/6 mice.
Metabolism 2010 May 20



Bijland S, Pieterman EJ, Maas ACE, van der Hoorn JWA, van Erk MJ, van Klinken JB, Havekes LM, Willems van Dijk K, Princen HMG, Rensen PCN. Fenofibrate increases VLDL-triglyceride production despite reducing plasma triglyceride levels in APOE*3-Leiden.CETP mice.
The Journal of Biological Chemistry 2010;285(33):25168-75

de Wilde J, Smit E, Mohren R, Boekschoten MV, de Groot P, van den Berg SAA, Bijland S, Voshol PJ, Willems van Dijk K, de Wit NW, Bunschoten A, Schaart G, Hulshof MF, Mariman EC. An 8-week high-fat diet induces obesity and insulin resistance with small changes in the muscle transcriptome of C57BL/6J mice.
Journal of Nutrigenetics and Nutrigenomics. 2009;2(6):280-91

de Vogel-van den Bosch J*, van den Berg SAA*, Bijland S, Voshol PJ, Havekes LM, Romijn HA, Hoeks J, van Beurden D, Hesselink MKC, Schrauwen P, Willems van Dijk K. High fat diets rich in medium- versus long-chain fatty acids induce distinct patterns of tissue specific insulin resistance.
The Journal of Nutritional Biochemistry 2010

Bijland S*, Rensen PCN*, Pieterman EJ, Maas ACE, van der Hoorn JW, van Erk MJ, Havekes LM, Willems van Dijk K, Butenhoff JL, Princen HMG. Perfluoroalkyl sulfonates cause alkyl chain-dependent hepatic steatosis and combined hypolipidemia in ApoE*3-Leiden.CETP mice.
Submitted.

Langeveld M*, van den Berg SAA*, Bijl N, Bijland S, van Roomen C, Houben-Weerts JH, Ottenhoff R, Houten SM, Willems van Dijk K, Romijn JA, Groen AK, Aerts JM, Voshol PJ. N-(5-adamantane-1-yl-methoxy-pentyl)-deoxynojirimycin (AMP-DNM) reduces body weight by decreasing energy intake and increasing fat oxidation in ob/ob mice.
Submitted

Bijland S*, de Haan W*, Smit JWA, Havekes LM, Princen HMG, Willems van Dijk K, Rensen PCN. Rifampicin decreases plasma cholesterol by impairing HDL and VLDL particle production in ApoE*3-LEIDEN.CETP mice.
Manuscript in preparation.

*Both authors contributed equally

**Curriculum Vitae**

Silvia Bijland werd geboren op 13 juli 1980 te Zaanstad. Na het doorlopen van de Mavo en Havo behaalde ze haar VWO diploma in juni 2000 aan het Bertrand Russell College te Krommenie. In september dat jaar begon zij haar studie Biomedische Wetenschappen aan de Universiteit van Utrecht. Ze behaalde haar propedeutisch examen in 2001 en haar Bachelor diploma in 2003. Tijdens haar Master Developmental Biology and Biomedical Genetics heeft zij een drietal stages doorlopen. Tijdens haar hoofdvakstage heeft ze onderzoek verricht binnen de vakgroep Fysiologische Chemie van het Universitair Medisch Centrum Utrecht onder leiding van Drs. JA Riedl en Prof. Dr. JL Bos met als onderwerp 'Small GTPase Rap1'. Haar tweede onderzoeksstage heeft ze verricht onder leiding van Drs. MJ Adjobo-Hermans en Prof. Dr. D. Gadella Jr. bij de afdeling Molecular Cytology van het Swammerdam Institute for Lifescience te Amsterdam met als onderwerp 'Visualisation of dimerization C terminal domain PLCβ'. Daarnaast heeft ze nog een onderzoeksstage verricht bij de afdeling Endocrinologie van het Leids Universitair Medisch Centrum Leiden onder leiding van Drs. JFP Berbée en Dr. PCN Rensen met als onderwerp 'Role of apolipoprotein AIV in inflammation'. In 2006 behaalde zij haar Master diploma en aansluitend startte zij als promovenda met haar promotieonderzoek op de afdelingen Humane Genetica en Endocrinologie onder begeleiding van haar promotor Prof. Dr. Ir. LM Havekes en copromotores Dr. Ir. K. Willems van Dijk en Dr. PCN Rensen.